

SHEAR LAG EFFECTS ON WELDED STEEL  
ANGLES AND PLATES

CENTRE FOR NEWFOUNDLAND STUDIES

---

**TOTAL OF 10 PAGES ONLY  
MAY BE XEROXED**

(Without Author's Permission)

RAJAPRAKASH MANNEM







**SHEAR LAG EFFECTS ON WELDED STEEL  
ANGLES AND PLATES**

by

**e Rajaprakash Mannem, B.E**

A thesis submitted to  
The School of Graduate Studies  
in partial fulfillment of the  
requirements for the degree of  
Master of Engineering

Faculty of Engineering and Applied Science  
Memorial University of Newfoundland

**March 2002**

St. John's

Newfoundland

To my father Late Dr. M Venkatakrishnaiah

my mother Mrs. M.V. Malathikrishna

and my sister M. Chethana

## **ABSTRACT**

The "Shear Lag Effect" reduces the ultimate net-section capacity of steel members due to uneven stress distribution at the connection zone. Bolted connections have been studied in detail for shear lag. The applicable design specifications for both bolted and welded members are currently based on the behavior of bolt-connected elements. There is a need for investigating such assumed similarities with weld-connected members.

An experimental study was therefore carried out on welded steel members in tension. It included twenty-seven steel plate specimens and twenty-two steel angle specimens with different weld configurations. Analytical studies using finite element techniques were carried out. Material non-linearity including strain hardening effects and large deformation effects were considered in the analysis. The effects of various parameters were studied experimentally and analytically. Physical parameters such as length of member, size of member, length of connection, configuration of connections and material parameters such as ratio of yield stress and ultimate stress were considered. A study was also carried out to obtain an elastic solution using Fourier Series for discontinuous tensile loading.

The relevant current design provisions of North American specifications have been examined. Efficiencies predicted by these standards were compared with the experimental results. Modifications to the standards have been recommended.

## ACKNOWLEDGEMENTS

I have great pleasure in expressing my gratitude to my supervisor Dr. Seshu Madhava Rao Adluri for his continuous guidance and encouragement.

I thank Dr. A.S.J. Swamidas for his cooperation with the experimental setup, and Dr. K. Munaswamy for his help with the lab setup, encouragement, valuable advice and persistent interest in my research work.

Thanks are due to Mr. Austin Burse and Mr. Calvin Ward for their continuous assistance during the experimental study. I also acknowledge the Technical Services of Memorial University for their cooperation in the fabrication of the test-setup, plate and angle specimens.

This research is made possible by grants from the Steel Structures Education Foundation (SSEF) of the Canadian Institute of Steel Construction (CISC) and the Natural Sciences and Engineering Research Council of Canada (NSERC).

I thank the School of Graduate Studies, which provided me a fellowship and needful help in completing my Master of Engineering Program. My thanks to Dr. J.J. Sharp and Dr. Haddara, Associate Dean of Engineering and Applied Science. The generous support from Computing Services (CCA) at Memorial University is very much appreciated.

Finally to all my friends, my thanks for their companionship and assistance offered during my Master's Program.

# TABLE OF CONTENTS

ABSTRACT .....	ii
ACKNOWLEDGEMENTS .....	iii
TABLE OF CONTENTS .....	iv
LIST OF FIGURES.....	viii
LIST OF TABLES .....	xii
LIST OF SYMBOLS .....	xiv

<b>Chapter 1 Introduction .....</b>	<b>1</b>
1.1 Tension Members.....	2
1.2 Shear Lag Phenomenon.....	3
1.3 Scope of Research.....	4
1.4 Objectives.....	5

<b>Chapter 2 Literature Review.....</b>	<b>7</b>
2.1 Earlier Studies .....	8
2.1.1 Shear Lag in Bolted Angle Tension Members [Kulak and Wu, 1997].....	8
2.1.2 Shear Lag Effects in Steel Tension Members [Easterling and Gonzalez, 1993] .....	11
2.1.3 Single Angles in Tension and Compression [Marsh, 1969].....	18
2.1.4 Truss-Type Tensile Connections [Munse and Chesson, 1963a].....	18
2.1.5 Riveted and Bolted Joints: Net Section Design [Munse and Chesson, 1963b] .....	20
2.1.6 Welded Connections for Angle Tension Members [Gibson and Wake, 1942] .....	21
2.1.7 Tension Tests of Welded and Riveted Structural Members [Davis and Boomsliter, 1934].....	21
2.2 Current Design Provisions for Tension Members.....	22
2.2.1 CAN/CSA-S16.1-94 [CSA, 1994] .....	23
2.2.2 Load and Resistance Factor Design [AISC-LRFD, 1993].....	24

2.2.3 Design of Latticed Transmission Tower Structures, ASCE/ANSI 10-90 [ASCE, 1990] .....	24
2.2.4 New Provisions for Shear Lag in Steel Tension Members [Albert, 1996]	25
2.3 Theoretical Analysis.....	25
2.3.1 Exact solution of Shear-Lag problems [Hildebrand, 1943] .....	26
2.4 Summary of Previous Studies .....	26
<b>Chapter 3 Theoretical analysis of Shear Lag in Tension.....</b>	<b>31</b>
3.1 Classical Solutions .....	31
3.2 Elastic Numerical Solution.....	34
3.3 Elastic Solution for Welded Plates.....	35
3.4 Nonlinear Analysis Using Finite Elements .....	38
3.5 Finite Element Model.....	39
<b>Chapter 4 Experimental Investigation .....</b>	<b>52</b>
4.1 Physical Properties .....	53
4.2 Material Properties .....	54
4.3 Test Setup.....	56
4.4 Specimen Description .....	57
4.4.1 Plate Specimens.....	58
4.4.2 Angle Specimens.....	59
4.5 Test Procedure.....	64
<b>Chapter 5 RESULTS AND DISCUSSION .....</b>	<b>74</b>
5.1 Experimental Results .....	74
5.1.1 Plate Specimens.....	75
5.1.2 Angle Specimens.....	79
5.2 Finite Element Analysis .....	85
5.3 Discussion of Results .....	88
5.3.1 Effect of Size of Member.....	89
5.3.2 Effect of Length of Connection.....	92

5.3.3 Effect of Material Properties .....	98
5.3.4 Effect of Eccentricity .....	100
5.3.5 Effect of Free Length of Member .....	100
5.3.6 Effect of Weld Configuration.....	101
5.3.6.1 Type-1 Configuration: Welds with both Longitudinal and Transverse Welds.....	102
5.3.6.2 Type-2 Configuration: Specimens with only Longitudinal Welds ...	108
5.3.6.3 Type-3 Configuration: Specimens with only Single Edge Longitudinal Welds.....	108
5.3.6.4 Angle Specimens.....	109
5.3.7 Effect of Specimen Configuration.....	111
5.3.8 Single and Double Specimen Configuration .....	112
5.4 Comparison of Current Net-Section Strength Formulae with Experimental Results .....	113
5.4.1 Evaluation of $1 - \bar{x}/L$ Rule [Chesson and Munse, 1963] .....	113
5.4.2 Net-Section Strength Formula by Kulak and Wu [1997].....	115
5.5 Evaluation of Current Specifications .....	117
5.6 Proposed Net-Section Strength Formula.....	118
5.6.1 Size Effect Parameter .....	119
5.6.2 Connection Length Parameter.....	120
5.6.3 Steel Grade Parameter.....	121
5.6.4 Breaking Strain Parameter .....	121
5.6.5 Combined Formula for Plates .....	122
5.6.6 Efficiency of Angles.....	122
5.7 Recommended Design Method .....	123
<b>Chapter 6 Conclusions and Recommendations .....</b>	<b>159</b>
6.1 Summary.....	159
6.2 Conclusions.....	160
6.3 Suggested Changes to the Current Design Practice.....	164
6.4 Recommendations for Further Research.....	166

<b>References</b>	.....	<b>168</b>
<b>Appendices</b>	.....	<b>171</b>
APPENDIX A	FE Model of Plate connected by Longitudinal Welds only .....	172
APPENDIX B	FE Model of Angle Specimens .....	177
APPENDIX C	FE Model for Evaluating Weld Stiffness .....	182
APPENDIX D	True Stress vs. Logarithmic Strain of Plates and Angles .....	184
APPENDIX E	Failure Pictures of Plate Specimens .....	187
APPENDIX F	Failure Pictures of Angle Specimens .....	194

## LIST OF FIGURES

Figure 1-1 Stress Variation due to “Shear Lag Effect” in Structural Steel Angle Section in Tension.....	6
Figure 3-1 Plate with Symmetrical Welds of Length transmitting Tensile Force .....	44
Figure 3-2 Plate with Symmetrical Concentrated Axial Loads at Corners .....	44
Figure 3-3 Stress Variation along the Length of Stiffened Plate .....	45
Figure 3-4 Elastic Stress Variation for Plate with Stiffeners .....	46
Figure 3-5 Elastic Stress Variation for Plate without Stiffeners .....	46
Figure 3-6 Variation of Stress across the Plate Width at the Critical Section .....	47
Figure 3-7 Variation of Longitudinal Stress along Center-line of the Plate ( $l/w = 1$ ).....	48
Figure 3-8 Typical Curve for True Stress Vs. Log Strain for Test Specimens .....	49
Figure 3-9 Finite Element Model of Plate Specimens (Typical) .....	50
Figure 3-10 Finite Element Model of Single Angle Specimen (Typical).....	50
Figure 3-11 Convergence Test for FEA Model .....	51
Figure 4-1 True Stress Vs. Log Strain Relation of Test Specimens .....	66
Figure 4-2 Self-Balancing Rectangular Frame Setup for 2700 kN Actuator.....	67
Figure 4-3 Details of Self-Balancing Rectangular Frame Setup.....	68
Figure 4-4 Test on Tinius-Olsen UTM .....	69
Figure 4-5 Typical Location of Strain Guages on Plate Specimens .....	70
Figure 4-6 Typical Location of Strain Guages on Angle Specimen .....	71
Figure 4-7 Measurement Devices on Plate Specimens .....	72
Figure 4-8 Measurement Devices on Angle Specimens .....	73
Figure 5-1 Propagation of Net-Section Failure .....	126
Figure 5-2 Failure of Angle in Tension-type Tearing .....	127
Figure 5-3 Failure of Weld under Bending and Shear .....	127
Figure 5-4 Failure of Angle in Shear-type Tearing.....	128

Figure 5-5 Lateral Deflection of Plate Specimens .....	129
Figure 5-6 Load Deformation Curve for Specimen UEA2 .....	130
Figure 5-7 Specimen Loaded through Gusset Plates .....	131
Figure 5-8 Specimen Loaded through Gusset Plates .....	131
Figure 5-9 Comparison of Load-Elongation Curve from FEA and Experimental Results. .....	132
Figure 5-10 Stress Variation at Ultimate Load for Specimen P120-1 (FEA) .....	133
Figure 5-11 Stress Variation at Ultimate Load for Specimen P120-1.5 (FEA) .....	133
Figure 5-12 Stress Variation at Ultimate Load for Specimen DEA1 .....	134
Figure 5-13 Stress Variation at Ultimate Load for Specimen UEA4 .....	134
Figure 5-14 Stress Variation at Ultimate Load for Specimen EA1 .....	135
Figure 5-15 Effect of Size of Specimen on Shear Lag .....	136
Figure 5-16 Effect of Width of Plate on Shear Lag (FEA) .....	137
Figure 5-17 Comparison of Experimental and FEA Results on Size of Specimen .....	137
Figure 5-18 Effect of Size of Angles on Shear Lag .....	138
Figure 5-19 Effect of Length of Connection on Plate Welded on Both Edges .....	139
Figure 5-20 Effect of Length of Connection on Plates Welded Only on Single Edge ...	139
Figure 5-21 Behavior of 75mm Wide Plate Specimens .....	140
Figure 5-22 Behavior of 120mm wide Plate Specimen .....	141
Figure 5-23 Plate Tear-Out in Shearing Mode .....	142
Figure 5-24 Failure of Specimen P75-0.87 in Shear-type Tearing .....	142
Figure 5-25 Effect of Length of Connection on Angles .....	143
Figure 5-26 Effect of Length of Connection on Angles (FEA Study) .....	143
Figure 5-27 Effect of $F_y/F_u$ (Steel Grade) on Efficiency of Plate Specimens .....	144
Figure 5-28 Stress Strain Pattern for FEA Parametric Study .....	145
Figure 5-29 Effect of $F_y/F_u$ on Plate Specimens ( $F_u$ kept Constant) .....	146
Figure 5-30 Effect of Initial Strain at Strain Hardening .....	146
Figure 5-31 Effect of Breaking Strain on Shear Lag .....	147
Figure 5-32 Effect of Eccentricity on Shear Lag .....	147
Figure 5-33 Effect of Free Length on Shear Lag .....	148
Figure 5-34 Finite Element Model of a Typical Fillet Weld .....	148

Figure 5-35 Plate Specimen with Both Longitudinal and Transverse Welds .....	149
Figure 5-36 Forces and Reactions on Transverse and Longitudinal Welds.....	149
Figure 5-37 Elastic Stress Variation in a Plate connected by both Longitudinal and Transverse Welds ( $L_{longitudinal\ weld-length} / w = 1.0$ ) .....	150
Figure 5-38 Elastic Stress Variation in Plate connected by both Longitudinal and Transverse Welds ( $L_{longitudinal\ weld-length} / w = 0.5$ ) .....	150
Figure 5-39 Elastic Stress Variation in a Plate connected by both only Longitudinal Welds ( $L_{longitudinal\ weld-length} / w = 1.0$ ).....	151
Figure 5-40 Comparison of $1 - \bar{x}/L$ with Experimental Results .....	151
Figure 5-41 Variation of Munse's Expression for Plate and Angle Specimens.....	152
Figure 5-42 Comparison of Kulak Predictions with Test Results.....	152
Figure 5-43 Comparison of CAN/CSA S16.1-94 Predictions with Test Results .....	153
Figure 5-44 Comparison of AISC-LRFD Predictions with Test Results.....	154
Figure 5-45 Comparison of ANSI/ASCE 10-90 Predictions with Test Results .....	155
Figure 5-46 Comparison of Proposed Expression with Test Results.....	156
Figure 5-47 Comparison of Theoretical Predictions with Experimental Results.....	157
Figure 5-48 Comparison of Mean Values of Predictions of Current Design Standards and Proposed Expression .....	157
Figure 5-49 Comparison of Standard Deviation of Predictions of Current Design Standards and Proposed Expression.....	158
Figure E-1 Failure of Specimen DP120-1.....	187
Figure E-2 Failure of Specimen P120-S .....	187
Figure E-3 Failure of Specimen DP75-S.....	188
Figure E-4 Failure of Specimen P120-1.5.....	188
Figure E-5 Failure of Specimen P120-1a.....	189
Figure E-6 Failure of Specimen P120-T-b.....	189
Figure E-7 Failure of Specimen P250-1 .....	190
Figure E-8 Failure of Specimen P75-S-b .....	190
Figure E-9 Failure of Specimen P75-0.87.....	191
Figure E-10 Failure of Specimen P75-1 .....	191

Figure E-11 Failure of Specimen P75-2.....	192
Figure E-12 Failure of Specimen P75-S .....	192
Figure E-13 Failure of Specimen P75-T .....	193
Figure E-14 Failure of Specimen OP120-1-a.....	193
Figure F-1 Failure of Specimen DEA2 .....	194
Figure F-2 Failure of Specimen DEA1 .....	195
Figure F-3 Failure of Specimen DEA5 .....	195
Figure F-4 Failure of Specimen DUEA1 .....	196
Figure F-5 Failure of Specimen DUEA2 .....	196
Figure F-6 Failure of Specimen EA1 .....	197
Figure F-7 Failure of Specimen EA2 .....	198
Figure F-8 Failure of Specimen EA3 .....	198
Figure F-9 Failure of Specimen EA4 .....	199
Figure F-10 Failure of Specimen EAm1 .....	199
Figure F-11 Failure of Specimen EAm2.....	200
Figure F-12 Failure of Specimen UEA1 .....	201
Figure F-13 Failure of Specimen UEA2 .....	202
Figure F-14 Failure of Specimen UEA3 .....	202
Figure F-15 Failure of Specimen UEA4 .....	203
Figure F-16 Failure of Specimen UEA5 .....	203
Figure F-17 Failure of Specimen UEA6.....	204
Figure F-18 Failure of Specimen UEA8.....	204
Figure F-19 Failure of Specimen UEA9.....	205

## LIST OF TABLES

Table 2-1 Properties and Experimental Results of Plates Specimens by Easterling and Gonzalez (1993).....	13
Table 2-2 Properties of Angle Specimens tested by Easterling and Gonzalez (1993)....	14
Table 2-3 Experimental Results of Angle Specimens by Easterling and Gonzalez (1993) .....	15
Table 2-4 Experimental Test Data by American Welding Society (1931) .....	16
Table 2-5 Experimental Test Data by American Welding Society (1931) .....	17
Table 2-6 Tension Tests by Davis and Boomsliiter [1934] .....	22
Table 3.1-1 Values of $\lambda_w$ for different ratios $\alpha$ .....	33
Table 5-1 Experimental Results of Plate Specimens .....	76
Table 5-2 Experimental Results of Plate Specimens .....	77
Table 5-3 Experimental Results of Plate Specimens .....	78
Table 5-4 Experimental Results for Angle Specimens .....	80
Table 5-5 Experimental Results for Angle Specimens .....	81
Table 5-6 Experimental and FE Results of Plate Specimens .....	87
Table 5-7 Experimental and FE Results of Angle Specimens .....	88
Table 5-8 Effect of the Size of Member -Plates.....	89
Table 5-9 Effect of Size of Member- Angles.....	91
Table 5-10 Effect of Length of Connection -Plate Specimens.....	92
Table 5-11 Effect of Length of Connection - Angle Specimens .....	95
Table 5-12 Effect of Grade of Steel .....	98
Table 5-13 Effect of Load Eccentricity on Plates .....	100
Table 5-14 Effect of Free Length of Member .....	101
Table 5-15 Effect of Weld Configuration - Both Edges Welded .....	104
Table 5-16 Effect of Weld Configuration - One Edge Welded .....	109
Table 5-17 Effect of Weld Configuration on Angle Specimens .....	110

Table 5-18 Effect of Specimen Configuration .....	111
Table 5-19 Effect of Single and Double Specimen Configuration .....	112
Table 5-20 Net Section Efficiency based on Munse's Expression for Shear Lag. ....	114
Table 5-21 Efficiency Predictions for Proposed Net-section and Munse's Expression .	125
Table D-1 Stress Vs. Strain for Plate Specimens .....	184
Table D-2 Stress Vs. Strain for Angle Sections .....	185
Table D-3 Stress Vs. Strain for Angle Section.....	186

## LIST OF SYMBOLS

The following symbols have been used in the present thesis:

$a$	=	Length of Weld, mm
$A_{cn}$	=	Net Area of Connected Leg, mm <sup>2</sup>
$A_f$	=	Area of Flange Plates
$A_g$	=	Gross Area of the Section
$A_{net}$	=	Net Total Area accounting for reduction due to holes and slots, mm <sup>2</sup>
$A_o$	=	Net area of Outstanding Leg, mm <sup>2</sup>
$b$	=	Free length of the Specimen
$B$	=	Bearing Factor
$c$	=	Half Width of the Plate Specimen
$C'$	=	Proportionality Constant
$C$	=	Efficiency Coefficient based on the Geometry of the Connection
$E$	=	Modulus of Elasticity, MPa
$F$	=	Elemental Load
$F_y$	=	Yield Stress, MPa
$F_u$	=	Ultimate Stress, MPa
$G$	=	Modulus of Rigidity, MPa
$H$	=	Fabrication Factor accounting for Drilled or Punched Holes

$k_l$	=	Stiffness of Longitudinal Weld of Unit length
$k_w$	=	Stiffness of Transverse Weld of Unit Length
$K$	=	Ductility Factor
$K_g$	=	Steel Grade Parameter
$K_b$	=	Breaking Strain Parameter
$K_l$	=	Connection Length Parameter
$K_w$	=	Size Effect Parameter
$L_p$	=	Plate of Finite Length
$L$	=	Length of Connection, mm
$L_f$	=	Free Length of the Test Specimen, mm
$L_{p1}, L_{p2}$	=	Longitudinal Weldlength on Test Specimen, mm
$L_t$	=	Transverse Weldlength on test Specimen, mm
$L_1$	=	Longitudinal Weldlength at the Heel of the Angle Specimen, mm
$L_2$	=	Longitudinal Weldlength at the Toe of the Angle Specimen, mm
$P$	=	Applied Force in the Longitudinal direction
$P_a$	=	Calculated Ultimate Capacity, kN
$R$	=	Percentage Reduction of Cross-Sectional Area
$S$	=	Weld Size, mm
$S_1$	=	Weld Size at the Heel of the Angle Specimen, mm
$S_2$	=	Weld Size at the Toe of the Angle Specimen, mm

$S_t$	=	Transverse Weld Size, mm
$t$	=	Thickness of the Test Specimen, mm
$t_g$	=	Thickness of the Gusset Plate, mm
$T_a$	=	Actual Test Capacity of the Test Specimen, kN
$T_n$	=	Nominal Capacity of the Tension Member, kN
$T_y$	=	Gross Yield Capacity of the Test Specimen, kN
$T_u$	=	Gross Theoretical Ultimate Capacity of the Test Specimen, kN
$T_r$	=	Ultimate Calculated Capacity
$U_c$	=	Net Section Efficiency
$V$	=	Shear Lag Factor as defined by Chesson and Munse
$w$	=	Width of the Plate Specimen, mm
$w_c$	=	Overall Width of the Connected Leg of the Angle Specimen, mm
$w_o$	=	Overall Width of the Outstanding Leg of the Angle Specimen, mm
$x'$	=	Any distance along the length of the plate, mm
$\bar{x}$	=	Distance between Centroid of the Member and the Plane of Force, mm
$X_u$	=	Ultimate Strength of the Weld Material, MPa
$y'$	=	Any distance from the centreline of Plate, mm
$Z$	=	Miscellaneous Factor such as Ductility
$\alpha'$	=	Ratio of Longitudinal Weld and Width of Plate
$\alpha$	=	Ratio of the Flange Area to Plate Area

- $\beta$  = Area Reduction Factor depending on the number of Bolts
- $\delta$  = Elongation of the Specimens
- $\sigma_t$  = Stress in Transverse Weld

# Chapter 1

## Introduction

Most civil engineering structures are assemblages of members. These members are made of steel, concrete, timber, fiber-reinforced plastics, etc. Of these, steel is widely used in engineering structures in the form of framework for buildings, bridges, cranes, oil platforms, towers, etc. High strength per unit weight, uniformity of material properties, ductility, ability to fasten together using simple connections, reuse, fatigue strength and speed and ease of erection are some of its many advantages that have made steel a most preferred material. Structural steel in tension members is quite common. Tension members are the most efficient form of transmitting forces between two points. Some of the examples of steel tension members can be found as tension chords in trusses, bracing members in frames, transmission towers and antenna supporting structures, hangers in suspended structures, etc. Recent advances in manufacturing processes have introduced the use of higher and better grades of steel for routine purposes. The use of steel in these structures is governed by design codes such as Canadian Standard CSA-S16.1 [CSA 1994]. These design codes need to be constantly revised to take advantage of the new developments in usage and production technologies. The present study is concerned with the investigation of steel tension members and their behaviour under certain conditions.

## 1.1 Tension Members

Steel tension members can be of various types. They include open sections such as angles, tees, channels, plates/flats, etc., closed sections such as hollow structural tubes, compound/built-up sections consisting mainly of double or multiple angles, double channels, channel with tee sections, etc., ropes and cables as in cable suspended bridges. Of these, the most commonly used are single or double angles.

Tension members may fail in one of three principal modes, viz.,

1. Complete yielding of the gross section which occurs away from the connection zone ( $T_y \leq A_g F_y$ ),
2. Failure of the end connection (bolts and/or welds) and
3. Fracture of the net section near the connection zone ( $T_u \leq A_{net} F_u$ )

In the above,  $T_y$  and  $T_u$  are the (unfactored) yield and ultimate tension capacity,  $A_g$  is the gross cross-sectional area,  $A_{net}$  is the net cross-sectional area accounting for reduction due to the presence of holes and other openings near the connection zone.  $F_y$  and  $F_u$  are the yield and tensile strengths of the material. Failure by fracture of the gross-section is not allowed, since this would result in excessive deformations.

Fracture of the net-section depends mainly on the geometry of the cross-section and the end connection.

Ideally, tension members must be connected to other members in such a way as to receive uniform stress throughout all parts of the cross-section. However, in most applications, it

is not possible to have the entire cross-section of the member connected to other members (Figure 1-1). Connecting only a part of the section causes non-uniform distribution of stress in the connection zone. This non-uniformity decreases the efficiency of the member at the time of collapse.

## 1.2 Shear Lag Phenomenon

Members that fail in net section fracture may not exhibit full efficiency. Their theoretical capacity should be  $A_{net}F_u$ . However, due to the presence of certain effects related to force transfer between different connected parts (or zones) of the member, this theoretical capacity is reduced. The efficiency of the net-section  $U_e$  in resisting loads is given by,

$$U_e = \frac{T_n}{A_{net}F_u} \quad \text{Eq. 1-1}$$

where,  $T_n$  is the tensile capacity of the member in net-section rupture, and  $A_{net} \leq A_g$ .

Net-Section efficiency depends mainly on an effect known as “Shear Lag.” Shear Lag occurs in members when forces are transferred only to part of the member instead of the entire cross-section.

In weld connected members, elements directly connected to longitudinal weld receive forces through the weldment. These elements in turn transfer their forces to sections adjacent to them. In this process, some amount of the applied load is resisted by direct tension of the element that is receiving it while the remaining load is transferred through shear to its adjacent elements. Such transfer of force occurs till the entire applied load is balanced. The elements that receive force through shear-transfer lags behind the elements

that receive the force directly from the weld. This transfer of forces results in unequal distribution of stresses in the cross-section. Such distribution of stresses persists even after parts of the end connection region have yielded and the member is about to rupture. This is known as Shear Lag Effect -primarily because the stress in an element lags behind the stress in elements closer to the weld. Figure 1-1 shows the force variation due to shear lag along the cross-section of the member.

As the load on the member increases, the regions with higher stresses enter into their plastic state, which on further loading tends to cause a complete failure of the member before the gross-section of the member reaches its ultimate capacity. This effect is prominent in certain tensile members. It reduces the load carrying capacity of such structural elements.

### **1.3 Scope of Research**

Considerable research has been carried out on tension members connected by bolts. Wu and Kulak [1993] studied in detail, the Shear Lag Effect on bolted angles. Their research lead to the current Canadian design provisions for angles in tension. However, there is only a limited amount of data on the efficiency of welded tension members. The Steel Structures Education Foundation (SSEF) and the Canadian Institute of Steel Construction (CISC) initiated a project to study these effects. The present study is an effort aimed at expanding the experimental and theoretical basis for design of welded steel tension members.

The current North American design provisions applicable to Shear Lag in welded members are based on research by Munse and Chesson [1963] on bolted connections and other studies by the American Welding Society [1931] on welded members. Easterling and Gonzalez [1993] had reviewed most of the available data and after an experimental study for welded members, concluded that there is a need for further testing. In the present study, it is proposed to examine experimentally and analytically the use of current code provisions for weld connected members.

#### **1.4 Objectives**

The following are the objectives for the present study:

- Conduct experimental investigation on welded single and double angles and plate specimens.
- Conduct analytical (FEA) investigation for the specimens studied experimentally.
- The parameters for the experimental and analytical investigation should include:
  - the effect of material property variation on the behavior of the member,
  - load eccentricity,
  - length of member,
  - stiffness of gusset plate,
  - effect of longitudinal and or transverse welds, and
  - P- $\delta$  curve and the strain distribution within the cross-section of the member, etc.

- Examine the current design provisions for welded members in tension and suggest recommendations for design.

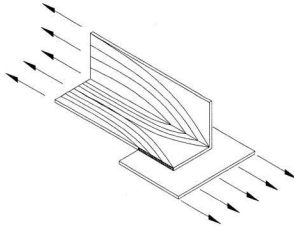


**Figure 1-1 Stress Variation due to “Shear Lag Effect” in Structural Steel Angle Section in Tension**

## **Chapter 2**

### **LITERATURE REVIEW**

The study of shear lag effect in structural steel members has been mainly concentrated on bolt-connected specimens. The influence of various parameters affecting shear lag on such bolt-connected members was examined in the past. Such studies on welded members were very limited. Geometric parameters such as length of connection, eccentricity, length of specimen, configuration of connection, etc., and material parameters such as ratio of yield stress to ultimate stress of material, breaking strain, etc., affecting shear lag were not studied in detail. The present chapter reviews available literature on both welded and bolted connection with respect to the shear lag phenomenon. Several of the parameters mentioned above were considered in the later chapters for experimental and finite element study on welded sections.

Changes in technology have evolved better and higher grade of steel for structural purposes. Hence, the effect of material properties on shear lag was given importance for the current study. The following review of previous literature is therefore presented in reverse chronological order to reflect the pattern of changes in net-section efficiency with the changes in the grade of steel.

## **2.1 Earlier Studies**

### **2.1.1 Shear Lag in Bolted Angle Tension Members [Kulak and Wu, 1997]**

Kulak and Wu [1997] (also, Wu and Kulak [1993]) studied the various parameters affecting shear lag on bolt-connected members. An experimental study was conducted on twenty-four single and double angle tension members. It was supplemented by numerical analysis.

The test specimens were of 300W Steel grade and were axially loaded with increasing magnitude until complete rupture of the specimen. These specimens failed by tearing at the critical cross-section as the ultimate load was reached. The reported failure occurred with necking followed by tearing from the edge of the connected leg through to the hole and then to the heel. It continued through to the outstanding leg of the angle. This confirms the fact that connected leg was stressed more compared to the outstanding leg.

Numerical analysis was conducted using ANSYS-finite element commercial software for predicting the ultimate capacity and the stress distributions at the critical cross-section. Actual material properties were reportedly used and large displacement analysis was performed. Displacement control was used throughout the loading history. The results of this study were used to update the Canadian standard CSA/S16.1-94 [CSA, 1994].

The following points of interest can be obtained from the study:

- Effect of different connection lengths: The specimen with the shortest connection indicated lowest ultimate loads, as expected. It was analytically observed that as the

length of connection was increased, the formation of compressive zone at the critical cross-section decreased.

- Effect of stiffness of the gusset plate: This study was conducted by varying the length of the gusset plate between the connected-end of angle section to the fixed boundary. Although, the test data was limited, it was judged that there is not a significant difference in efficiencies among the specimens.
- Effect of same cross-section with different dispositions: Long-leg connected versus short-leg connected configurations were studied. The ductility as well as the efficiency of connection was better in the case when the long-leg was connected.
- Effect of leg thickness: It was judged that angle leg thickness has little effect on the net section efficiency.
- Single angle or double angle specimens: The difference in the behavior of single and double angle specimens was mainly reflected in the amount of lateral deflection perpendicular to the gusset plate, and the strain distribution at the critical cross-section. However, the efficiencies were generally the same for both cases with the overall average efficiency of single angle members being 7% higher than that for double angle members.
- Strain profile at the critical cross-section: The strain was largest in the connected leg and smallest at the edge of the outstanding leg. For long connection length cases in single angle specimens, the edge of the outstanding leg was in compression under loads up to 90% of its ultimate capacity. For angles with short connection lengths, the

edge of the outstanding leg was in compression throughout the loading range. However, in most specimens at ultimate loads, the gross member had reached the tensile yield stress.

- Strain profile at mid-length section: At low loads, the strain distribution was non-uniform and the edge of the outstanding leg was in compression. At ultimate loads, the strain of the whole section was almost uniform as the centroid of the angle coincided with the applied load.
- Stress profile: This study (numerical analysis) indicated that at failure, the average stress at critical section of the connected leg approached the ultimate strength of the material. Also, the average stress in the outstanding leg was almost equal to its yield strength. This is especially so for specimens with longer connection lengths (four or more bolts per line of connection). The stress in the outstanding leg at failure was less than the yield stress in the case of specimens with shorter connection lengths. In view of this observation, the proposed expression for the net section efficiency was:

$$U_e = \frac{A_{cn} + \beta \frac{F_y}{F_u} A_o}{A_{net}} \quad \text{Eq. 2-1}$$

where,  $A_{cn}$  is the net area of the connected leg

$A_o$  is the net area of the outstanding leg

$A_{net}$  is the net total area

$F_y$  and  $F_u$  represent the yield and ultimate tensile strength of the material

$\beta$  is the factor accounting for reduction in area depending on number of bolts/row

### 2.1.2 Shear Lag Effects in Steel Tension Members [Easterling and Gonzalez, 1993]

Easterling and Gonzalez [1993] studied the effects of shear lag on welded members experimentally (also, Gonzalez and Easterling [1989]). Twenty-seven specimens consisting of plates, angles, and channels were tested with three different weld configurations (Longitudinal welds only, transverse welds only, and combination of longitudinal and transverse). These specimens (75mm and 100mm wide plate specimens, L2x2x3/16 and L4x3x1/4 angle specimens, and C3x4.1 and C4x5.4 channel specimens) consisted of double members welded back to back on either sides of the gusset plate. Hence, the eccentricity effects on shear lag were reduced by minimizing the distortion due to out-of-plane eccentricity. All specimens were loaded statically in tension up to failure.

Analytical study was conducted using linear elastic finite element methods and the stress patterns were compared in the elastic region.

The following can be concluded from the investigation:

- Shear lag controlled the strength of both plate and angle specimens.
- For plates connected by longitudinal welds, connection length has little influence on the shear lag coefficient. This is a somewhat surprising result. The experimental shear lag coefficient for plate specimens connected by use of longitudinal welds only ranged from 0.94 to 1.00. For the ratio of weldlength to width of specimen ( $L/w$ ) equal to 1.4, the average experimental shear lag coefficient for a 75mm width

specimen was 0.97. For  $L/w$  equal to 1.67 and same width of specimen, the average shear lag coefficient was again at 0.97.

- Transverse welds in angle members welded both longitudinally and transversely did not increase the shear lag coefficient as expected.
- Recommended upper limit for the shear lag coefficient is 0.9.
- The predominant limit state observed in channel tests was rupture in the cross-section away from the welded region. This indicated that the combined state of stress induced in the member due to out of plane eccentricity is more dominant compared to the shear lag effect on the member capacity.
- Effects on large size specimens were to be investigated. Additional tests were recommended to study the effects of various parameters in detail.

The experimental results on plate and angles sections conducted by Easterling and Gonzalez have been tabulated in Table 2-1, Table 2-2 and Table 2-3.

In addition, the American Bureau of Welding [1931] conducted experiments on welded specimens. Some data values of this study was reported and discussed briefly in the Easterling and Gonzalez study [1993]. The results are shown in Table 2-4 and Table 2-5.

Table 2-1 Properties and Experimental Results of Plates Specimens by Easterling and Gonzalez (1993)

Specimen ID	Width $w$ , mm	Thick $t$ , mm	Stress, MPa		Weld Length, mm			$A_p F_u$ kN	$T_u$ kN	Efficiency $U_e$
			$F_y$	$F_u$	$L_{pl}$	$L_{p2}$	$L_i$			
P-L1-1a	101.1	9.3	334	505	139.7	139.7	Nil	478	440.3*	-
P-L1-1b	76.7	6.6	358	503	108	108	Nil	255	239	0.94
P-L1-2	76.8	6.6	358	503	108	108	Nil	255	249	0.98
P-L1-3	76.8	6.6	358	503	108	108	Nil	255	256	1.00
P-L2-1	76.2	6.6	358	503	127	127	Nil	253	249	0.98
P-L2-2	76.2	6.6	358	503	127	127	Nil	253	248	0.98
P-L2-3	76.2	6.6	358	503	127	127	Nil	253	242	0.96
P-B-1	76.2	6.6	358	503	76.2	76.2	76.2	253	228	0.9
P-B-2	76.2	6.6	358	503	76.2	76.2	76.2	253	249	0.99
P-B-3	76.2	6.6	358	503	76.2	76.2	76.2	253	248	0.98

Table 2-2 Properties of Angle Specimens tested by Easterling and Gonzalez (1993)

Specimen ID	Angle Type	Leg, mm		Thick $t$ , mm	Stress, MPa		Weld Length and Size, mm					
		$w_c$	$w_o$		$F_y$	$F_u$	$L_1$	$S_1$	$L_2$	$S_2$	$L_r$	$S_r$
L-L-1	L50x50x5	50.5	51.1	5.1	373	559	114.3	4.8	114.3	9.5	Nil	Nil
L-L-2	L50x50x5	50.5	51.1	5.1	373	559	114.3	4.8	114.3	9.5	Nil	Nil
L-L-3	L50x50x5	50.8	51	5.1	373	559	114.3	4.8	114.3	9.5	Nil	Nil
L-B-1a	L100x75x6	75.6	100.9	6.4	330	492	88.9	6.4	88.9	6.4	101.6	6.4
L-B-1B	L50x50x5	50.5	51.1	5.1	373	559	76.2	4.8	76.2	11.1	50.8	4.8
L-B-1c	L50x50x5	50.5	51.1	5.1	373	559	76.2	4.8	76.2	11.1	50.8	4.8
L-B-2	L50x50x5	50.5	51.1	5.1	373	559	76.2	4.8	76.2	11.1	50.8	4.8
L-B-3	L50x50x5	50.5	51.1	5.1	373	559	76.2	4.8	76.2	11.1	50.8	4.8
L-T-1	L100x75x6	75.6	100.9	6.3	330	492	Nil	Nil	Nil	Nil	101.6	6.4

Table 2-3 Experimental Results of Angle Specimens by Easterling and Gonzalez (1993)

Specimen ID	Angle Type	Weld Length and Size, mm						$A_g F_u$ kN	$T_u$ kN	Efficiency $U_e$
		$L_1$	$S_i$	$L_2$	$\delta_2$	$L_r$	$S_r$			
L-L-1	L50x50x5	114.3	4.8	114.3	9.5	Nil	Nil	274	222	0.81
L-L-2	L50x50x5	114.3	4.8	114.3	9.5	Nil	Nil	274	225	0.82
L-L-3	L50x50x5	114.3	4.8	114.3	9.5	Nil	Nil	275	224	0.82
L-B-1a	L100x75x6	88.9	6.4	88.9	6.4	101.6	6.4	533	439	0.82
L-B-1b	L50x50x5	76.2	4.8	76.2	11.1	50.8	4.8	274	-	Weld failure
L-B-1c	L50x50x5	76.2	4.8	76.2	11.1	50.8	4.8	274	222	0.81
L-B-2	L50x50x5	76.2	4.8	76.2	11.1	50.8	4.8	274	206	0.75
L-B-3	L50x50x5	76.2	4.8	76.2	11.1	50.8	4.8	274	217	0.79
L-T-1	L100x75x6	Nil	Nil	Nil	Nil	101.6	6.4	529	-	Weld failure

Table 2-4 Experimental Test Data by American Welding Society (1931)

Specimen ID	Width $w$ , mm	Thick $t$ , mm	Stress, MPa		Weld Length, mm			$A_g F_u$ kN	$T_u$ kN	Efficiency $U_e$
			$F_y$	$F_u$	$L_{p1}$	$L_{p2}$	$L_t$			
2200a	190.5	19.05	250	393	304.8	304.8	Nil	1426	983	0.69
2200b	190.5	19.05	229	392	304.8	304.8	Nil	1423	1463	1.03
2400a	190.5	9.525	246	400	152.4	152.4	Nil	1451	1103	0.76
2400b	190.5	12.7	256	415	203.2	203.2	Nil	2008	1806	0.9
2400c	190.5	12.7	255	408	203.2	203.2	Nil	1974	1348	0.68
2400d	190.5	12.7	270	429	203.2	203.2	Nil	2074	1699	0.82
2400e	190.5	19.05	252	408	304.8	304.8	Nil	2962	1922	0.65
2400f	190.5	19.05	251	411	304.8	304.8	Nil	2982	2153	0.72
2400g	190.5	19.05	228	393	304.8	304.8	Nil	2852	2669	0.94
2500	101.6	19.05	245	416	101.6	101.6	101.6	805	758	0.94
2600a	190.5	12.7	255	409	101.6	101.6	190.5	989	662	0.67
2600b	190.5	19.05	252	408	203.2	203.2	190.5	1481	827	0.56
2600c	190.5	19.05	251	411	203.2	203.2	190.5	1491	889	0.6

Table 2-5 Experimental Test Data by American Welding Society (1931)

Specimen ID	Width w, mm	Thick t, mm	Stress, MPa		Weld Length, mm			$A_g F_u$ kN	$T_u$ kN	Efficiency $U_e$
			$F_y$	$F_u$	$L_{pi}$	$L_{p2}$	$L_t$			
2700a	101.6	12.7	254	428	50.8	50.8	101.6	1104	1057	0.96
2700b	101.6	19.05	245	416	101.6	101.6	101.6	1611	1557	0.97
2700c	101.6	19.05	245	416	101.6	101.6	101.6	1611	1535	0.95
2800a	190.5	9.5	246	400	50.8	50.8	190.5	1451	1254	0.86
2800b	190.5	9.5	246	400	50.8	50.8	190.5	1451	1063	0.73
2800c	190.5	9.5	259	401	50.8	50.8	190.5	1456	1237	0.85
2800d	190.5	9.5	259	401	50.8	50.8	190.5	1456	1223	0.84
2800e	190.5	12.7	270	429	101.6	101.6	190.5	2075	1855	0.89
2800f	190.5	15.8	252	425	152.4	152.4	190.5	2568	2224	0.87
2800g	190.5	15.8	257	393	152.4	152.4	190.5	2377	2113	0.89
2800h	190.5	15.8	230	393	152.4	152.4	190.5	2377	2220	0.93
2800i	190.5	15.8	230	393	152.4	152.4	190.5	2377	2313	0.97
2800j	190.5	19.05	251	411	203.2	203.2	190.5	2982	2695	0.9
2800k	190.5	19.05	251	411	203.2	203.2	190.5	2982	2624	0.88

### 2.1.3 Single Angles in Tension and Compression [Marsh, 1969]

Marsh [1969] derived mathematical expressions for calculating the ultimate capacity of angles loaded eccentrically in tension. The expression accounted for both bending and tension and was confirmed by tests conducted on nine aluminum specimens. A simplified expression to obtain the capacity of the angle was given as,

$$P_u = F_u A_{net} = F_u \frac{w_c^2 + w_o t}{w_c - 0.04L} t \quad \text{Eq. 2-2}$$

where,  $L$  is the distance from the point of loading to the inner most bolt, (assumed to be the length of the connection)

$P_u$  is the calculated ultimate capacity, N

$w_c$  is the width of connected leg, mm

$w_o$  is the width of outstanding leg, mm

$A_{net}$  is the net area of the specimen, mm<sup>2</sup>

### 2.1.4 Truss-Type Tensile Connections [Munse and Chesson, 1963a]

The current North American design provisions (CAN/CSA S16.1-94 and AISI LRFD-1993) are based in part on the study by Munse and Chesson [1963]. Tests were performed to obtain the general behaviour and ultimate strength of large truss type and bolted steel connections composed of plates and rolled shapes. The average properties of the angle specimens conformed to the requirements of the ASTM A7 specification.

Upon comparison of results and computed efficiencies, a simple relationship (Eq. 2-3) to predict the strength of sections in tension was presented. This empirical relationship was given for riveted and bolted connections.

$$U_e = \left( 1 - \frac{\bar{x}}{L} \right) \quad \text{Eq. 2-3}$$

where,  $\bar{x}$  is the distance from the centroid of the member to the face of the gusset plate.

The distance  $\bar{x}$  was selected as a measure of the eccentricity of the area. When angles or channels were used on both sides of the gusset, the value of  $\bar{x}$  was calculated based on single member section. For wide-flange or other members connected by both flanges, the eccentricity of the section  $\bar{x}$  was computed for tee-shape or shape formed by considering one half of the section only. Thus, expression Eq. 2-3 improved accuracy in predicting the net area of tension members in which all the area is not directly connected to the gusset.

The test results indicated that unequal distribution of stress in tension tests of double plane members at small loads had little effect on the ultimate loads, since the same at higher load levels had a nearly uniform distribution of stress. The usual gross area formula,  $\delta = PL/AE$ , was satisfactory for use in elongation computations for truss members.

An upper limit of 0.85 was recommended on gross area provided, the difference in the behaviour of drilled and punched members was separately accounted for. (At the time of the study, the current practice of adjusting the hole diameter depending on its mode of

preparation, i.e., drilled or punched was not adopted. Instead, allowable stresses were adjusted.)

### 2.1.5 Riveted and Bolted Joints: Net Section Design [Munse and Chesson, 1963b]

Based on a wide range of joint sizes, single and double angle configurations, specimen fabrication, an expression for net-section efficiency was assumed as a function of number of factors.

$$U_e = f(A_{net}, C, H, B, V, Z) \quad \text{Eq. 2-4}$$

where,  $C$  is the efficiency coefficient, which is based on the geometry of the connection,

$H$  is the fabrication factor that corresponds to whether holes for connections were punched or drilled. This aspect could be related to the effect of welding that involves high temperatures thereby inducing residual stresses,

$B$  is known as the bearing factor,

$V$  is known as the shear lag factor which has considerable effect on the efficiency of the member, and

$Z$  represents miscellaneous effects such as the ductility factor.

It was suggested that unless ductile materials were used in tension connections, some of the expected efficiencies may be lost. The relationship that was recommended to account for the ductility is

$$K = 0.82 + 0.032R \leq 1.0 \quad \text{Eq. 2-5}$$

where,  $R$  refers to the percentage reduction of area and  $K$  is known as the ductility factor

### **2.1.6 Welded Connections for Angle Tension Members [Gibson and Wake, 1942]**

Gibson and Wake [1941] studied experimentally, the necessity to adhere to theoretically balanced weld design for steel angles. For this study, fifty-four ultimate strength tests were conducted with 15 different types of weld configurations on angle  $L2\frac{1}{2} \times 2\frac{1}{2} \times \frac{5}{16}$ ". The angles used were structural steel (ASTM A7) with yield stress ranging from 267 to 275 MPa (38.8 to 39.9 ksi) and tensile strength from 444 to 485 MPa (64.4 to 70.4 ksi). Weld failure was the required criteria for each of these specimens and would not have been of use for the present study. However during the testing program, it was noticed that one third of the angle test specimens fractured through the angle section despite the fact that welds were designed to fail. This was due to the fact that, the effect of shear lag on the reduction of section capacity was not considered. The large deformation of single angle tests showed that the most important factor affecting the strength of single angle connections is their eccentricity normal to the plane of welds. Connections with lower eccentricity were found to give higher strengths. It may however be noted that only two such tests were conducted to confirm the above. The lateral deflection behavior of single angle specimens was independent of the weld configuration.

### **2.1.7 Tension Tests of Welded and Riveted Structural Members [Davis and Boomsliiter, 1934]**

Single angles, double angles on same side of the gusset plate, double angles with connecting plates in between them, double angles with two connecting plates, all with welded or riveted joints were tested in tension by Davis and Boomsliiter [1934]. Angle

3 x 3 x  $\frac{5}{16}$  was used for this study. The values of yield strength and ultimate tensile strength were 206.4 MPa (30 ksi), and 394.4 MPa (57.2 ksi) respectively. Specimen W-3 composed of two angles welded back to back on opposite sides of gusset plate, and Specimen W-4 with two angles welded to two gusset plates (Table 2-6) with configurations having minimum eccentricity experienced failure through the angle. Unlike specimens W-3 and W-4, single angle specimens W-1 and W-1A and double angle specimens W-2 and W-2A welded on to the same side of the gusset plate having larger connection eccentricity experienced weld failures. Such specimens with eccentric loading exhibited considerable deformations with bending occurring in the plane of the eccentricity.

**Table 2-6 Tension Tests by Davis and Boomsliiter [1934]**

Member	Test Load, kN	Efficiency Based on Ultimate Strength, %	Efficiency based on Elastic Limit, %	Failure Type
W-1	322	71	47	Weld Failure
W-1A	300	66	56	Weld Failure
W-2	451.1	50		Weld Failure
W-2A	654	72	56	Weld Failure
W-3	783	87	86	Section Failure
W-4	782.5	87	75	Section Failure

## 2.2 Current Design Provisions for Tension Members

Current specifications for design of members subjected to tensile loading account for the reduction of net-section efficiency caused by shear lag using various approaches. The main North-American design specifications are summarized below:

### 2.2.1 CAN/CSA-S16.1-94 [CSA, 1994]

Design of tension members with welded connections in accordance with CAN/CSA S16.1-94 specification requires the effective area to be calculated by considering the given section as a number of independent plates connected together. The reduced effective area of the cross-section,  $A_{net}$  is represented by the sum of the effective net areas of the various connected plate elements.

$$A_{net} = A_{ne1} + A_{ne2} + A_{ne3} \quad \text{Eq. 2-6}$$

where,  $A_{ne1}$ ,  $A_{ne2}$  and  $A_{ne3}$  are net areas for different situations as described below.

1. For elements connected by transverse welds,

$$A_{ne1} = wt$$

2. Elements connected by longitudinal welds along two parallel edges,

$$A_{ne2} = 1.00wt \quad \text{for } L \geq 2w$$

$$A_{ne2} = 0.87wt \quad \text{for } 2w > L \geq 1.5w$$

$$A_{ne2} = 0.75wt \quad \text{for } 1.5w > L \geq w$$

where,  $w$  and  $t$  are the width and thickness of the specimen, respectively.

3. For elements connected by a single line of weld,

$$A_{ne3} = \left(1 - \frac{x}{L}\right)$$

where,  $L$  is the length of weld

$\bar{x}$  is the eccentricity of the weld with respect to the centroid of the outstanding element

### **2.2.2 Load and Resistance Factor Design [AISC-LRFD, 1993]**

Design of plate type members in accordance with LRFD is very similar to the method described in CAN/CSA S16.1-94 with minor variations as outlined here. Explicit mention has been made for plates connected only by transverse welds wherein the shear lag reduction coefficient is considered equal to unity. For other structural sections connected by longitudinal welds only, and sections connected by both longitudinal and transverse welds, the recommendations of Chesson and Munse [1963] were considered. LRFD uses Eq. 2-3 with an upper limit of 0.9 for determining the reduction coefficient of the specimen. It may also be noted that the same equation (Eq. 2-3) without any upper limits is allowed (commentary of [CISC 2000]) for calculating the shear lag reduction coefficients for structural sections in the CAN/CSA S16.1-94 specifications.

### **2.2.3 Design of Latticed Transmission Tower Structures, ASCE/ANSI 10-90 [ASCE, 1990]**

Design specifications for tension members as per ASCE/ANSI 10-90, Design of Latticed Steel Transmission Structures is for bolt connected members. For plates under tension, the allowable stress is yield stress of the material. The capacity of the member is calculated based on the assumption that its cross-sectional area is uniformly stressed.

$$T = A_g F_y \quad \text{Eq. 2-7}$$

For angle members connected by one leg, the allowable stress,  $F_t$ , is taken as 90% of the yield stress.

$$F_t = 0.9F_y \quad \text{Eq. 2-8}$$

For unequal angle sections, if only the short leg of the angle is connected, the outstanding unconnected long leg is considered to be of the same size as the connected short leg in calculating the net-section area. Based on this, the ultimate capacity of the member can be expressed by the following expression, where the max value of the ratio  $A_o/A_{cn} = 1.0$ .

$$\text{Ultimate Capacity } T_r = F_t \left( 1 + \frac{A_o}{A_{cn}} \right) A_{cn} \quad \text{Eq. 2-9}$$

#### 2.2.4 New Provisions for Shear Lag in Steel Tension Members [Albert, 1996]

Albert [1996] investigated the influence of Grade 300W Steel and Grade 350W Steel on the behavior of angles with different weld configurations using the relationships given in the CAN/CSA-S16.1-94. The effect of thickness of the angle affecting the shear lag was neglected. This study concluded that shear lag is likely to be more significant in angles with its long leg as outstanding section and in angles with longitudinal weld along its heel shorter than that along its toe. According to the current design rules, tension members with 350W grade were more influenced by shear lag than those with 300W.

### 2.3 Theoretical Analysis

Some of the studies mentioned above carried out theoretical studies in addition to experimental investigations, e.g., Kulak and Wu [1997], and Gonzalez and

Easterling [1989]. These studies are meant for simply verifying experimental results using theoretical finite element models. They were not used to derive substantial conclusions. Stand alone theoretical studies considering material and geometric non-linearity's have not been carried out for shear lag phenomenon in tension members. However, Hildebrand [1943] studied elastic behaviour of shear lag problems.

### **2.3.1 Exact solution of Shear-Lag problems [Hildebrand, 1943]**

Hildebrand [1943] developed mathematical procedures for obtaining the "exact solutions" of Shear-Lag problems. Only elastic behaviour was included. The study was based on the assumption that the amount of stretching of the plates in the direction perpendicular to the direction of essential normal stresses is negligible. Orthotropic material with Modulus of Elasticity in the direction perpendicular to the essential normal stress taken as infinity, and the Poisson's ratio in the direction of the essential normal stress is taken equal to zero. Solutions for various cases have been given. The case wherein concentrated forces are introduced into flat sheets by means of stiffeners, with forces acting in the plane of the sheet was also taken into consideration. This example has been described in detail in Chapter 3.

## **2.4 Summary of Previous Studies**

A review of past research indicates that several factors affect the shear lag phenomenon. These in turn influence the tensile load carrying capacity of the member. The current understanding is that the behaviour of welded members in tension is similar to that of

bolted members in tension. Some of the points in this regard as noticed from previous works are summarized below:

- It is assumed in the current design practice that the connection efficiency increases with the length of connection. However, it was reported by Easterling and Gonzalez [1993] that the connection length has little influence on the experimental shear lag coefficient.
- The stiffness of the gusset plate had no significant effect on the efficiency of the specimen. Wu and Kulak [1993] tested two such specimens. More data would be desirable.
- Specimen configuration has an important effect with long leg as connected leg having better efficiencies compared to short leg as connected leg. This understanding was based on the study of bolted connections by Kulak and Wu [1997]. In their study, single L102x76x6.4 had efficiencies of 0.92 and 0.84, respectively, while double L102x76x6.4 had average efficiencies of 0.87 and 0.82, respectively. Current understanding that this behavior is acceptable for welded members needs some experimental validation.
- Thickness of specimen is assumed to have negligible effect on the net section efficiency. Tests by the AWS [1931] showed that 100mm wide specimens (No. 2700a and 2700b) with thicknesses of 12.7mm and 19.05mm had efficiencies of 0.96 and 0.97, respectively. Similarly 190.5mm wide specimens (No. 2800e and 2800f) with

thicknesses of 12.7mm, 15.8mm and 19.05mm had efficiencies of 0.89, 0.87 and 0.90, respectively.

- Load eccentricity had little effect on the tension capacity of bolted members. Efficiencies were generally the same for both single and double angle members tests by Wu and Kulak [1993] with the overall efficiency of single angle members being 7% higher than double angle members. Unlike the results reported by Wu and Kulak [1997], the test results by Gibson and Wake [1941] seem to suggest that the double angle members had better efficiencies compared to their counterpart single angle members. However, the data from Gibson and Wake is not very clear to make a firm conclusion on this aspect. It is noticed that large eccentricity causes considerable bending and twisting of the member. Considerable strain variation was also noticed in the cross-section. The lateral deflection behavior of single angle specimens was independent of the weld configuration.
- Test results showed that failure of specimens occurred only after gross yielding of the section over its free-length. This was true in the case of both bolt and weld connected members irrespective of the grade of steel used. Hence, the net-section equation of various standards rarely governs the design of the member.
- Eq. 2-1 given by Kulak and Wu [1997] for bolted members, indicates that the efficiency of the member is a function of the grade of the material. Parametric study on the current design provisions by Albert [1996] concludes that according to CSA-S16.1-94, tension members with a 350W steel grade are more influenced by shear lag than those with 300W. This needs to be verified for welded members, especially for

higher grade steels. Hence, there is a need to study the effect of material properties on shear lag.

- Comparison of current North American Design Standards indicates some differences among these specifications in the design of tension members. Some of these differences are listed below.
  - AISC-LRFD [1993] uses Eq. 2-3 for the entire cross-section of angles. This is used only for the outstanding leg of angles in CSA-S16.1-94. However, CSA-S16.1-94 does allow the use of the same for angle specimens.
  - AISC LRFD specification [1993] allows a reduction coefficient of unity to be considered, when load is transferred through the use of only transverse welds. However, CSA-S16.1-94 uses a coefficient equal to unity when elements are connected by transverse welds. Shear lag effect of connections with longitudinal welds in combination with transverse welds have not been stated explicitly. It seems to infer that for such connections too, the shear lag effect is negligible and therefore the reduction coefficient is equal to unity. Unlike the CSA-S16.1-94 specification, LRFD specification recommends an upper limit of 0.9 as reduction coefficient for such connections.
  - No consideration has been given for the effect of length of connection in the ASCE/ANSI 10-90.
  - Net section for the determination of ultimate capacity in ASCE/ANSI 10-90 is based on the yield stress and the ratio of the areas of the outstanding leg to the connected leg.

The above discussion briefly reviewed the previous experimental and theoretical studies and the current North American codes. It can be seen that there is a need for further study

of welded steel tension members with reference to the effect of shear lag on its tensile capacity.

Initial review of available experimental data indicates the importance of material properties on shear lag effect. Hence, attempts were made to study this effect on different grades of steel. Review of previous literature has therefore been presented in reverse chronological order, due to importance given for the type and grade of material tested. Current design specifications indicate that length of connection has a major affect on the net-section capacity. Hence, this parameter was studied in detail both experimentally and analytically.

## **Chapter 3**

### **Theoretical analysis of Shear Lag in Tension**

The shear lag phenomenon in welded tension members was studied theoretically and experimentally. The present chapter outlines the main approaches used for the theoretical examination of the problem. Two separate techniques were followed, viz., classical and numerical. The classical solutions were elastic while the numerical work was both linear and nonlinear.

#### **3.1 Classical Solutions**

The effect of 'shear lag' due to welded connections in plate elements is similar to the behaviour of plates loaded discontinuously with line loads parallel to their edges (Figure 3-1). Elastic solutions using classical techniques to problems of this type are examined in this section. The real problem of shear lag under consideration is not elastic. However, elastic solutions can still prove to be of good use. They can be used for the validation of the finite element models to be used. They are also useful in the sense that they can suggest the form of the design equation that can be used with nonlinear material properties. They could also suggest the inter-relationships between different physical parameters.

Mathematical solutions for certain standard problems subjected to 'shear lag' were developed by Hildebrand [1943]. He derived "exact" solution to plates with concentrated loads acting at the edge of a sheet or a panel with or without flange plates. The problem

with restricted load transfer regions (Figure 3-1) caused by welded connections was not examined by Hildebrand [1943]. The closest problem to the present one that Hildebrand examined is shown in Figure 3-2. The plate is infinitely long and has a width of  $w$  and thickness  $t$ . It is loaded at the end  $x' = 0$  by axial forces  $P/2$  acting on stiffeners of equal cross-sectional area  $A$  attached to edges along  $y' = \pm w/2$ . The stiffeners participate in transferring part of the force to the support at the other end of the plate.

Hildebrand used a function  $H$  to satisfy the equilibrium condition. This stress function unlike the Airy's stress function was chosen such that the axial normal stress  $\sigma_x = \partial H / \partial y$  and shear stress  $\tau = -\partial H / \partial x$ . The stress function for this example is,

$$H = \frac{P}{t} \left[ \frac{1}{\alpha + 1} \frac{2y'}{w} + 2 \sum_{n=1}^{\infty} \frac{\cos \lambda_n \sin \left( \lambda_n \frac{2y'}{w} \right)}{\lambda_n (1 + \alpha \cos^2 \lambda_n)} e^{-\sqrt{\frac{\sigma}{E}} \lambda_n \frac{2x'}{w}} \right] \quad \text{Eq. 3-1}$$

where,  $\alpha$  represents the ratio of flange and sheet areas and is given by

$$\alpha = \frac{2A}{tw} \quad \text{Eq. 3-2}$$

and the parameters  $\lambda_n$  are the positive solutions of the equation

$$\tan \lambda_n + \alpha \lambda_n = 0 \quad \text{Eq. 3-3}$$

Some values of  $\lambda_n$  are listed in Table 3-1.

Table 3-1 Values of  $\lambda_n$  for different ratios  $\alpha$

	$\alpha = 1$	$\alpha = 5$	$\alpha = 0.77101$
N	$\lambda_n$	$\lambda_n$	$\lambda_n$
1	2.0288	1.6887	2.1199
2	4.9132	4.7544	4.9678
3	7.9787	7.8794	8.0144
4	11.0855	11.0137	11.1118
5	14.2074	14.1513	14.2281
6	17.3364	17.2903	17.3534
7	20.4692	20.4301	20.4836
8	23.6043	23.5704	23.6168
9	26.7409	26.711	26.7520
10	29.8786	29.8518	29.8885
11	33.017	32.9928	33.0260
12	36.156	36.1339	36.1642
13	39.2954	39.275	39.3029
14	42.4351	42.4162	42.4421
15	45.575	45.5575	45.5815

The longitudinal and shear stresses are given by,

$$\sigma_x = \frac{\partial H}{\partial y'} = \frac{2P}{tw} \left\{ \frac{1}{\alpha+1} + 2 \sum_{n=1}^{\infty} \frac{\cos \lambda_n \cos \left( \lambda_n \frac{2y'}{w} \right)}{(1 + \alpha \cos^2 \lambda_n)} e^{-\sqrt{\frac{G}{E}} \lambda_n \frac{2z'}{w}} \right\} \quad \text{Eq. 3-4}$$

$$\tau_{x'y'} = -\frac{\partial H}{\partial x'} = 2\sqrt{\frac{G}{E}} \frac{2P}{tw} \left\{ \sum_{n=1}^{\infty} \frac{\cos \lambda_n \sin \left( \lambda_n \frac{2y'}{w} \right)}{1 + \alpha \cos^2 \lambda_n} e^{-\sqrt{\frac{G}{E}} \lambda_n \frac{2x'}{w}} \right\} \quad \text{Eq. 3-5}$$

If the plate is finite in length ( $L_p$ ), the solution can be obtained by replacing the term

$e^{-\sqrt{\frac{G}{E}} \lambda_n \frac{2x'}{w}}$  by  $\cosh \left( 2\lambda_n \frac{L_p - x'}{w} \sqrt{\frac{G}{E}} \right) / \cosh \left( 2\lambda_n \frac{L_p}{w} \sqrt{\frac{G}{E}} \right)$  in the expression for the stress

function.

### 3.2 Elastic Numerical Solution

The elastic behaviour of the shear lag problem as analyzed by Hildebrand [1943] was examined using a numerical model. Finite element analysis of elastic problems is well established. Numerous software packages with powerful options are available commercially. For the present purposes, Finite Element software ANSYS [1997] and ABAQUS [1999] were both used.

The example problem (Figure 3-2) consisted of a plate with a width of 120mm, thickness of 12.97mm and length of 1000mm. The Young's modulus  $E$  was 210000 MPa and the modulus of rigidity  $G$  was 77000 MPa. A force of 100kN was applied onto a flange plate of thickness 20mm and depth 30mm located at the edge of the specimen. The analysis was conducted using both thin shell and thick shell elements. The plate model had a mesh grid of 20x300 4-node quadrilateral elements. The results of both ABAQUS and ANSYS software differed negligibly from each other. The use of thick vs. thin shell elements also did not show any appreciable difference. The stress variation across the width at various lengths was collected and compared with the variation obtained by

Hildebrand's expression (Eq. 3-4 and Eq. 3-5) after changing it to account for the finite length of plate. In Hildebrand's derivation, it was assumed that the plate does not stretch in the lateral direction (along the width). This has been simulated by manipulating the Poisson's ratio as well as by explicitly applying restraints. Some of the results are plotted in Figure 3-3. When the plate was analyzed numerically without Hildebrand's assumption, the stress pattern showed that his prediction was slightly different from that of FEA near the origin. Away from the origin, the two were very close to each other. Thus, the numerical models that will be used for the analysis of shear lag problem were justified in view of their good comparison with classical solutions.

Results of both FE model and Hildebrand's expression showed that significant variation of stress profile ceased to occur beyond a length of 1.3 times the width of the specimen. Beyond a length of 2.5 times the width (as shown in Figure 3-4 and Figure 3-5), the stress profile is completely uniform. As seen in Figure 3-4 and Figure 3-5 the stress variation for a plate with and without stiffeners is quite similar. If the flanges can be assumed to represent the effect of size of welds, then, this result may conclude that the effect of size of weld on the variation of stress and 'shear lag' is negligible.

### **3.3 Elastic Solution for Welded Plates**

The example used the previous section was a stiffened panel wherein the load was applied to the flange plate located at the edge of the specimen. In the case of plates welded to gussets at the end, stiffening effect due to absence of the flange plates is not present along the full length of the plates. For the case without stiffeners,  $\alpha = 0$ . For such

unstiffened panels,  $\lambda_n = n\pi$  (Eq. 3-3) and the series solution presented in Section 3.1 becomes a Fourier series. The stress function can be summed in closed form giving,

$$H = \frac{2F}{\pi} \tan^{-1} \left( \tanh \frac{\xi}{2} \tan \frac{\eta}{2} \right) \quad \text{Eq. 3-6}$$

The stresses can be obtained by simple differentiation as,

$$\sigma_{x'} = \frac{2F}{tw} \frac{\sinh \xi}{\cosh \xi + \cos \eta} \quad \text{Eq. 3-7}$$

$$\tau_{x'y'} = -\frac{2F}{tw} \sqrt{\frac{G}{E}} \frac{\sin \eta}{\cosh \xi + \cos \eta} \quad \text{Eq. 3-8}$$

$$\text{where, } \xi = \sqrt{\frac{G}{E}} \frac{2\pi x'}{w}, \quad \eta = \frac{2\pi y'}{w}$$

The results presented above are applicable for single concentrated loads applied at each corner of the plate along the end  $x=0$ . However, in case of welded plate, the load is actually distributed along a weld of length  $l$ . For such cases, the load can be assumed to have been made of a series of elemental concentrated loads being transferred over an elemental length of  $dx_1$ . Typical elemental load of  $F=(P/2l)dx_1$  is shown in Figure 3-1.

The total stress at any point  $(x,y)$  is found as the sum of the contributions of all such elemental loads. Let  $x'$  be the distance of the point of interest from that of the elemental load. The elemental load itself is at a distance of  $x_1$  from the origin. Noting that  $x'=x-x_1$ , and using Eq. 3-7 and Eq. 3-8,

Eq. 3-9

$$\sigma_x = \int_0^l \frac{P}{tw} \frac{\sinh \xi}{\cosh \xi + \cos \eta} dx_1, \quad \xi = \sqrt{\frac{G}{E}} \frac{2\pi(x-x_1)}{w}, \quad \eta = \frac{2\pi y}{w}$$

Integrating,

$$\sigma_x = a \ln \frac{\cosh \xi_0 + \cos \eta}{\cosh \xi_l + \cos \eta}, \quad \text{Eq. 3-10}$$

$$a = \frac{P}{tw} \frac{1}{\pi} \frac{2l}{w} \sqrt{\frac{G}{E}}, \quad \xi_0 = 2\pi \frac{x}{w} \sqrt{\frac{G}{E}}, \quad \xi_l = 2\pi \frac{(x-l)}{w} \sqrt{\frac{G}{E}}$$

Similarly, the total shear stress can be found by integrating as,

$$\tau_{xy} = \frac{P}{2ml} \left[ \tan^{-1} \frac{v_l}{\sin \eta} - \tan^{-1} \frac{v_0}{\sin \eta} \right], \quad v_0 = e^{\xi_0} + \cos \eta, \quad v_l = e^{\xi_l} + \cos \eta \quad \text{Eq. 3-11}$$

In the derivation of stresses above, the plate stretching in the direction of the width is assumed to be negligible. This assumption might be justified since the actual plate under consideration is welded to a gusset plate, which in turn is connected to the joint. In the weld region, this additional gusset plate material and the restraint offered by the joint, would render the displacements in the lateral (width) direction small compared to those in the longitudinal direction.

Eq. 3-10 and Eq. 3-11 can be used as a guide to the interrelationships between various parameters that effect shear lag stresses. A plot of the normalized stresses predicted by Eq. 3-10 and Eq. 3-11 is shown in Figure 3-6 and Figure 3-7. The figures also show the results of FEA for the example problem of Section 3.2 where the stiffeners are only of

length  $l$ . These stiffeners are used for load transfer only. They are not restrained and hence simulate the effect of the welds.

It can be seen that the stresses predicted by FEA are 'flatter' (or less severe) than those by Eq. 3-10. Thus Eq. 3-10 is conservative. It can therefore be used to study the inter-relationships between parameters, if so desired.

### **3.4 Nonlinear Analysis Using Finite Elements**

The effect of 'shear lag' on welded steel sections in tension was studied using non-linear finite element analysis. The purpose of the finite element model was to re-create mathematically the behavior of angle and plate specimens in tension for a parametric study of the 'shear lag' Effect.

The objectives of the nonlinear finite element analysis were:

- To study the effect of material properties such as
  - Ratio of yield and ultimate stress (Grade of Steel),
  - Ductility of steel (Breaking strain),
  - Strain at the onset of strain hardening.
- To study the effect of geometric properties of member such as,
  - Length of member,
  - Thickness of member,

- Size of member,
  - Length of connection,
  - Eccentricity of load,
  - Orientation of member (Short leg and Long leg connected),
  - Single and double specimen,
  - Stiffness of gusset plate, etc.
- To obtain the load vs. deflection behaviour, and
  - To study the strain variation in the cross-section at various load levels

### **3.5 Finite Element Model**

The nonlinear analysis of structural problems is well established. Commercial Finite Element software Package ANSYS [1997] was used for the purpose of analyzing the shear lag problem. The actual theory behind the analysis is not being explained here since it can be found in standard references and software manuals.

Finite element models comprising of quadrilateral elements were used for the nonlinear analysis. Linear elements were used instead of quadratic or higher order elements, since the models were regular shaped with few or no curved regions. These linear elements also obtained good accuracy at lower CPU times.

Both plate and angle members were considered in this study. They were modeled using element Shell181 of ANSYS. This element was suited for thin to moderately thick shells. As a linear four-noded element with six degrees of freedom at each node, it can accommodate large rotation, large strain non-linear plastic analysis with a multi-linear curve representing elastic, plastic and strain hardening zones. Changes in the shell thickness were accounted for in the non-linear analysis. The element formulation was based on logarithmic strain and true stress measures. Hence, stress-strain relationships obtained from tension coupon tests were converted to true stress vs. logarithmic strain and idealized into multi-linear curves. A sample curve shown in Figure 3-8 was used to define the material properties. These material properties were defined such that the stress would drop rapidly beyond the rupture strain.

The finite element model was created by controlled generation. Length of specimen was modeled along the x-axis, and its width along the y-axis. Thickness of the connected plate, eccentricity of load and the width of outstanding length was along the z-axis. This model comprised mainly of rectangular shaped elements with varying aspect ratios. Symmetric conditions due to geometry and loading were used in minimizing the number of elements in the model. Most plate specimens were symmetric about their longitudinal axis and also along their width. Only a quarter portion of such specimens (Figure 3-9) with symmetric boundary conditions were used in the analysis. Angle members were modeled considering two plates each perpendicular to one another (Figure 3-10). Single angle specimens being symmetric only about their longitudinal axis required modeling of one half of the length. Double angle specimens were analyzed using quarter models and appropriate boundary conditions.

Gusset plate and welds were also modeled using the same (Shell 181) element. Gusset plate with elastic perfectly plastic material property was considered to compare the finite element analysis with the experimental study. However, for parametric study, elastic material properties were considered, since there was no significant effect of the gusset plate material properties on the ultimate capacity of the specimen. Weld elements connecting the test plate and the gusset plate were specified with high stiffness and elastic material properties. Rectangular and trapezoidal shaped elements with various sizes were considered. The mesh density was higher near the welds and decreased at sections away from the welded region. Mesh density of gusset was lower compared to that of the test specimen.

The boundary conditions simulating the actual test conditions were used in the analysis. Nodes at the gusset end of the model had all degrees of freedom restrained except for the axial translation of the specimen. At mid-length cross-section of the member, longitudinal axis symmetric boundary condition, i.e., x-direction translation degree of freedom and y and z rotational degree of freedom were restrained. Similarly, y-axis symmetry for single plate specimens and z-axis symmetry for outstanding plate specimens and double angle specimens were used.

Consideration of actual material properties and large deformation effects required the use of nonlinear analysis. This was achieved through step by step incremental approach. Standard automatic time stepping procedure was adopted for this. The incremental analysis used full Newton-Raphson algorithm (due to large deformation analysis) with

tangent stiffness being formulated at every equilibrium iteration. Displacement control method was used throughout the entire loading history.

Mesh Convergence test (Figure 3-11) was performed to obtain the necessary mesh density. Based on these results, general input data files (Appendix B and C) for finite element modeling of various problems was created. Actual test specimens with appropriate material properties, and boundary conditions were incorporated and analyzed. Comparisons of these finite element results with the test results have been shown in Chapter 5. To study the reason for termination of each finite element analysis, the force variation at the net section cross-section and the mid-section cross-section were examined. The effect of 'shear lag' was quite noticeable at the net section cross-section while at the mid-section cross-section, the stress variation was quite uniform. Cross-sectional area near the mid-section of the specimen was increased over 50% of its free length. This study was to investigate, if the failure or termination of analysis was due to yielding of the gross-section under the combined action of bending and tensile force. Results of this analysis exhibited the same ultimate load as that of the corresponding actual specimen of uniform cross-section. However, the ultimate load was obtained at a lower axial displacement, which is justified by the smaller length of angle being subjected to yielding. The effect of inclined loading on the test specimens was also studied. Examination of results between direct axial loading and inclined loading indicated no significant change on the ultimate capacity of the test specimen.

Thus, on validation of the finite element model, a parametric study was conducted on both the material and the geometric properties. The trends and behaviour of both plate and angle specimens have been presented in Chapter 5.

The combined effects of transverse and longitudinal welds were examined by studying the stiffness of both welds independently. Weld assumed to be a right angle isosceles triangular shaped prism was modeled using brick element (ANSYS element-SOLID45). Elastic analysis on various sizes and mesh densities (Appendix C) assuming material properties of steel for the weld material was performed. The results of this analysis have been discussed in detail in Chapter 5.

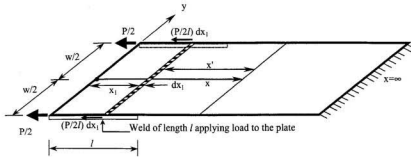


**Figure 3-1 Plate with Symmetrical Welds of Length  $l$  transmitting Tensile Force**

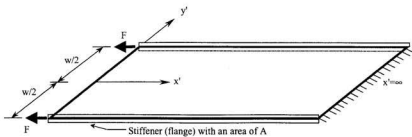


**Figure 3-2 Plate with Symmetrical Concentrated Axial Loads at Corners**

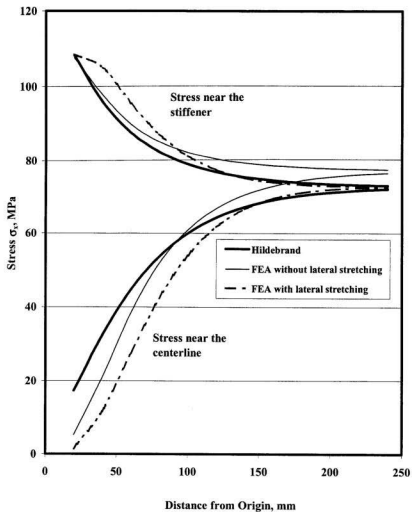


Figure 3-3 Stress Variation along the Length of Stiffened Plate

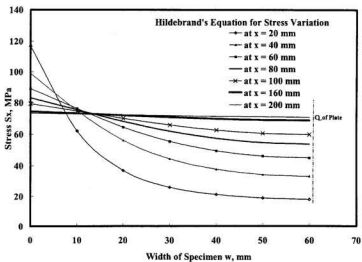


Figure 3-4 Elastic Stress Variation for Plate with Stiffeners

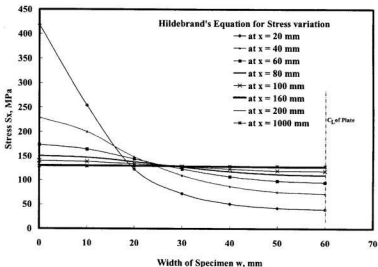


Figure 3-5 Elastic Stress Variation for Plate without Stiffeners

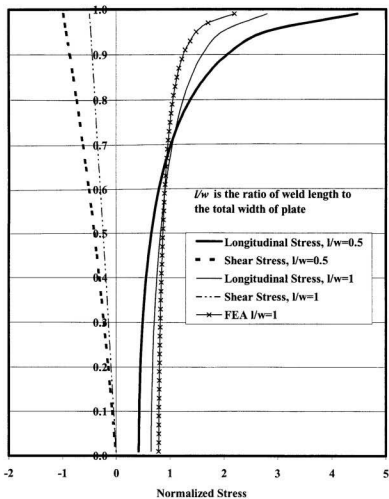


Figure 3-6 Variation of Stress across the Plate Width at the Critical Section

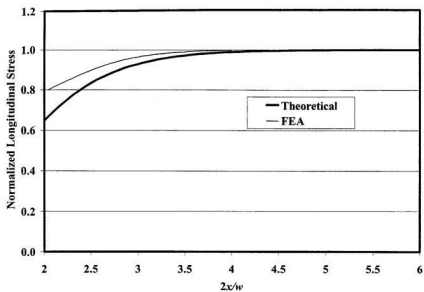


Figure 3-7 Variation of Longitudinal Stress along Center-line of the Plate ( $l/w = 1$ )

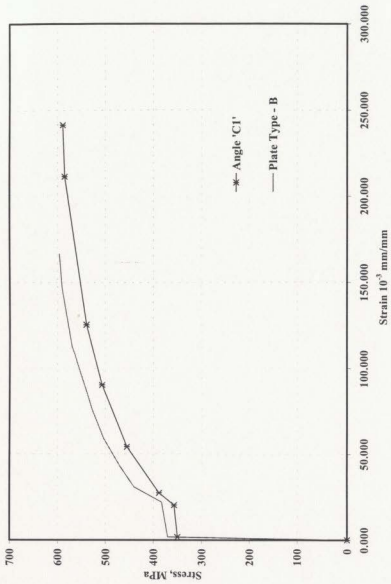


Figure 3-8 Typical Curve for True Stress Vs. Log Strain for Test Specimens

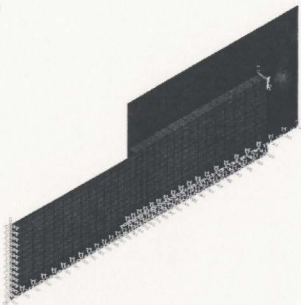


Figure 3-9 Finite Element Model of Plate Specimens (Typical)

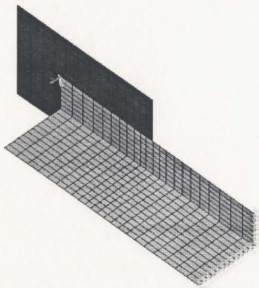


Figure 3-10 Finite Element Model of Single Angle Specimen (Typical)

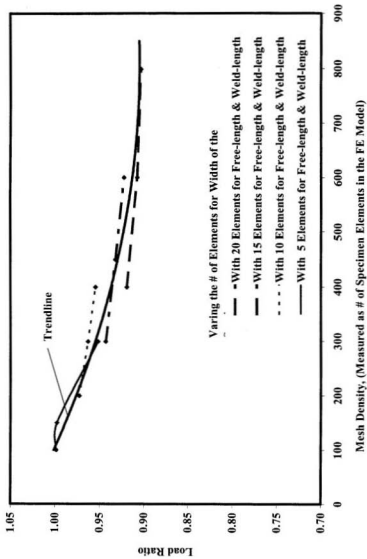


Figure 3-11 Convergence Test for FEA Model

## Chapter 4

### Experimental Investigation

An experimental program was carried out to study the ultimate capacity of structural steel angle and plate members in tension. The experimental program was designed to understand the Shear Lag effect. There was a limited amount of experimental data available from previous studies. Based on the recommendations of Easterling and Gonzalez [1993] and Kulak and Wu [1997], the following parameters were considered in the experimental study:

1. Size of member,
2. Length of connection,
3. Effect of eccentricity,
4. Length of member,
5. Size and configuration of the test specimen (short leg or long leg connected, single specimen or double specimen), and
6. The effect of grade of steel.

A total of twenty-seven plate specimens and twenty-two angle specimens were tested. As far as possible, the welds were provided with 25%-50% more capacity than the design capacity of specimens calculated as per the current code.

#### 4.1 Physical Properties

Plate specimens were obtained from two stocks of plate. Plate type 'A' had a non-Canadian origin and had a yield strength of 210 MPa and tensile strength of 432 MPa (roughly conformed to CAN/CSA-S39 Grade Steel [1935]). Plate type 'B' conformed to the requirements of CAN/CSA-G40.21-M and was of grade 350W. Gusset plates were obtained from plate stocks 'C', 'D' and 'E'. The thickness of these plates are reported in Table 4-1. The thickness is the average of at least 10 measurements at different locations across the original stock.

**Table 4-1 Physical Properties of Plates**

Plate Name	Steel Grade	Thickness t, mm	Category
A	S39	12.82	Test Specimen
B	350W	12.97	Test Specimen
C	350W	19.18	Gusset Plate
D	N/A	26	Gusset Plate
E	N/A	30	Gusset Plate

Angle specimens were fabricated from six individual angle sections which conformed to the requirements of CAN/CSA-G40.21~300W Steel. Several angles were tested and those that had a yield strength higher than 350 MPa were chosen in order to study the effect on higher grade such as 350W angles. The cross-section of each of the angles was measured at three locations along the length and the average values have been tabulated in Table 4-2.

**Table 4-2 Physical Properties of Angles**

Angle Name	Angle Type	Leg 1, mm	Leg 2, mm	Thickness t, mm	Gross Area, mm <sup>2</sup>
A1	L152x152x9.5	151.6	151.4	9.74	2857
B1	L152x102x7.9	152.4	102.1	8.18	2016
C1	L127x76x6.4	125	75	6.62	1280
D1	L127x76x6.4	126.1	75.7	6.58	1285
E1	L102x102x6.4	101.4	101.6	6.81	1336
F1	L102x102x6.4	101.7	101.4	6.78	1330

## 4.2 Material Properties

The material properties of both plates and angles were obtained from standard tensile coupon tests. Three coupons from each plate type 'A', 'B', 'C' and two from each angle type were made. Coupons were made in accordance to the SHEET-TYPE specimen details as per ASTM~E8-96 Standard Test Methods for tension testing of Metallic Materials [Metric]. The width of these coupons was 12.5 mm.

An extensometer of gauge length 51.3 mm was used to measure the strain in the coupon. In most specimens, the overall elongation of the coupon was also measured using two Linear Variable Differential Transformers (LVDTs). A data acquisition unit was used to collect the load, strain and the overall elongation simultaneously. In some cases, 'Electrical Resistance Strain Gauges' were also used in addition to the extensometer. The elongation over the gauge length was measured after rupture.

Tensile loading was applied using a Tinius-Olsen universal testing machine (UTM). Standard friction grips were used to grip the coupons. Rate of loading upto yield point was maintained at 2-5MPa/sec and beyond yield point at strain rate of 0.1- 0.3m/m/min.

In some tests, necking occurred outside the gauge length. In such cases, the breaking strain value was obtained only from its co-coupon made from the same specimen. The results of these tests have been tabulated in Table 4-3 and Table 4-4. For some test specimens, the true stress versus logarithmic strain is shown Figure 4-1 The overall elongation used as a measure of ductility was calculated based on the elongation of a 125mm long stem length of the tension coupon.

**Table 4-3 Material Properties of Plates**

Plate Type	Coupon ID	Gauge Length, mm	Stress $F_y$ , MPa	Stress $F_u$ , MPa	Elongation %	Reduction in Area
A	R1	51.3	208	430	28	54
A	R2	51.3	208	430	28	55
A	R3	51.3	214	435	28	51
B	NT1	51.3	365	500	17	66
B	NT2	51.3	370	505	21	64
B	NT3	51.3	365	515	19	67
C	GP1	51.3	370	530	N/A	65
C	GP2	51.3	365	530	N/A	64
C	GP3	51.3	365	511	N/A	64

Note: N/A indicates data is not available

**Table 4-4 Material Properties of Angle Specimens**

Angle Type	Coupon Name	Gauge Length, mm	Stress $F_y$ , MPa	Stress $F_u$ , MPa	Overall Elongation %	Reduction In Area	Gaugelength Elongation, %
A1	A1	51.3	358	525	20	63	36.0
A1	AA1	51.3	362	525	22	63	23.8*
B1	B1	51.3	358	483	23	64	26.2*
B1	BB1	51.3	375	488	21	63	35
C1	C1	51.3	350	476	23	62	36.4
C1	CC1	51.3	356	484	24	59	36.4
D1	D1	51.3	360	482	22	64	36
D1	DD1	51.3	353	480	17	53	17.0*
E1	E1	51.3	352	500	21	54	32
E1	EE1	51.3	357	510	21	56	32
F1	F1	51.3	360	507	21	58	32
F1	FF1	51.3	359	515	21	58	33

Note: \* indicates that specimen ruptured at a section beyond the gauge length of the extensometer.

### 4.3 Test Setup

A 2700kN hydraulic actuator and a 1300kN capacity Tinius-Olsen UTM were used for the experimental program. For the 2700kN actuator, a completely new frame capable of

applying load both in tension and compression was designed and fabricated. The setup was designed keeping in view the limitations on the availability of structural sections and restriction in space. Following a thorough investigation on the available materials, various options were considered. Each of these options was analyzed using empirical relations (Young, 1989) and compared. The final configuration, whose details are shown in Figure 4-2 and Figure 4-3, was analyzed using various structural analysis programs. The configuration chosen was such that the service load deflections were well within the limitations of CSA S16.1-94 to minimize the secondary effects on collection of load-deflection data during the experimental program. The frame was designed as a self-straining rectangular reaction frame made of two WWF sections carrying the end reactions and braced against lateral movement at suitable points. Axial deflection of the frame due to axial forces was allowed from both ends but restrained only at the mid-section, in order to prevent transfer of horizontal reaction forces to the strong floor of the laboratory. This new frame was capable of testing members of lengths between 0.3m to 11.1m with 0.6m increments. Grips with one to six pins at each end were used to hold the specimen.

The Tinius-Olsen UTM was used to obtain the material properties and to test specimens of smaller length (Figure 4-4) Standard friction grips were used to hold coupons and gusset plates of the test specimens.

#### **4.4 Specimen Description**

All specimens considered in this study were welded to gusset plates. The gusset plates used on the actuator specimens were of plate type 'C' with dimensions of 500 mm in

width, 19.1 mm in thickness and 1220 mm in length including a grip length of 480 mm. Plate types 'D' and 'E' were used on the UTM. These plates were Tee-shaped. This reduction of cross-section was necessitated since the grip width of the UTM was limited. Hence, larger thickness was used to avoid failure of these plates.

Hildebrand's elastic solution (Eq. 3.10) indicated that the stress profile across the cross-section and along the length is independent of the thickness of the specimen. Hence it was assumed that thickness of specimen has a negligible effect on shear lag and was not considered in the parametric study. The ratio of weld size to specimen cross-section being small, the effect of size and type of weld was also neglected. Weld electrodes of type E760XX were used for welding. This is a high-strength welding rod compared to the normally used E480XX rod used to match the plate tensile strength. It has allowed minimizing the weld lengths needed to examine the shear lag effects. The minimum weld length requirements were calculated using the actual material properties and current code provisions. The material resistance factors were taken to be unity, and weld lengths were designed for gross ultimate capacity. The lengths obtained were increased by 25% for plate specimens and 50% for angle specimens due to eccentricity of loading. Thus, weld failures were minimized in order to obtain net section failure of the test specimens.

#### **4.4.1 Plate Specimens**

Twenty-seven plate specimens having different parameters were tested. The free length of the plate specimens was 480 mm. Instrumentation on these specimens is shown in Figure 4-5 and Figure 4-7. The details of each of the plate specimen have been tabulated in Table 4-5 and Table 4-6. The plate specimens were labeled such that P denotes single

plate specimen, DP a double plate specimen, OP a single plate specimen belonging to the old grade steel i.e., plate A type, UP a single plate specimen with unequal welds on both edges of the specimen, etc. For example, specimen P120-1.0 denotes a 120 mm wide single plate specimen for which, the ratio of weld length to the width of the plate is 1.0. Similarly, T denotes plate with transverse weld, S is a plate welded on one edge (longitudinal weld) only. Specimens with some parameters different while having same weld length to width ratio are differentiated by using a, b or c.

#### **4.4.2 Angle Specimens**

Twenty-two angle specimens were prepared from six individual pieces of angle. The free length of angle specimens was either 480 mm or 760mm. Instrumentation on these specimens is shown in Figure 4-8. The location of strain gauges on the angle is shown in Figure 4-6. Details of various angle specimens are given in Table 4-7 and Table 4-8. These angle specimens were labeled such that EA denotes single equal angle specimen, UEA a single unequal angle specimen, DEA a double equal angle specimen, DUEA as double unequal angle specimen, etc.

Table 4-5 Details of Plate Specimens

Sl	Specimen Name	Width w, mm	Thickness t, mm	Length $L_f$ , mm	WeldLength,mm			Plate type	Gusset type	Gusset width, mm
					$L_{p1}$ , mm	$L_{p2}$ , mm	$L_o$ , mm			
1	OP120-1-a	120	12.82	120	115	115	-	A	D	180
2	OP120-1-b	119.9	12.82	120	115	115	-	A	D	180
3	OP120-T	120	12.82	120	55	55	120	A	D	180
4	OP120-S-a	120	12.82	120	230	-	-	A	D	180
5	OP120-S-b	120.9	12.82	120	226	-	-	A	D	180
6	P120-1-a	120.6	12.97	480	120	120	-	B	C	500
7	P120-1-b	121.1	12.97	120	120	120	-	B	C	180
8	P120-1-c	120.8	12.97	120	120	120	-	B	C	180
9	P120-1.5	120.8	12.97	480	180	180	-	B	C	500
10	DP120-S	121.7	12.97	480	180	-	-	B	C	500
11	DP120-1	122	12.97	480	120	120	-	B	C	500
12	P120-T-a	121.4	12.97	450	100	100	121.4	B	C	500
13	P120-T-b	120.3	12.97	450	50	50	120.3	B	C	500

**Table 4-6 Details of Plate Specimens**

Sl	Specimen Name	Width $w$ , mm	Thickness $t$ , mm	Length $L_f$ , mm	WeldLength,mm			Plate type	Gusset type	Gusset width, mm
					$L_{p1}$ , mm	$L_{p2}$ , mm	$L_t$ , mm			
14	P120-2	120.2	12.97	480	235	235	-	B	C	500
15	P120-S	118	12.97	480	235	-	-	B	C	500
16	P75-0.87	76.2	12.97	480	65	65	-	B	C	500
17	P75-1.0	77.5	12.97	480	75	75	-	B	C	500
18	P75-1.6	77.8	12.97	472	120	120	-	B	C	500
19	P75-2.0	76	12.97	480	153	153	-	B	C	500
20	P75-T	75.5	12.97	480	30	30	75	B	C	500
21	P75-e3/4	75	12.97	120	75	75	-	B	C	180
22	P75-e5/4	75.5	12.97	120	75	75	-	B	E	180
23	UP75-3/4	73.8	12.97	480	95	70	-	B	C	500
24	P75-S	76	12.97	480	170	-	-	B	C	500
25	P75-S-b	76	12.97	480	137	-	-	B	C	500
26	DP75-S	76.1	12.97	480	110	-	-	B	C	500
27	P250-1	250.5	12.97	480	250	250	-	B	C	500

**Table 4-7 Details of Test Angle Specimens**

Sl No	Specimen Name	Angle Type	Leg $w_1$ , mm	Leg $w_2$ , mm	Length $L_f$ , mm	Weldlength and Size, mm						$A_{gross}$ mm <sup>2</sup>
						$L_1$ , mm	$s_1$ , mm	$L_2$ , mm	$s_2$ , mm	$L_3$ , mm	$s_3$ , mm	
1	DEA1	F1	101.4	101.7	480	100	18	100	6.7	101.7	6.7	2660
2	DEA2	F1	101.4	101.7	480	400	18	400	6.7	Nil	Nil	2660
3	DEA3	E1	101.4	101.4	480	150	14	150	6.8	101.4	6.8	2672
4	DEA4	E1	101.4	101.4	480	150	14	150	6.8	101.4	6.8	2672
5	DEA5	F1	101.4	101.7	480	100	18	100	6.7	101.7	6.7	2660
6	EA1	E1	101.4	101.4	480	140	12	140	6.8	101.4	6.8	1336
7	EA2	E1	101.4	101.4	480	135	16	135	6.8	Nil	Nil	1336
8	EA3	A1	151.4	151.6	460	210	18	210	9.7	151.6	9.7	2857
9	EA4	A1	151.4	151.6	460	215	18	215	9.7	Nil	Nil	2857
10	EAm1	E1	101.4	101.4	480	150	14	150	6.8	101.4	6.8	1336
11	EAm2	E1	101.4	101.4	480	150	14	150	6.8	101.4	6.8	1336

Table 4-8 Details of Test Angle Specimens

SI No	Specimen Name	Angle Type	Leg $w_o$ , mm	Leg $w_e$ , mm	Length $L_f$ , mm	Weldlength and Size, mm						$A_{gross}$ , mm <sup>2</sup>
						$L_1$ , mm	$s_1$ , mm	$L_2$ , mm	$s_2$ , mm	$L_o$ , mm	$s_o$ , mm	
12	DUEA1	D1	126.1	75.7	480	125	14	125	6.5	75.7	7.5	2570
13	DUEA2	C1	125	75	480	125	14	125	6.5	75.7	6.5	1285
14	UEA1	D1	75.7	126.1	480	125	14	125	6.5	126.1	6.5	1285
15	UEA2	D1	126.1	75.7	480	135	14	135	6.5	75.7	8.5	1285
16	UEA3	D1	75.7	126.1	480	155	14	155	6.5	Nil	Nil	1285
17	UEA4	D1	126.1	75.7	480	190	16	190	6.5	Nil	Nil	1285
18	UEA5	C1	125	75	480	250	16	250	6.6	Nil	Nil	1280
19	UEA6	C1	125	75	760	190	16	190	6.6	Nil	Nil	1281
20	UEA7	D1	126.1	75.7	480	190	16	190	6.58	Nil	Nil	1285
21	UEA8	B1	102.1	152.4	480	230	16	230	8.1	Nil	Nil	2016
22	UEA9	B1	102.1	152.4	760	300	16	300	8.1	Nil	Nil	2017

## 4.5 Test Procedure

The weld and other details of the test specimens were selected based on the objectives outlined earlier. Each test specimen was welded to gusset plates such that the gusset centerline and the specimen centerline are aligned with each other. The specimen along with the gusset plate is then mounted on the test frame. All specimens were instrumented to measure the axial elongation and the lateral deflections, which in some cases were both in-plane and out-of-plane deformations and the strains at net-section and mid-length cross-section.

All specimens were loaded statically in tension up to failure or complete rupture. The behaviour of these specimens was monitored using electrical resistance Strain Gauges and Linear Variable Differential Transformers (LVDT). All strain gauges were oriented to measure the strains in the longitudinal direction. In most specimens, strain gauges were glued at locations near the net-section cross-section and at mid-section of the specimen to examine the strain variation at various load levels.

LVDTs were used at appropriate locations to obtain the load-elongation behavior, load vs. lateral deflection for specimens in eccentric loading. The overall elongation that includes the elongation of specimen and the gusset plate as well as the effect of the load application mechanism was measured by the stroke of the actuator. All lateral deflections both in plane and out of plane deflections were measured using LVDTs located at the mid-section of the specimen. Data from all these devices including the load measurement

and the stroke of the actuator were recorded simultaneously using Data acquisition units and Labtech software. The pattern of failure of each of these specimens was noted.

Specimens OP120-1-a, OP120-1-b, OP120-T, OP120-S-a, OP120-S-b, P120-1-b, P120-1-c, P75-e3/4, P75-e5/4, P75-S were tested on the UTM and the remaining specimens were tested on the large self straining frame. Specimens tested on the UTM (Figure 4-4) were installed in a direction such that the load application was vertical. These were gripped at the top end and their alignment was checked. Then the lower end of the specimen was gripped, and a small pre-load was applied. After the specimen was gripped to a sufficiently tight condition, the axial load was released and specimen returned to zero load condition. Initial readings of all the strain gauges and LVDTs were noted, and the tensile load was then applied by controlling the movement of the grip end. Readings of strain gauges, LVDT's, and load were recorded continuously during the loading process up to rupture.

Specimens tested in the self straining frame were installed (Figure 4-2) such that the load application was horizontal. The far end of the actuator was initially held by use of 40mm diameter pins. The actuator end was then moved in line with the pinholes of the gusset plate and gripped. Care was taken to ensure no portion of the gusset or specimen was in contact with the floor and no external means for resistance was applied. A small pre-load was applied to ensure proper grip of the test specimen. Initial values of all mounted devices including the stroke of the actuator and load were noted. Tensile load was applied under displacement control. Each specimen was loaded until rupture, and the pattern of

rupture was noted. Digital pictures were taken at various load levels and also during various stages of rupture.

In order to ensure that the large reaction frame containing the actuator and the arrangement made for testing functioned as expected, the results of simple tension test on a plate specimen were compared with the results of the corresponding tensile coupon. This comparison showed that the two behaviours are very similar thus validating the use of the test frame.

Details of the test data and the observations and discussion of the results are presented in the next Chapter.

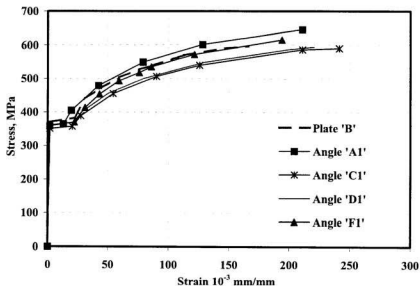


Figure 4-1 True Stress Vs. Log Strain Relation of Test Specimens

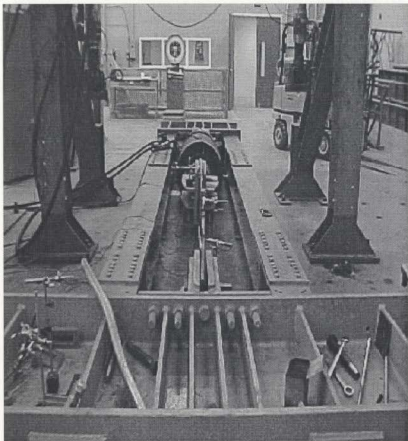


Figure 4-2 Self-Balancing Rectangular Frame Setup for 2700 kN Actuator

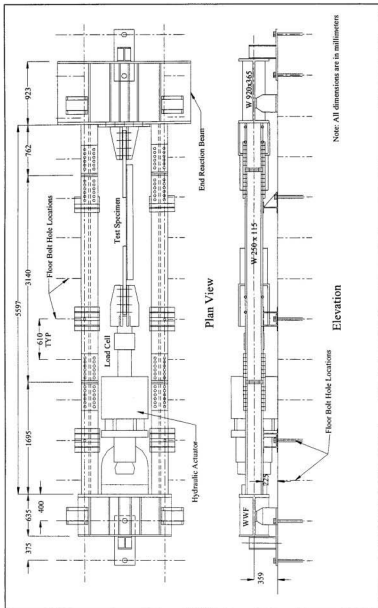
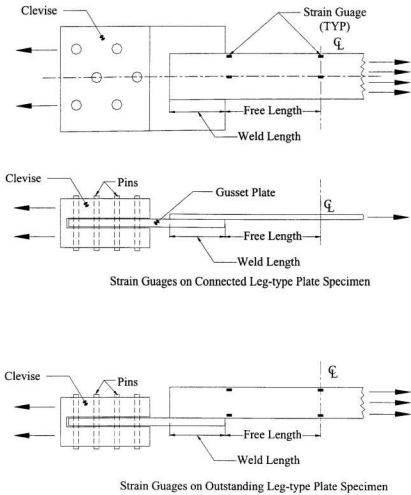


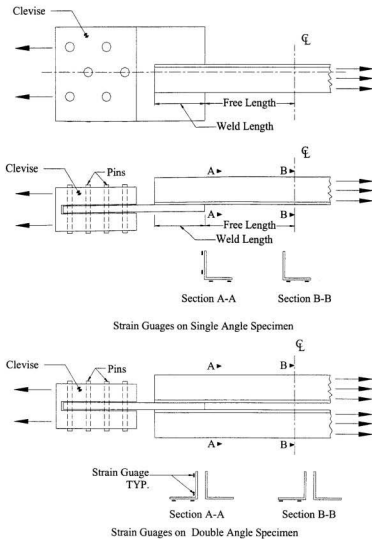
Figure 4-3 Details of Self-Balancing Rectangular Frame Setup



Figure 4-4 Test on Tinius-Olsen UTM



**Figure 4-5 Typical Location of Strain Gauges on Plate Specimens**



**Figure 4-6 Typical Location of Strain Gauges on Angle Specimen**

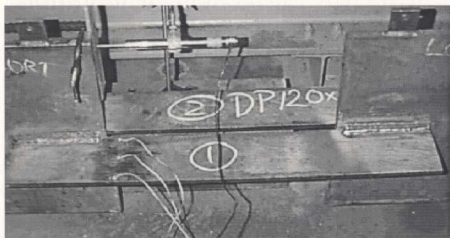
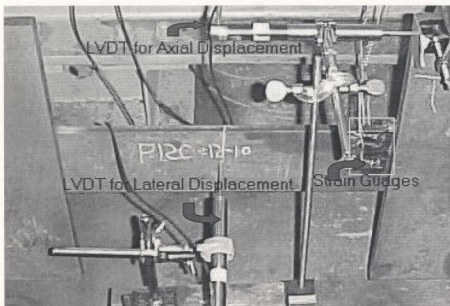


Figure 4-7 Measurement Devices on Plate Specimens



Figure 4-8 Measurement Devices on Angle Specimens

## Chapter 5

### RESULTS AND DISCUSSION

#### 5.1 Experimental Results

Results of tests on weld connected plates and angles under tension subjected to shear lag effect are presented in this chapter. The loads were applied through a displacement-controlled mechanism. Most of the specimens experienced net-section failure due to shear lag by tearing across the member at its critical cross-section. However, a few specimens failed through their weld. The effect of out of plane eccentricity of angle specimens contributed to such weld failures. Only one specimen (P75-1.6) failed at gross-section. This is mainly due to a defect in the plate itself. Typical failure modes are shown in Figure 5-1, Figure 5-2, Figure 5-3 and Figure 5-4. Several other failures of specimens are shown in Appendix E and Appendix F.

All the specimens yielded completely at critical sections before the ultimate capacity was attained. Yielding was first visible at the critical cross-section near the welds, and propagated towards the regions away from the weld. On further loading, yielding over the cross-section at the net-section extended into the free-length of the member. Necking effect was quite prominent near the critical section at the weld end. This effect was followed by tearing from the weld ends leading to complete rupture of the specimen. These specimens showed near constant ultimate loads as the displacement increased.

Specimens with weld lengths lesser than its width exhibited signs of shearing and tearing of plates parallel to the length of weld. Such specimens failed at lower loads compared to specimens with larger weld length.

All specimens with symmetry (double section specimens) exhibited only small out of plane deflections. Their tendency was to reduce the free gap between the two sections. However, all single section specimens showed considerable out of plane bending. The bending was prominent both in the gusset plate and the specimen. After rupture of the specimen, the gusset plates tended to regain their original shape thereby exhibiting no signs of yielding. As expected, due to nonlinear deformations, the specimen deformation was quite prominent and out of plane deflection remained even after the complete rupture of the specimen.

### 5.1.1 Plate Specimens

Single and double plate specimens with transverse and longitudinal welds, longitudinal welds on two edges, and longitudinal welds on only one edge configurations were tested in tension. The results of these test specimens have been tabulated Table 5-1, Table 5-2 and Table 5-3. The net-section efficiency was computed using,

$$U_e = \frac{T_u}{A_g F_u} \quad \text{Eq. 5-1}$$

where,  $U_e$  is the net-section efficiency,  $T_u$  is the actual test capacity,  $A_g$  is the gross cross-sectional area,  $F_u$  is the tensile strength of the material.

Table 5-1 Experimental Results of Plate Specimens

Sl No.	Specimen Name	Width w, mm	Weld Length, mm			Specimen Capacity			Efficiency $U_e$	Failure Type
			$L_1$	$L_2$	$L_t$	$T_p$ , kN	$T_w$ , kN	$T_w$ , kN		
1	OP120-1-a	120	115	115	nil	323	669	531	0.79	Net section
2	OP120-1-b	119.9	115	115	nil	322	668	508	0.76	Net section
3	OP120-T	120	55	55	120	323	669	569	0.85	Net section
4	OP120-S-a	120	230	nil	nil	323	669	333		Weld failure
5	OP120-S-b	120.9	226	nil	Nil	325	674	440	0.65	Net section
6	P120-1-a	120.6	120	120	nil	580	796	750	0.94	Net section
7	P120-1-b	121.1	120	120	nil	582	799	556		Weld failure
8	P120-1-c	120.8	120	120	nil	581	797	733	0.92	Net section
9	P120-1.5	120.8	180	180	nil	581	797	756	0.95	Net section
10	P120-2	120.2	235	235	nil	576	797	740	0.94	Net-section
11	DP120-1	122	120	120	nil	1172	1609	1521	0.95	Net section

Note: \* Indicates Net-Section Efficiency could not be obtained since it wasn't a Net-section Failure

**Table 5-2 Experimental Results of Plate Specimens**

Sl No.	Specimen Name	Width w, mm	Weld Length, mm			Specimen Capacity			Efficiency $U_e$	Failure Type
			$L_1$	$L_2$	$L_t$	$T_p$ , kN	$T_u$ , kN	$T_n$ , kN		
12	P120-T-a	121.4	100	100	121.4	583	800	763	0.95	Net-section
13	P120-T-b	120.3	50	50	120.3	577	793	770	0.97	Net-section
14	DP120-S	121.7	180	nil	nil	1168	1604	1431	0.89	Net-section
15	P120-S	118	235	nil	nil	566	777	664	0.85	Net-section
16	P75-0.87	76.2	65	65	nil	366	503	478	0.95	Net-section
17	P75-1.0	77.5	75	75	nil	372	511	489	0.96	Net-section
18	P75-1.6	77.8	120	120	nil	374	514	500	0.97*	Gross section
19	P75-2.0	76	153	153	nil	365	501	489	0.97	Net-section
20	UP75-3/4	73.8	95	70	nil	354	487	471	0.97	Net-section
21	P75-T	75.5	30	30	75	363	499	489	0.98	Net-section
22	P75-c3/4	75	75	75	nil	360	495	480	0.97	Net-section

Note: \* Indicates Net-Section Efficiency could not be obtained since it wasn't a Net-section Failure

Table 5-3 Experimental Results of Plate Specimens

Sl No.	Specimen Name	Width w, mm	Weld Length, mm			Specimen Capacity			Efficiency $U_e$	Failure Type
			$L_1$	$L_2$	$L_t$	$T_p$ , kN	$T_m$ , kN	$T_n$ , kN		
23	P75-e5/4	75.5	75	75	nil	363	498	475	0.95	Net-section
24	P75-S	75.2	170	nil	nil	362	497	413	0.83	Net-section
25	P75-S-b	76	137	nil	nil	365	501	480	0.96	Net-section
26	DP75xS	76.1	110	nil	nil	732	1005	942	0.94	Net-section
27	P250x1	250.5	250	250	nil	1205	1645	1456	0.89	Net-section

Note: \* Indicates Net-Section Efficiency could not be obtained since it wasn't a Net-section Failure

Using this expression, the average efficiency of plate specimens made from lower steel grade (S39 Grade) and connected on both edges was 80%. The corresponding value for plates connected on one edge only was 65%. Specimens made from Grade 350W Steel connected on both edges exhibited net section efficiency  $U_e$  of 94%.

Behaviour of these specimens was monitored during all the loading stages. Due to the low moment of inertia of the plate specimen, eccentric loading caused significant out of plane deflection even at loads considerably lower than the ultimate capacity of the section. Most of the total deflection as shown in Figure 5-5 occurred within 40% of its ultimate test capacity. Beyond this load, the free length of these specimens oriented along the line of force, and the lateral deflection became minimal. Thus the effect of eccentricity was counteracted by the lateral deformation of plate specimen.

In double plate specimens the gusset plates remained straight throughout their loading stages. Test plates of these specimens, exhibited only a small out of plane deflections by bending inwards with a tendency to reduce the free gap existing between them. The in-plane deflections of all plate specimens, however, were negligible.

### **5.1.2 Angle Specimens**

A total of twenty-two angle specimens with different geometric and weld configurations were tested in tension. Results for the angle specimens have been presented in Table 5-4 and Table 5-5.

Table 5-4 Experimental Results for Angle Specimens

Sl No	Specimen Name	Angle Size, mm	Weld Length and Sizes, mm			$A_g * F_y$ kN	$A_g * F_u$ kN	Test Load $T_m$ kN	$U_e$ %	Failure type
			$L_1$	$L_2$	$L_r$					
1	DEA1	101.7x101.4x6.78	100	100	101.7	958	1357	995	0.73	Net-Section
2	DEA2	101.7x101.4x6.78	400	400	Nil	958	1357	1181	0.87	Net-Section
3	DEA3	101.4x101.6x6.81	150	150	101.4	962	1363	931	0.68	Weld Failure
4	DEA4	101.4x101.6x6.81	150	150	101.4	962	1363	1023	0.75	Weld Failure
5	DEA5	101.7x101.4x6.78	100	100	101.7	958	1357	1067	0.79	Weld Failure
6	EA1	101.4x101.6x6.81	140	140	101.4	481	681	577	0.85	Net-Section
7	EA2	101.4x101.6x6.81	135	135	Nil	481	681	547	0.80	Net-Section
8	EA3	151.6x151.4x9.74	210	210	151.6	1023	1500	1250	0.83	Net-Section
9	EA4	151.6x151.4x9.74	215	215	Nil	1023	1500	1225	0.82	Net-Section
10	EAm1	101.4x101.6x6.81	150	150	101.4	481	681	577	0.85	Net-Section
11	EAm2	101.4x101.6x6.81	150	150	101.4	481	681	556	0.82	Net-Section

**Table 5-5 Experimental Results for Angle Specimens**

Sl No	Specimen Name	Angle Size, mm	Weld Length and Sizes, mm			$A_g * F_y$	$A_g * F_u$	Test	$U_e$	Failure
			$L_1$	$L_2$	$L_t$	kN	kN	Load, kN	%	type
12	DUEA1	75.7x126.1x6.58	125	125	75.7	925	1239	874	0.71	Weld Failure
13	DUEA2	75x125x6.62	125	125	75.7	914	1244	925	0.75	Net-Section
14	UEA1	126.1x75.7x6.58	125	125	126.1	463	619	562	0.91	Net-Section
15	UEA2	75.7x126.1x6.58	135	135	75.7	463	619	485	0.78	Net-Section
16	UEA3	126.1x75.7x6.58	155	155	Nil	463	619	558	0.90	Net-Section
17	UEA4	75.7x126.1x6.58	190	190	Nil	463	619	502	0.81	Weld Failure
18	UEA5	75x125x6.62	250	250	Nil	456	620	556	0.90	Net-Section
19	UEA6	75x125x6.62	250	250	Nil	456	620	520	0.84	Net-Section
20	UEA7	75.7x126.1x6.58	190	190	Nil	463	619	502	0.81	Weld Failure
21	UEA8	152.4x102.1x8.18	230	230	Nil	746	984	920	0.94	Net-Section
22	UEA9	152.4x102.1x8.18	300	300	Nil	746	984	901	0.92	Net-Section

Behaviour of angle specimens, like the plate specimens, was monitored throughout the loading stage up to rupture of the specimen. Twisting of angle sections was prominent in single angle specimens but negligible in double angle specimens. Due to the unsymmetric nature of the angle section, single angle specimens experienced considerable in-plane and out-of-plane deformations. All specimens were aligned such that the geometric centre of the specimen was in line with the force application. Hence, nominal eccentricity was zero in the plane of the connected leg. These specimens still exhibited in-plane deformations. Such behaviour could be attributed to the 'shear lag' effect resulting in non-uniform distribution of stress, causing the force centroid for the angle to be not at the force centroid for the gusset. Also, out-of-plane deformations causing twisting can cause additional in-plane bending. (Figure 5-6) Such behaviour of these specimens caused significant deformation of the gusset plates. But, the revival of the gusset's original shape after rupture of the angle specimen indicated that the gusset plate did not experience yielding.

EAm1 and EAm2 tests were conducted on single equal angle specimens that were unloaded to zero load condition after being loaded to levels beyond their gross yield load. These were then tested for the ultimate capacity of the angle. These specimens had similar efficiencies in comparison to EA2 that was loaded to failure without any unloading. This indicates that partial yielding of the angles during loading and unloading cycles does not have any appreciable effect on the ultimate capacity. Such behaviour on ultimate capacity is attributed to the fact that the specimen, never loaded in compression, experienced no significant change to the ultimate strength of the material as a result of Bauschinger effect. This seems to indicate that Bauschinger effect did not significantly

change the section efficiency. However, such loading and reloading reduced the rupture strain measured during the second loading stage. This was noticed in both the specimens EAm1 and EAm2 in comparison to Specimen EA2.

In the case of short-leg connected specimens such as UEA4 and UEA7, its out of plane eccentricities caused specimen to experience failures through the weld by pull out at the outer edge on the heel of the angle. Such failure (as shown in Figure 5-3) was a result of the combined action of bending and shear. These specimens had no transverse welds. It must be noted however, that these specimens had nearly reached their ultimate capacities before the weld tear-out, since tearing at the heel of the angle section was noticed very clearly. Therefore, we can use this data from these experiments to estimate the shear lag effect on the specimens.

Such weld failure/tearing in some of the angle specimens points to the fact that although the design equations used in practice do not explicitly account for the effect of eccentricity that causes weld tear-out, it is actually a governing failure mode in certain cases. It must be pointed out that the eccentricity in this case is difficult to determine since significant out of plane bending as well as some twisting occurs well before the onset of tear out. Such bending is meant to reduce the overall eccentricity of the applied load with respect to the centroid of the resisting force. However, at the connection zone, the profile of the member, the gusset plate and the alignment of the force are difficult to determine. They depend on several factors such as the actual shape of the gusset plate and restraints placed on it, etc. The actual eccentricity of the weld with respect to the centroid of the resisting force will be different from the distance between the angle centroid and

the weld measured before the application of load. Besides, the weld line will not be parallel to the resisting force because of bending and twisting of the angle, especially at the connection zone. As a minimum, the weld design must account for the out of plane eccentricity caused by the distance between the member centroid and the weld line. Referring to Figure 5-7, the weld design is normally carried out by not including the eccentricity since the weld line and the applied load from the gusset plate are almost collinear at the beginning. As the load approaches limit load, however, (Figure 5-8) the bending of the gusset plate and the member near the connection zone produce an eccentric inclined force acting on the weld. This can cause tearing of the weld as noticed during the tests.

In these specimens, two types of section failures were noticed.

- Tearing at the toe of the connected leg of the angle, which extended towards the heel and then to the outstanding leg of the angle was most common type of section failure noticed in the angle specimens. Figure 5-1 and Figure 5-2 show such failure type commonly called as net-section failure of the specimen. The toe is the most common failure initiation point since the effective area available for load transfer at the toe is less than that available for load transfer at the heel. The actual force transferred, however, will be the same at the heel as well as the toe (assuming that the weld lengths and sizes on both sides are equal to each other).
- Specimens DEA1 and DUEA2 with weld lengths lower than or equal to the width of the outstanding leg, failed by tearing at the net-section in the connected leg and along the weld in the outstanding leg. Tearing was first noticed at the heel of the angle

followed by tearing at the toe of the connected leg. Figure 5-4 shows a typical failure of the specimen. Designers do not commonly account for this type of failure. This is further discussed in the following sections.

In all angle specimens failing at the net-section, complete rupture occurred through the connected leg prior to the outstanding leg. Such behaviour was noticed even in large size angle specimens and unequal angle specimens with its long-leg as the connected leg. For the angles considered for this study, at load ranges between 70%-93% of the ultimate capacity of single angle specimens, the extreme fibre of the outstanding-leg of the angle specimen was subjected to compressive stresses. Due to the large deformation behaviour of angle specimens, the outstanding-leg experienced reversal of its stresses. From the experimental and FEA results, when the extreme fibre of the outstanding-leg was at its tensile yield stress, the stress in the connected leg was well beyond its yield capacity approaching its ultimate strength. This difference in the load carrying behaviour of the legs of the angle specimen results in complete failure of the connected leg prior to the outstanding leg. Since, such trends were observed in angle specimens L102x102x6.4 and L152x152x9.5, it could be assumed that other sizes exhibit similar trends as well.

## **5.2 Finite Element Analysis**

Numerical models for most test specimens were developed incorporating their measured physical and material properties (as opposed to their nominal properties). These models were analyzed using non-linear finite element techniques. Results and behaviour of these finite element models have been compared with the experimental results as shown in Table 5-6 and Table 5-7 .

The average ratio of FEA to experimental results for plates with welds on both longitudinal edges (connected leg type) was 1.01. For outstanding-leg type plate specimens, the ratio is 0.88. FE results of angle specimens overestimated their corresponding test capacity with a mean of 1.05 and standard deviation of 0.04. ANSYS element Shell-181 seems very efficient in simulating the material tension coupon behaviour. Hence, the prediction of connected leg type plates in tension had a variation of  $\pm 8\%$  variation. However, in outstanding-leg type plates, the effect of eccentricity causes significant bending stress along with tensile forces. Under the combined effect, the variation in predictions of ultimate capacity is  $-8$  to  $+15\%$ . Predictions of angle specimens, modeled as a combination of connected & outstanding leg type plates, varied between  $-2\%$  to  $+12\%$ . It must be pointed out that in general non-linear analysis give deviations larger than above. The somewhat small deviations noticed in the present study are perhaps common to tensile strength measurements. This trend is also noticeable in the few non-linear analysis carried out by Wu and Kulak [1993] on bolted angles in tension. Thus, FEM can be successfully used to examine the effects of various parameters.

The load vs. elongation response obtained analytically was compared with the experimental results (Figure 5-9). The contours of the longitudinal stresses mapped by linear interpolation from the averaged nodal stresses were collected from the ANSYS FE program. Figure 5-10, Figure 5-11 show the stress pattern at ultimate loads in specimen P120-1 and P120-1.5 obtained from non-linear FE analysis. At net-section, comparison of the stress variation clearly indicates that the effect of longitudinal weldlength is negligible on 'shear lag'. Figure 5-12, Figure 5-13 and Figure 5-14 show the axial stress variation at ultimate loads for specimen DEA1, UEA4 and EA1 respectively.

**Table 5-6 Experimental and FE Results of Plate Specimens**

SI No.	Specimen Name	Width w, mm	Plate Type	Test Capacity, kN	FEM Results, kN	FEM/Test Ratio
1	OP120x1-a	120	A	531	537	1.01
2	OP120xT	120	A	569	589	1.03
3	P120x1-a	120.6	B	752	757	1.01
4	P120x1-c	120.8	B	734	675	0.92
5	P120x1.5	120.8	B	756	775	1.03
6	P120x2	120.2	B	740	790	1.07
7	DP120x1	122	B	1521	1588	1.05
8	P75x0.87	76.2	B	479	502	1.05
9	P75x1.0	77.5	B	489	510	1.04
10	P75x2.0	76	B	489	505	1.03
11	P75xT	75.57	B	489	488	1
12	P75xe3/4	75	B	480	463	0.96
13	P75xe5/4	75.5	B	476	468	0.98
14	P75xS	76	B	480	437	0.91
15	DP75xS	76.1	B	934	790	0.85
16	P250x1.0	250.5	B	1456	1457	1

**Table 5-7 Experimental and FE Results of Angle Specimens**

Sl No	Specimen Name	Angle Type	Test Load, kN	FEM Load, kN	Ratio FEM/Test
1	DEA1	F1	995	980	0.98
2	DEA2	F1	1181	1320	1.12
3	EA1	E1	577	589	1.02
4	EA2	E1	547	590	1.08
5	EA3	A1	1250	1229	0.98
6	EA4	A1	1225	1226	1.00
7	DUEA2	C1	925	1026	1.11
8	UEA1	D1	562	605	1.08
9	UEA2	D1	485	495	1.02
10	UEA3	D1	558	612	1.10
11	UEA5	C1	556	581	1.04
12	UEA6	C1	520	545	1.05
13	UEA7	D1	510	544	1.07
14	UEA8	B1	920	955	1.04
15	UEA9	B1	901	931	1.03

### 5.3 Discussion of Results

This section briefly discusses the various results obtained experimentally and numerically and their implications with respect to the shear lag effect on welded steel plates and

angles. Most of the tables referred to here consider the data from the basic results in Table 5-1 to Table 5-5 and regroup them to obtain the required comparisons.

### 5.3.1 Effect of Size of Member

Plot of average experimental stress based on the gross-section area and the average strain based on total axial deformation for various specimens is shown in Figure 5-15. It compares the behaviour of plate specimens of various sizes. All these specimens were made from the same plate type 'B'. The general trends are all consistent with each other as well as with the material behaviour.

**Table 5-8 Effect of the Size of Member -Plates**

Specimens	Plate size, mm	$\frac{L}{w}$	$U_e$	Notes
P75-1.0	72x12.97	1.0	0.96	
P120-1.0-a	120x12.97	1.0	0.94	
P250-1.0	250x12.97	1.0	0.89	
P75-S	75x12.97	2.23	0.96	Single weld
P120-S	120x12.97	1.5	0.85	Single weld
P75-2	75x12.97	2.0	0.97	
P120-2	120x12.97	2.0	0.94	
P75-T	75x12.97	0.4	0.97	
P120-T-b	120x12.97	0.41	0.97	

The relevant experimental results for plates are grouped in Table 5-8.

The comparison of results of the plate specimens indicates that shear lag effects generally increased with an increase in the size of the specimen. Decrease in ductility with increasing size of the specimen is also noticeable from Figure 5-15. Such behaviour with increase in size of specimen was also predicted by the analytical results. FE analysis results shown in Figure 5-16 indicate that the effect of size on shear lag is more prominent in materials with low  $F_y/F_u$  ratio such as material type "A". The increase in shear lag effect with the size is clearly visible for all plates whether they are welded on both ends (similar to the connected leg of the angle) or welded on one edge only (similar to the outstanding leg of the angle). Figure 5-17 shows a comparison between experimental and FEA trends. The trends show reasonable agreement.

It can thus be seen that the shear lag effect is not a simple function of  $L/w$  ratio. The width influences the shear lag more than the length. For members connected on two edges, this difference is not very high. However, for plates connected at one end only, the effect of width is much more pronounced since the eccentricity of load with respect to the weld line is also high.

The relevant experimental results for angles are grouped in Table 5-9. Unlike plate specimens, experimental angle specimens exhibited no clear pattern with respect to the effect of shear lag with increase in size of specimen. Finite element studies on angles with different sizes having similar material properties are shown in Figure 5-18. For this parametric study, numerical analysis was conducted with its material properties similar to

that of Coupon-F1. The figure also shows the relevant experimental data taken from Table 5-9. The figure shows that the experimental and FEA results are agreeable. The FEA results clearly indicate that if the material property is kept the same, the net section efficiency decreases with increase in angle size. This result is not clearly reflected in experimental data since it corresponds to angles of different material properties. The influence of angle size on shear lag is larger than the corresponding influence of plate size on shear lag. This is attributable to the larger eccentricities of load in case of angles.

**Table 5-9 Effect of Size of Member- Angles**

Specimen	Angle Size	$\frac{L}{w_o}$	$U_e$	Notes
EA2	L101.4x101.6x6.81	1.35	0.80	
EA4	L151.6x151.4x 9.7	1.41	0.82	
EA1	L101.4x101.6x 6.81	1.4	0.85	
EA3	L151.6x151.4x 9.74	1.38	0.83	
DEA2	L101.7 x 101.4 x 6.78	4.0	0.87	Double Angle
L-L-1	L50 x 50 x 5	2.3	0.81	Easterling's Double Angle
L-L-2	L50 x 50 x 5	2.3	0.82	Easterling's Double Angle
L-L-3	L50 x 50 x 5	2.3	0.82	Easterling's Double Angle
EAm1	L101.4 x 101.6 x 6.81	1.5	0.85	Single Angle Section
Eam2	L101.4 x 101.6 x 6.81	1.5	0.82	Single Angle Section
L-B-1c	L50 x 50 x 5	1.5	0.81	Easterling's Double Angle
L-B-2	L50 x 50 x 5	1.5	0.75	Easterling's Double Angle
L-B-3	L50 x 50 x 5	1.5	0.79	Easterling's Double Angle

### 5.3.2 Effect of Length of Connection

The effect of the length of connection of plates on shear lag is shown in Table 5-10 .

**Table 5-10 Effect of Length of Connection -Plate Specimens**

Specimen	Plate Size, mm	$\frac{L}{w}$	$U_e$	Notes
P75-0.87	75x 12.97	0.87	0.95	Easterling & Gonzalez [1993]
P75-1.0	75x 12.97	1.0	0.96	
P75-2.0	75x 12.97	2.0	0.97	
P-L1-1b	76.7 x 6.6	1.41	0.94	
P-L1-2	76.8 x 6.6	1.41	0.98	
P-L1-3	76.8 x 6.6	1.41	1.0	
P-L2-1	76.2 x 6.6	1.67	0.98	
P-L2-2	76.2 x 6.6	1.67	0.98	
P-L2-3	76.2 x 6.6	1.67	0.96	
P120-1a	120x 12.97	1.0	0.94	
P120-1c	120x 12.97	1.0	0.92	
DP120-1	120x12.97	0.98	0.95	
P120-1.5	120x 12.97	1.5	0.95	
P120-2	120x 12.97	2.0	0.94	
P75-S	75x 12.97	2.26	0.96	Single Plate
P75-S-b	75x 12.97	1.87	0.97	Single Plate
DP75-S	75x12.97	1.46	0.93	Double Plate

In the results reported above, for plates connected by welds on two edges (both 75 and 120 mm plates), an increase in the length of weld did not show appreciable effect on the net section efficiency. In all cases, when  $L/w$  is at least 1.0, the efficiency is above 90%. This is somewhat surprising in view of the current code provisions where this parameter is given the highest prominence. Result from finite element analysis shown in Figure 5-19 indicates that when the  $L/w$  ratio is above 1.0, the variation in efficiency is within 3-4%.

For plates connected on one edge only, there is a marginal effect on ultimate capacity with an increase in the length of weld. Figure 5-20 shows that this variation (FEA analysis) is significant for plates connected by single weld. The FEA predictions were lower than those from experiments. The FEA prediction for 120 mm wide plate is close to the  $1 - \bar{x}/L$  curve currently being used by the CSA-S16.1-94 code [CSA, 1994]. The efficiency of these specimens increased with the length of connection up to a ratio of  $L/w$  equal to 2.0.

The behaviour of 75mm wide specimens with increasing load is compared in Figure 5-21. These specimens with different weld configurations showed similar efficiencies. Similarly Figure 5-22 shows, among other things, the behaviour of P120-1.0, P120-1.5 and P120-T-a. All three show similar pattern. This would imply that for plates connected by two longitudinal edges, the efficiency is not seriously effected by the  $L/w$  ratio. For plates connected by one edge only, the efficiency is at least equal to or considerably better than that predicted by the  $1 - \bar{x}/L$  rule.

In addition to the above observations, it may be noted that plate specimens with small connection lengths exhibited failure of plates by tearing parallel to the weld length as shown in Figure 5-23. Typical failure of such experimental specimens is shown in Figure 5-24. Designers do not usually anticipate this mode of failure. This mode governs the strength of small weld lengths, where as for larger weld lengths, the usual net-section tearing failure (Figure 5-1) governs.

Such specimens failed at lower net-section efficiencies. Specimen P75-0.87 connected by longitudinal welds on both edges exhibited shearing failure while Specimen DP120-S showed signs of such failure. Such failures could be avoided by increasing minimum limits on connection lengths. In Figure 5-23, the capacity for failure on path 1-1 is  $2Lt(0.6F_u)$ . The capacity for failure along 2-2 is  $U_{e-c}wt(F_u)$ , where,  $L$  is the weld length,  $w$  is the plate width, and  $U_{e-c}$  is the net section efficiency. As per the current code, for very small weld lengths,  $U_{e-c}$  is 0.75. Using this value implies that failure along 1-1 governs only if  $L/w \leq 0.625$ . However, during experiments, this failure governed for  $L/w$  values of 0.87. This implies that the choice of  $U_{e-c} = 0.75$  by the code is conservative. This may be satisfactory for design purposes, but between this mode of failure and tensile failure mode, there is a marked difference in the ductility of the specimen.

Failure modes of this kind are also predicted by FEA. Figure 5-19 shows a noticeable drop in efficiency for  $L/w$  ratio below 0.9. This could be attributed to the fact that below this, the net section failure does not govern the strength. Instead, the plate failure by shearing parallel to weld governs.

The effect of the length of connection of angles on shear lag is shown in Table 5-11.

**Table 5-11 Effect of Length of Connection – Angle Specimens**

Specimen	Angle Size	$\frac{L}{w_o}$	$U_e$	Notes
DEA1	L101.7x101.4x 6.78	1.0	0.74	Double Angle (not full net section failure)
EA1	L101.4x101.6x 6.81	1.4	0.85	Single Angle
Eam1	L101.4x101.6x6.81	1.5	0.85	Single Angle
EA2	L101.4x101.6x 6.81	1.35	0.80	Single Angle
DEA2	L101.7x101.4x 6.78	4.0	0.87	Double Angle
UEA6	L75x125x 6.62	1.5	0.85	
UEA5	L75x125x6.62	2.0	0.90	
DUEA2	L75.7x126.1x 6.58	1.0	0.75	Double Angle (not full net section failure)
UEA2	L75x125x 6.62	1.1	0.78	Single Angle (not full net section failure)

The results above show that as the  $L/w$  values increase, the efficiencies for full net-section failure increase slightly. Numerical analysis on equal angle specimens exhibited behaviors similar to the test results. Figure 5-25 and Figure 5-26 show that the efficiency of angles changes only a few percentage points beyond  $L/w_o = 1.5$ , where,  $w_o$  is the width of outstanding leg of the angle. From the results of plates, we can see that for the connected legs of angles, the efficiency does not vary much in the range  $L/w > 1.5$ . For outstanding legs of angles, the  $1 - \bar{x}/L$  rule is conservative. This rule predicts only a 7% change in the outstanding leg efficiency for the range  $1.5 \leq L/w \leq 2.0$ . Therefore, the combined efficiency of the two legs of the angle will not differ by more than 3 – 4% in that range. Experimental results have indicated this range to be in the order of 5 – 12%.

Angle specimens DEA1, DUEA2, and UEA2 with  $L/w$  ratio of 1.0 exhibited net-section failure in the connected leg and tearing due to shear in the outstanding leg (similar to that in Figure 5-4). These specimens had lower efficiencies compared to specimens that experienced complete net-section tearing failure (as in Figure 5-2). As in the case of plates, the current provisions of CAN/CSA S16.1-94 for design of members in tension do not predict tearing in shear type behaviour of the specimen. This is examined below.

According to the design specifications of CAN/CSA-S16.1-94, the weld capacity of the connection is the lower of its base metal capacity or the weld capacity.

$$T_r = \min(0.67\phi_w A_m F_u, 0.67\phi_w A_w X_u) \quad \text{Eq. 5-2}$$

where,  $A_m = L s$  is the product of weld length on outstanding leg and the size of weld,

$$A_w \text{ is the net weld area obtained by } Ls/\sqrt{2}$$

The tensile tearing capacity of the outstanding leg (capacity in shear lag) is given by,

$$T_r = 0.85\phi \left(1 - \frac{\bar{x}}{L}\right) w_e t F_u \quad \text{Eq. 5-3}$$

$$\text{where, } \bar{x} = \frac{w_p - t}{2}$$

The shearing capacity of the specimen along the weld edge is given by

$$T_r = 0.85\phi t 0.6F_u \quad \text{Eq. 5-4}$$

Comparison of the tearing capacity of the specimen as given in Eq. 5-3 and Eq. 5-4 indicates that the weld length  $L$  is the influencing factor behind the demarcation between the two types of failure. The limiting length of weld  $L$  required to ensure tensile tearing failure could be obtained by equating the two kinds of failure capacities, thus,

$$0.85\phi\left(1 + \frac{\bar{x}}{L}\right)wtF_u = 0.85\phi Lt0.6F_u$$

substituting for  $\bar{x}$  and simplifying,

$$L = \frac{w \pm \sqrt{1.2wt - 0.2w^2}}{1.2} \quad \text{Eq. 5-5}$$

For real roots of  $L$  in Eq. 5-5,  $w/t \leq 6.0$ . However, for practical angles,  $w/t$  is greater than 6.0. Hence, according to the current specifications for angles, there is no such weld length 'L' that causes shearing type failure of the angle outstanding leg. If the radical in Eq. 5-5 (within the square-root) is neglected for such angles, it is noticed that the current specification (CSA S16.1-94) shows no such weld length wherein the block shear capacity of the angle governs the capacity of the member. However, as explained above, shear-type failures were noticed in Specimens DEA1 and DEA2. This is because the  $1 - \frac{\bar{x}}{L}$  rule for 'shear lag' under-estimates the Net-Section Efficiency of outstanding legs. The effect of this rule is further discussed in the subsequent sections.

### 5.3.3 Effect of Material Properties

The shear lag is affected by several material properties such as the yield and ultimate strengths, onset of strain hardening, strain at tensile strength, strain at breaking (rupture), etc. Some of those are examined in this subsection.

The effect of yield strain on the shear lag has been examined using FEA. The modulus of elasticity was varied, thus affecting the yield strain parameter. It is found that this has no significant impact on the shear lag for the range of geometric properties used in the investigation. This study also showed that most of the specimens were more or less completely yielded through out the critical cross-section at the time of failure. Such behaviour causing complete cross-sectional yielding was confirmed by the strain gauge measurements taken from the experimental results.

**Table 5-12 Effect of Grade of Steel**

Specimen	Plate Size, mm	$\frac{L}{w}$	$U_e$	Notes
P120-1-c	120.8x 12.97	1.0	0.92	Plate type 'B'
OP120-1-a	120x 12.8	1.0	0.79	Plate type 'A'

Test specimens labeled OP and P (or DP) indicate the two different steel grades considered in this study. Results of these specimens showed that the effect of shear lag is more prominent in specimens of lower steel grade. Although only a limited number of such specimens were tested, results of American Welding Society [Easterling and Gonzalez, 1993] on single plate specimens shown in Table 2.1 on lower steel grade had an average efficiency value of 75%, while results by Easterling and Gonzalez [1993] on

higher steel grade indicated an average efficiency of 96%. This difference should be attributed to the ratio of yield stress to ultimate stress ( $F_y/F_u$ ). Figure 5-27 and Figure 5-29 show that the lower the ratio  $F_y/F_u$ , the more prominent is the shear lag effect.

To study the various effects of material properties on shear lag, the stress-strain data relating to plate type 'A' was suitably modified and considered in the numerical model. Figure 5-28 shows the pattern of stress strain relationship used to obtain a realistic material property parameter for this study.

The effect of the location of the onset of strain hardening within the practical range of 0.4% to 2.0% strains was investigated. Figure 5-30 shows no significant variation in the efficiency of the section within the above range.

The effect of breaking strain on plate types 'A' and 'B' is shown in Figure 5-31 for a 120mm wide plate. The analytical results show that between the 16% and 22% ultimate strain, the efficiencies have shown a marked increase. Breaking strain of approximately 22% in both plate types yielded near maximum efficiencies. It must be noted that most practical steels differ widely in their breaking strain values. Guaranteed values of more than 18% ultimate strain are difficult to assure except in case of special steels. This would imply that we are better off in not using the higher efficiencies accrued at larger breaking strain values. As is also seen from the figure, the larger the value of yield stress  $F_y$  with respect to the ultimate stress  $F_u$ , the lower the effect of breaking strain. Therefore, for higher steel grades (e.g., from 300W to 350W), the effect of breaking strain diminishes.

### 5.3.4 Effect of Eccentricity

The effect of gusset plate is to cause a load eccentricity, among other things. This is examined by varying the thickness of the gusset plates. The limited test data presented in Table 5-13 shows a minor variation of net-section efficiency. Some of the results of a finite element study on plates are shown in Figure 5-32. It shows that the eccentricity caused by the thickness of the gusset plate had no significant effect on the ultimate capacity of the specimen.

**Table 5-13 Effect of Load Eccentricity on Plates**

Specimen	Plate Size, mm	$\frac{L}{w}$	$U_e$	Notes
P75-e3/4	75x 12.97	1.0	0.97	Eccentricity of 19mm
P75-e5/4	75.5x 12.97	1.0	0.95	Eccentricity of 30mm

### 5.3.5 Effect of Free Length of Member

The critical section for welded members is at the end of the weld. The length of weld is usually in the order of the width of the member and is quite small compared to the length of member. Elastic stress distribution equations presented in Chapter 3 clearly show that the variation of stress across the width is negligible after a length of 2.5 time the width from the end of the member. Most practical members are at least that long. To illustrate the point further, a comparison is presented in Table 5-14 and Figure 5-33.

**Table 5-14 Effect of Free Length of Member**

Specimen	Plate size, mm	$\frac{L}{w}$	$U_e$	Notes
P120-1-a	120.6x 12.97	1.0	0.94	Free length of 480mm
P120-1-c	120.8x 12.97	1.0	0.92	Free length of 120mm
P75-1	77.5x 12.97	1.0	0.96	Free length of 480mm
P75-c3/4	75x 12.97	1.0	0.97	Free length of 120mm
Specimen	Angle size	$\frac{L}{w_o}$	$U_e$	Notes
UEA6	L75x125x 6.62	1.5	0.85	Free length of 760mm
UEA4	L75.7x126.1x 6.58	1.5	0.82*	Free length of 480mm
UEA7	L75.7x126.1x 6.58	1.5	0.83*	Free length of 480mm

Note: \* Estimated value (Actual failure was in the weld. However, prior to the weld failure, partial rupture in the angle was observed.)

Experimental results on both plate and angle specimens showed a small increase of about 2-3% in the net-section capacity with increase in free-length of the member. However, finite element analysis predicted no significant increase in the member capacity within the practical member length ranges.

### 5.3.6 Effect of Weld Configuration

Specimens with three types of connections were tested to study the effect of geometry and weld configuration, viz.,

1. Combination of both longitudinal and transverse welds (both Plates and Angles),
2. Longitudinal welds on both edges (both Plates and Angles),

### 3. Longitudinal weld on one edge only (Plates only).

#### **5.3.6.1 Type-1 Configuration: Welds with both Longitudinal and Transverse Welds**

Experimental results of plate and angle specimens connected by the use of both longitudinal and transverse welds clearly showed the presence of shear lag effect. Easterling and Gonzalez [1993] reported similar results. This is unlike the current design practice, wherein the presence of transverse welds should eliminate the shear lag effect in plates and in the connected-leg of angles completely.

The addition of transverse welds did not significantly increase the net-section capacity. Tests on plate specimens showed increase in efficiencies of sections with transverse welds by about 2%. This effect was studied further by providing different longitudinal weld lengths in combination with transverse welds. Specimen P120xT-b with lower longitudinal weld length experienced better efficiency compared to specimen P120-T-a with longer longitudinal weld-lengths. This seemingly paradoxical effect of increased efficiencies with lower longitudinal welds in combination with transverse welds could be attributed to the difference in stiffness of the two welds.

Figure 5-34 shows a finite element model of a typical fillet weld. If this weld is used along the transverse edge of a tensile specimen, the loading will be such as to cause in-plane stresses in the cross-section. If this weld is used along the longitudinal edge of the specimen, the loading will be such as to cause shear stresses on the throat of the cross-section. Figure 5-35 shows a specimen with combination of both longitudinal and

transverse welds and the corresponding forces acting on these welds are indicated in Figure 5-36.

The finite element model was used to determine the relative stiffness of the weld for the two types of loading. Force on the weld model was applied normal to the vertical face of the weld model for transverse weld behaviour, while for longitudinal weld behaviour, this was applied along the length of weld acting on the plane of vertical face of weld. The maximum deflection in the direction of application of force was obtained. The ratio of applied force and maximum deflection (known as stiffness) of longitudinal weld was approximately twice (2 - 2.34) that of transverse welds of similar dimensions. Hence, the stiffer longitudinal weld was assumed to be more effective in the force transfer through the welds. Figure 5-37 shows the elastic stress variation for a plate connected using both longitudinal and transverse welds, with longitudinal weld-length to width ratio of 1.0. Similarly, Figure 5-38 shows the same variation for a plate subjected to similar conditions, except that the ratio of longitudinal weld-length to width is equal to 0.5. Comparison of the two stress variations indicates that increased length of longitudinal welds tends to decrease the effect of transverse weld. This tendency confirming the above assumption causes shear lag to be more dominant on the ultimate capacity of the specimen.

Based on the above conclusion, if the welded plate has both the transverse and longitudinal welds, the load transferred through a unit length of longitudinal weld is higher than that transferred through a unit length of transverse weld. However, if only one type of weld is present (longitudinal or transverse), all the force is transferred

through that weld. The component of the total force transferred through the longitudinal weld causes and exhibits shear lag behaviour. Therefore, irrespective of the presence of transverse weld, there will be a significant amount of shear lag effect if longitudinal weld is present. This effect becomes smaller if the longitudinal welds get shorter. This is the reason why specimen P120xT-b with shorter longitudinal weld experienced better efficiency compared to specimen P120-T-a with longer weld lengths. For elements connected by only transverse welds throughout the whole width, the net-section efficiency could be considered equal to unity.

**Table 5-15 Effect of Weld Configuration – Both Edges Welded**

Specimen	Plate size	$\frac{L}{w}$	$U_e$	Notes
P75-T	75.5x 12.97	0.4	0.98	With transverse weld
P75-1.0	77.5x 12.97	1.0	0.96	No transverse weld
P120-T-a	121.4x 12.97	0.84	0.95	With transverse weld
P120-T-b	120.3x 12.97	0.42	0.97	With transverse weld
P120-1-a	120.6x 12.97	1.0	0.94	No transverse weld
P-B-1	76.2x 6.6	1.0	0.90	Easterling's Test
P-B-2	76.2x 6.6	1.0	0.99	Results Data
P-B-3	76.2x 6.6	1.0	0.98	with Transverse weld

This observation has implications to the code design. From the above discussion it can be seen that the current practice of assuming full efficiency of transverse weld is not correct if longitudinal weld is present.

This can be illustrated using the following example of a plate specimen as shown in Figure 5-35 having both longitudinal welds and transverse weld (extending the complete width of the plate). Assume that the weld remains elastic and the force transmitted to the weld is proportional to its length. For the sake of simplicity, let the displacement  $\delta$  be uniformly transmitted to all the welds.

Let,  $k_l$  represent the stiffness of longitudinal weld per unit length,  
 $k_w$  represent the stiffness of transverse weld per unit length and  
 $\alpha$  the ratio of the length of longitudinal weld and the width of the plate.

If  $\delta$  is the total displacement, then the total force in the weld is,

$$F = (2k_l\alpha w + k_l w)\delta \quad \text{Eq. 5-6}$$

As mentioned earlier, elastic finite element analysis indicates that the stiffness of the longitudinal weld is at least twice the stiffness of the transverse weld.

Hence considering,  $k_l = k_t/2$ , then

$$\text{Force in the longitudinal welds } F_l = (2k_l\alpha w)\delta ,$$

$$\text{Force in the transverse weld } F_t = k_l w\delta = k_l w\delta /2 ,$$

and the total force in the weld group is given by,

$$F = \frac{4\alpha + 1}{2} k_l w\delta \quad \text{Eq. 5-7}$$

$$\text{Therefore, } F_l = \frac{4\alpha}{4\alpha + 1} F \quad ; \quad F_t = \frac{1}{4\alpha + 1} F$$

The stress in the plate due to the force being carried by transverse weld is:

$$\sigma_t = \frac{1}{4\alpha + 1} \frac{F}{A_g} \quad \text{Eq. 5-8}$$

Let the efficiency of the longitudinal welds by themselves be equal to  $U_{lo}$ . The overall efficiency is  $U_e$  while the efficiency of transverse weld is 1.0. At failure,

$$F_t = U_{lo} A_g (F_u - \sigma_t)$$

Using,  $U_e = F/A_g F_u$  we can show that,

$$U_e = \frac{4\alpha + 1}{4\alpha + U_{lo}} U_{lo} \quad \text{Eq. 5-9}$$

The above equation can be used to obtain an estimate of the combined efficiency when both transverse and longitudinal welds are present. For the efficiencies listed by CAN/CSA-S16.1-94, we get a marginal improvement by the addition of transverse welds as shown in the Table below:

$\alpha$	$U_{lo}$	$U_e$
2.00	1.00	1.00
1.50	0.87	0.89
1.00	0.75	0.79

Several possible scenarios need to be examined.

1. *Specimen with only transverse weld:* This situation arises if the element width is sufficient to provide a transverse weld capable of carrying the element's ultimate load. For such cases, the efficiency can be taken as unity. It must be noted that

this occurs rarely since it can lead to premature base metal failure if both gusset and specimen are of the same grade of steel.

2. *Specimen with mainly transverse weld and small longitudinal welds:* This might be the situation in cases where both gusset and specimen are of the same material. In such cases, we need longitudinal weld-lengths of at-least  $0.33w$  on either side (in addition to full transverse weld) to offset base metal failure. These longitudinal extensions are stiffer than the transverse weld. Therefore, they will attract larger amount of force per unit length than is normally assumed. As explained earlier, this leads to efficiencies that are less than unity. Increasing the length of longitudinal welds could lead to the longitudinal welds attracting larger portion of the total applied force and would diminish the contribution of the transverse welds. It is recommended that in such cases, the specimen be provided with full transverse weld and a longitudinal weld of length of  $0.5w$ . The recommended efficiency for this case is 93%.
3. *Specimens with mainly longitudinal weld (with small amounts of transverse weld):* This situation arises if the element has a limited amount of space available for longitudinal weld and needs a small amount of transverse weld to complete the capacity requirement. If small transverse weld extensions to the longitudinal weld are provided to achieve a small additional capacity, these extensions may not provide as much strength as was originally contemplated. Hence, a doubling of the computed length of transverse welds can be recommended. In most practical

situations, this might probably mean providing transverse weld along the full width of the connected plate (see below).

4. *Specimens with significant longitudinal welds and full transverse welds:* In case both the welds are significantly long, it is recommended that the efficiency be calculated using Eq. 5-9.

#### **5.3.6.2 Type-2 Configuration: Specimens with only Longitudinal Welds**

The similarity in behaviour of all connected-leg type plate specimens (Figure 5-21 showing 75mm width specimens and Figure 5-22 with 120mm width specimens) exhibiting net-section failure indicate that the effect of length of longitudinal weld on efficiency is minor.

Comparison of the elastic stress variation, Figure 5-37 for type 1 configuration ( $L/w = 1.0$ ) and Figure 5-39 for type 2 configuration ( $L/w = 1.0$ ), indicate that the ultimate capacity of specimens with sufficiently long longitudinal weld-lengths (i.e., weld-lengths sufficient to cause tensile failure Figure 5-1) are not affected significantly by the addition of transverse welds. Both experimental and numerical analyses indicate the above tendency of transverse weld behaviour. Thus, there is only a marginal difference in the ultimate capacity of the test specimens.

#### **5.3.6.3 Type-3 Configuration: Specimens with only Single Edge Longitudinal Welds**

Single-edge welded specimens (type-3 configuration) were also examined to study the behaviour of plates representing the outstanding-leg of angle specimens. These

specimens exhibited considerable bending due to out of plane eccentricity. The outer fiber of the outstanding leg was subjected to compressive strains up to a load of about 60% of the ultimate capacity of the section. Also, due to this eccentricity, the yield load of these specimens was not well defined (Figure 5-21 and Figure 5-22). As mentioned earlier (Figure 5-20), the efficiency of these members increased with length of connection up to a ratio  $L/w$  equal to 2.0.

**Table 5-16 Effect of Weld Configuration – One Edge Welded**

Specimen	Plate Size	$\frac{L}{w}$	$U_e$	Notes
P120-S	118x 12.97	2.0	0.85	
P120-2	120.2x 12.97	2.0	0.94	
P75-S-b	76x 12.97	1.83	0.97	
P75-2	76x 12.97	2.0	0.97	

#### 5.3.6.4 Angle Specimens

Angles with single edge weld configurations were not tested, since such configuration would necessitate long weld lengths due to bi-axial eccentricity. Such configuration is highly unlikely in practical conditions. Figure 5-26 compares the behaviour of equal angle specimen with and without transverse welds. Angles experienced increased efficiencies of about 1% to 5% with the addition of transverse welds. Finite element analysis on the behaviour of equal angle specimens showed no significant increase in ultimate capacity with addition of transverse welds. This trends shown by angle specimens could be attributed to the similarity shown by the behaviour of both plates

connected by longitudinal welds only and plates connected by combination of both longitudinal and transverse welds. Similar to plates, connected leg of the angle specimen had no significant increase in member capacity with the addition of transverse welds, thereby having negligible effect on the overall member capacity. This behaviour is consistent with that reported by Easterling and Gonzalez [1993].

**Table 5-17 Effect of Weld Configuration on Angle Specimens**

Specimen	Angle size	$\frac{L}{w_o}$	$U_e$	Notes
EA1	L101.4x101.6x 6.81	1.4	0.85	With transverse weld
EA2	L101.4x101.6x 6.81	1.35	0.80	No transverse weld
EA3	L151.6x151.4x 9.74	1.38	0.83	With transverse weld
EA4	L151.6x151.4x 9.74	1.40	0.82	No transverse weld
UEA1	L126.1x75.7x 6.58	1.67	0.91	With transverse weld
UEA3	L126.1x75.7x 6.58	2.0	0.9	No transverse weld
L-B-1a	L100x 75x 6	1.2	0.82	Easterling's Test
L-B-1c	L50x50x 5	1.5	0.81	Results Data
L-B-3	L50x50x 5	1.5	0.79	With Transverse Weld

### 5.3.7 Effect of Specimen Configuration

**Table 5-18 Effect of Specimen Configuration**

Specimen	Angle Size	$\frac{L}{w_o}$	$U_e$	Notes
UEA8	L102.1x152.4x 8.18	2.25	0.94	Free length of 480mm Free length of 760mm Longitudinal weld of 125mm Longitudinal weld of 135mm
UEA9	L152.4x102.1x 8.18	2.0	0.92	
UEA3	L126.1x75.7x 6.58	2.06	0.90	
UEA5	L75x125x 6.62	2.0	0.90	
UEA1	L126.1x75.7x 6.58	1.67	0.91	
UEA2	L75.6x126.1x 6.58	1.06	0.78	
Specimen	Angle Size	$\frac{L}{w_o}$	$U_e$	Notes
UEA3	L126.1x75.7x 6.58	2.06	0.90	Longitudinal weld of 155mm
UEA6	L75x125x 6.62	1.5	0.85	Longitudinal weld of 190mm

L127x76x6.4 and L152x102x7.9 were the two unequal-leg angles considered to study the effect of long-leg connected and short-leg connected configurations. In all such specimens, as can be expected, angles with long-leg as connected leg exhibited higher net-section efficiencies compared to their corresponding specimens whose short-leg was the connected leg. The above set of experimental results shows that specimens with equal  $L/w_o$  ratio have similar efficiencies. However, specimens with almost equal length of longitudinal weld but with different configurations exhibited considerable difference in their net-section efficiencies. This difference is attributed to the efficiency of the

outstanding leg, which is dependent on the length of weld connecting itself to the gusset plate.

### 5.3.8 Single and Double Specimen Configuration

**Table 5-19 Effect of Single and Double Specimen Configuration**

Specimen	Plate Size	$\frac{L}{w}$	$U_e$	Notes
P75-S-b	76x 12.97	1.8	0.97	Single Plate Specimen
DP75-S	76.1x 12.97	1.47	0.93	Double Plate Specimen
P120-1-a	120.6x 12.97	1.0	0.94	Single Plate Specimen
DP120-1	122x 12.97	1.0	0.95	Double Plate Specimen
Specimen	Angle Size	$\frac{L}{w_o}$	$U_e$	Notes
UEA2	L75.6x126.1x 6.58	1.06	0.78	Single Angle Specimen
DUEA2	L75.6x126.1x 6.58	1.0	0.75	Double Angle Specimen

Experimental results of plate and angle specimens showed no significant difference and pattern in shear lag effect on single and double member configuration. This is in spite of the fact that single members will undergo considerable bending at the connection zone. This can be explained by the fact that single members bend in such a way that well before the onset of partial yielding, the centroid of the member is drawn in line with the applied force. This is consistent with the results reported by Kulak and Wu [1997]. Finite element analysis on equal angle sections exhibited similar behaviour with approximately 2% difference in efficiency of double angle members.

## 5.4 Comparison of Current Net-Section Strength Formulae with Experimental Results

Approximately 64 plate specimens and 25 angle specimens (from current and previous studies) were considered to examine various net-section strength formulae. Of the available data only 29 plate specimens conformed to the current grades (300W and above) of steel. All the angle specimens considered for this study conformed to the requirements of 300W (or 350W) steel. Only those specimens that experienced net-section failures were considered in this evaluation.

### 5.4.1 Evaluation of $1 - \bar{x}/L$ Rule [Chesson and Munse, 1963]

Chesson and Munse [1963a] proposed Eq. 5-10 for predicting the net-section efficiency of outstanding leg type plate sections, angle legs and other structural sections.

$$U_e = 1 - \bar{x}/L \quad \text{Eq. 5-10}$$

Comparison of the efficiency predicted by this equation with the experimental results has been shown in Figure 5-40. The average ratio of predicted capacity to the experimental capacity is 0.95 with a standard deviation of 0.11. This equation reasonably predicts the efficiencies of welded connections, but has a larger than usual scatter.

The variation of predictions of net-section efficiency using Eq. 5-10 with  $L/w$  for plates and  $L/w_o$  for angle specimens is shown in Figure 5-41. Angles of various sizes and configurations were included in this comparison by use of  $\bar{x}/w_o$ . Angle sections currently available indicated the following ranges of  $\bar{x}/w_o$ .

0.27 to 0.34 for equal angle sections

0.21 to 0.30 for unequal angle sections with short leg as outstanding leg

0.29 to 0.38 for unequal angle sections with long leg as connected leg

The value  $\bar{x}/w_o$  is independent of the size of angle i.e., for eg.  $L25 \times 25 \times 3.2$  and  $L203 \times 203 \times 25$  both have same  $\bar{x}/w_o$  of 0.30. Hence, if the weld-length is, a constant 'k' times the width of outstanding leg, then the predicted efficiency of such sections with same  $\bar{x}/w_o$ , using Eq. 5-10 is equal. The calculated efficiency for  $\bar{x}/w_o$  equal to 0.30 is  $1 - 0.30/k$  and is given in the following table for various values of k. Table 5-20 shows that the effect of size on Shear Lag is neglected by the Eq. 5-10.

**Table 5-20 Net Section Efficiency based on Munse's Expression for Shear Lag.**

$k = L/w_o$	Net-section efficiency	Angle Size, $\bar{x}/w_o = 0.30$
1.0	0.7	$L25 \times 25 \times 3.2$ ,
1.5	0.8	$L102 \times 102 \times 13$
2.0	0.85	$L152 \times 152 \times 19$ , & $L203 \times 203 \times 25$

Use of this expression for prediction of net-section capacity has various limitations.

1. Although there is only a limited amount of experimental data, it can be seen that the equation overestimates the efficiency of specimens having low  $F_y/F_u$  ratio and underestimates the capacity of plate with high  $F_y/F_u$  ratio connected on one edge only. Importance of the ratio of  $F_y/F_u$  is not considered in predicting the net-section capacity of the member though this equation.
2. The effect of size of specimens on efficiency as explained in Section 5.3.1 is not properly indicated by this rule.
3. Effect of members with and without transverse welds was not differentiated.
4. This expression fails to predict the net-section efficiency of plates connected with longitudinal welds on both edges. This is recognized in CSA-S16.1 that uses this formula only in case of weld on one edge.
5. Although the trends of this rule and the finite element analysis appear to be similar, for plates as outstanding legs, the equation shows an increase in capacity as against a constant capacity shown by finite element analysis beyond  $L/w$  ratio of 2.0.

#### **5.4.2 Net-Section Strength Formula by Kulak and Wu [1997]**

Kulak and Wu [1997] proposed an expression for net-section efficiency of bolt-connected angle members in tension.

$$U_e = \frac{A_{cn} + \beta \frac{F_y}{F_u} A_o}{A_n}$$

where,  $A_{cn}$  is the net area of connected leg,

$\beta$  is a factor based on the length of connection,

$A_o$  is the area of the outstanding leg,

$A_n$  is the total net cross-sectional area of the specimen ( $A_{cn} + A_o$ )

In evaluating Eq. 5-11 for welded members, the value of  $\beta$  has been considered to be unity if the length of connection was equal to or greater than twice the width of the outstanding leg, and value of 0.75 for all other lengths. These values of  $\beta$  were considered on the basis of the current specifications and the example of Wu and Kulak for bolted members. Also, Figure 5-20 shows that the efficiency of outstanding leg type specimens had their best efficiencies when the weld-length was approximately twice the width of the plate and had a marked decrease in efficiency at lower weld-lengths. The net-section strength predicted by this expression is compared with the test results in Figure 5-42. The average ratio of these predicted results to the test results was 0.95 with a standard deviation of 0.05. The disadvantage of this expression is its discontinuity in the value of  $\beta$ . Also, this expression is applicable only to angle sections **and** the efficiency of the connected leg was assumed to be unity.

## 5.5 Evaluation of Current Specifications

Current design provisions have been compared with the experimental results. CSA standard CAN/CSA-S16.1-94 suggests the use of coefficients that are dependent on the length of connection for plate specimens and Munse's expression for outstanding-leg type plate specimens. Two methods to obtain the net-section efficiency of angle sections are suggested.

Angle specimen is assumed to be a combination of two plates (connected-leg type and outstanding-leg type) with its total efficiency being calculated as a cumulative sum of the independent efficiencies of both plates. In actual condition, the efficiency of the outstanding leg varies (tends to decrease) under the combined action of both legs of the angle. This behaviour is discussed in more detail in Section 5.6.6. Hence, caution should be exercised in adopting the current provisions of superimposing the effects of each leg of the angle in determining its net section efficiency. The prediction of such approach in comparison with the experimental results is shown in Figure 5-43. The average ratio of these predictions of angles with experimental results was 0.90 with a standard deviation of 0.10. However on plate specimens this expression showed considerable deviation with a standard deviation of 0.22. It is also noticed that the predictions of the current provisions are conservative, but overestimates the capacity of angles and plates connected by welds of length ratios  $L/w$  greater than 2.

Use of Munse's Equation Eq. 5-10 is also allowed by CSA-S16.1 to obtain the net-section efficiency of angle sections. This is done by considering  $\bar{x}$  to be the distance between the centroid of the entire cross-section (connected and outstanding leg together).

AISC-LRFD method adopts the use of Munse's equation (Eq. 5-10) exclusively to obtain the net-section capacity of the structural sections (excluding connected leg type plate specimens) in tension. Figure 5-44 compares the predicted results with experimental results. With a mean value of 0.97 on angle specimens and 0.96 on plate specimens, this rule is quite suitable for predicting the net-section capacity. However, since the effect of grade of steel was not considered, considerable scatter of results exists with a standard deviation of 0.07 for angles and 0.18 for plate sections. As this specification adopts Munse's expression for prediction of net-section efficiency, most of the limitations outlined in the discussion on use of Munse's expression (Section 5.4.1) are applicable to this method.

The design provisions for welded members in tension as per ANSI/ASCE 10-90 specifications is shown Figure 5-45. The method adopted for bolted connection was assumed for welded connection, and this yielded highly conservative result, with an average efficiency of 0.79 and standard deviation of 0.08.

## **5.6 Proposed Net-Section Strength Formula**

The discussion of experimental and FEA results presented above indicates that several parameters such as: the yield strain of the material, the strain at the on set of strain hardening behaviour, the eccentricity of connection generated because of the gusset thickness, single or double member configuration and free length of member, etc., do not have a significant effect on the shear lag.

The Shear Lag in welded steel plates and angles is mainly influenced by:

physical parameters - Size (or width) of the specimen and the length of connection (in  
outstanding leg type specimens)

and material parameters -  $F_y/F_u$  and Breaking Strain

A generalized expression for net-section efficiency of plates welded either on both edges  
or on one edge (i.e., plates that look like the connected leg or outstanding leg of angles)  
considering the above parameters can be given by:

$$U_e = C^* K_w K_l K_b K_g \quad \text{Eq. 5-12}$$

where,  $C^*$  is the proportionality constant

$K_g$  is the steel grade parameter

$K_w$  is the size effect parameter

$K_b$  is the breaking strain parameter

$K_l$  is the connection length parameter. Parameters  $K_g$ ,  $K_w$ ,  $K_b$ ,  $K_l$  are described in  
the following section

### 5.6.1 Size Effect Parameter $K_w$

Experimental and analytical results as shown in Figure 5-15 to Figure 5-18 show that  
net-section capacity decreases with increase in the size of the specimen. It can be  
expressed as

$$K_w = a_1 \left( 1 - \frac{w}{200t} \right) \quad \text{for Connected-Leg type Plates, and}$$

$$K_w = \left(\frac{t}{w}\right)^{0.08} \quad \text{for Outstanding-Leg type Plates} \quad \text{Eq. 5-13}$$

where,  $w$  is the width of the outstanding leg,  $t$  is the thickness of the leg

$$a_1 = 0.975 \text{ (these constants can be absorbed in to } C' \text{ of Eq. 5-12)}$$

### 5.6.2 Connection Length Parameter

Results from this study and the study by Easterling and Gonzalez (1993) indicate that plates welded on both edges with weld lengths causing tensile failure showed negligible increase in the net-section capacity of the section with increasing weld lengths.

CAN/CSA-S16.1-94 predicts no Shear Lag Effect in such plates, when the weld length is greater than twice the width of the member. Experimental results showed that such specimens failed at efficiencies slightly lower than 1.0.

The present study indicated that the increase in connection length increased the section capacity in the case of out-standing leg type plate specimens. This increase was similar to the predictions of Munse's equation. Hence, such variation in plate specimens could be expressed as given below.

$$K_l = a_3 \text{ for connected leg type plates,} \\ = a_3 \left(1 - \frac{w}{2L}\right) \text{ for Outstanding-leg type plates,} \quad \text{Eq. 5-14}$$

where,  $L$  is the length of connection,  $t$  is the thickness of the leg, constant  $a_3 = 0.95$

### 5.6.3 Steel Grade Parameter

Of the various material parameters considered in this study, steel grade expressed as a ratio of  $F_y/F_u$  was a major factor influencing shear lag effect. Influence of this parameter can be included using

$$K_g = 0.35 + 0.7 \left( \frac{F_y}{F_u} \right) \quad \text{Eq. 5-15}$$

where,  $F_y$  and  $F_u$  are the yield strength and ultimate strength of the material, respectively

### 5.6.4 Breaking Strain Parameter

The effect of breaking strain has been described in Section 5.3.3. This effect of breaking strain on shear lag can be simply expressed as

$$\begin{aligned} K_b &= 1.0 \text{ when breaking strain is } \geq 22\% \\ &= 0.95 \text{ when breaking strain is } < 22\% \end{aligned} \quad \text{Eq. 5-16}$$

It must be noted that it is highly likely that the slopes of the ascending portion of the strain hardening zone and the descending line during the failure (necking) influence the actual failure load. These influences are effectively being considered by the parameters  $K_g$  and  $K_b$ .

The proportionality constant for connected leg specimens and out-standing leg specimens obtained using the experimental results is 1.26 and 1.65 respectively.

### 5.6.5 Combined Formula for Plates

Substituting the various parameters discussed in Section 5.6, the net-section efficiency expression, Eq. 5-12 can be simplified and is given below for the case with yield stress ( $F_y$ ) 300 MPa and ultimate stress ( $F_u$ ) of 450 MPa.

For Connected Leg type plate specimens, simplified net-section efficiency is

$$U_e = 0.9 \left( 1 - \frac{w}{200t} \right) \quad \text{Eq. 5-17}$$

For Outstanding Leg type plate specimens,

$$U_e = 1.28 \left( \frac{t}{w} \right)^{0.08} \left( 1 - \frac{w}{2L} \right) \quad \text{Eq. 5-18}$$

### 5.6.6 Efficiency of Angles

Similarly for angle specimens with yield stress of 300 MPa and ultimate stress of 450 MPa, the net-section efficiency expression is

$$U_e = \frac{\left( 0.9 \left( 1 - \frac{w}{200t} \right) A_{cs} + 1.28 \beta \left( \frac{t}{w'} \right)^{0.08} \left( 1 - \frac{w'}{2L} \right) A_o \right)}{A_{net}} \quad \text{Eq. 5-19}$$

where,  $w' = w - t$  and the term  $\beta$  accounts for difference in behaviour of an outstanding leg specimens acting independently and the outstanding leg acting in combination with the connected leg type plate occurring with the angle specimen.

$A_{net}$  is the net cross-sectional (c/s) area accounting for reduction due to the presence of holes and other openings near the connection zone.  $A_{cn}$  being the net c/s area of connected leg and  $A_o$  as the net c/s area of out-standing leg, both after the reduction for any holes.

Figure 5-22 shows that when the connected leg (P120-1.5) attained its ultimate capacity, then at the corresponding displacement the outstanding leg type specimen (DP120-S) had attained only 96% of its maximum capacity. The weld length on both P120-1.5 and DP120-S were equal. Hence, the value of  $\beta$  equal to 0.95 is considered in obtaining the net-section efficiency of the angle specimens. Experimental study on other structural sections may be necessary to obtain the  $\beta$  value for use in the new expression.

Comparison of this study with the test results is shown in Figure 5-46. With average ratio of the predicted values to test results of 0.99 for plates and 0.95 for angle specimens, this expression accounting for all the parameters affecting shear lag has a narrower scatter band with a standard deviation of 0.06 and 0.14 for angles and plates respectively. It is thus seen that the steel grade, size and the length of connection is incorporated in obtaining the net-section efficiency.

## 5.7 Recommended Design Method

The factored resistance of the plate specimens calculated in a format consistent with the current specifications can be expressed as

$$T_r = 0.85 \phi \left( 0.9 \left( 1 - \frac{w}{200t} \right) A_{cn} + 1.28 \beta \left( \frac{t}{w} \right)^{0.08} \left( 1 - \frac{w'}{2L} \right) A_o \right) F_u \quad \text{Eq. 5-20}$$

A study of 230 angle sizes listed by CISC Handbook [CISC 2000] showed that the term  $0.9\left(1 - \frac{w'}{200t}\right)$  in the proposed expression (Eq. 5-19) for net-section efficiency varied from 0.89 to 0.98 with an average value of 0.95. Similarly for the outstanding plate portion of the angle, the term  $1.28\left(\frac{t}{w'}\right)^{0.08}$  varied between 0.99 to 1.15 with an average value of 1.07. For design purposes, a simplified expression opting on the conservative side is proposed using the lower coefficients of 0.9 and 1.0, respectively, as calculated above. Using these, Eq. 5-19 can be reduced to the following form

$$U_e = \frac{0.9 A_{cs} + \beta\left(1 - \frac{w'}{2L}\right)A_o}{A_{net}} \quad \text{Eq. 5-21}$$

The factored resistance of the net-section is then calculated in a format consistent with the current specifications, and is of the form

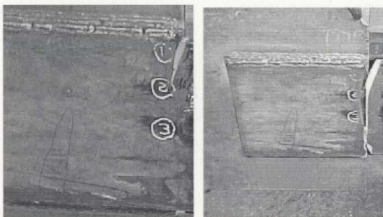
$$T_r = 0.85 \phi \left(0.9 A_{cs} + \beta\left(1 - \frac{w'}{2L}\right)A_o\right)F_u \quad \text{Eq. 5-22}$$

where,  $\phi$  known as the resistance factor is equal to 0.90.

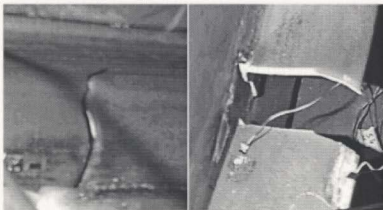
The following table (Table 5-21) compares the net-section efficiency predictions of both the proposed net-section expression and the Munse's equation. It can be seen that for  $F_y$  and  $F_u$  equal to 300 MPa and 450 MPa respectively, the predictions are quite similar. However, as indicated in Section 5.4.1, Munse's equation (Eq. 5-10) neglects the effect of angle size and grade of steel on shear lag effect. Most of the major limitations of the Munse's equation outlined in Section 5.4.1 can be addressed by the use of the proposed expression given by Eq. 5-19.

**Table 5-21 Efficiency Predictions for Proposed Net-section and Munse's Expression**

Angle Designation	Connected Leg, mm	Net-section efficiency for connection length					
		L = 1.0w		L = 1.5w		L = 2.0w	
Equal-leg angle		Eq. 5-20	Eq. 5-10	Eq. 5-20	Eq. 5-10	Eq. 5-20	Eq. 5-10
203x 203 x28.6	203	0.73	0.70	0.80	0.80	0.83	0.85
203x 203 x12.7	203	0.71	0.73	0.78	0.82	0.82	0.86
152x 152 x7.94	152	0.71	0.73	0.78	0.82	0.82	0.87
102x 102 x6.35	102	0.71	0.73	0.78	0.82	0.81	0.86
50.8x 50.8 x4.76	50.8	0.72	0.71	0.79	0.81	0.82	0.86
38.1x 38.1 x4.76	38.1	0.73	0.70	0.79	0.80	0.83	0.85
31.8x 31.8 x4.76	31.8	0.74	0.70	0.80	0.80	0.83	0.85
25.4x 25.4 x4.76	25.4	0.75	0.68	0.80	0.79	0.83	0.84
203x 152 x25.4	203	0.77	0.72	0.82	0.82	0.84	0.86
203x 152 x11.1	203	0.74	0.76	0.80	0.84	0.83	0.88
152x 102 x22.2	152	0.79	0.72	0.83	0.81	0.85	0.86
102x 76.2 x6.35	102	0.74	0.75	0.80	0.84	0.83	0.88
76.2x 50.8 x4.76	76.2	0.76	0.76	0.81	0.84	0.84	0.88
203x 152 x25.4	152	0.70	0.67	0.78	0.78	0.82	0.83
203x 152 x11.1	152	0.68	0.69	0.76	0.80	0.80	0.85
152x 102 x6.35	102	0.66	0.68	0.75	0.79	0.80	0.84
102x 76.2 x6.35	76.2	0.68	0.69	0.76	0.79	0.80	0.85
76.2x 50.8 x4.76	50.8	0.67	0.68	0.76	0.78	0.80	0.84



**Net-section failure propagation in Plate Specimen P250-1**



**Net-section failure propagation in Angle Specimen UEA5**

**Figure 5-1 Propagation of Net-Section Failure**



Figure 5-2 Failure of Angle in Tension-type Tearing



Figure 5-3 Failure of Weld under Bending and Shear

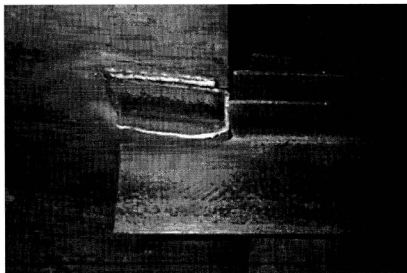
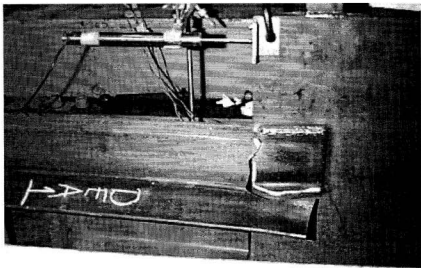


Figure 5-4 Failure of Angle in Shear-type Tearing

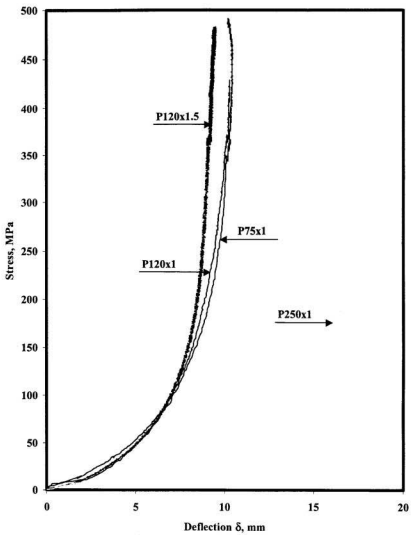


Figure 5-5 Lateral Deflection of Plate Specimens

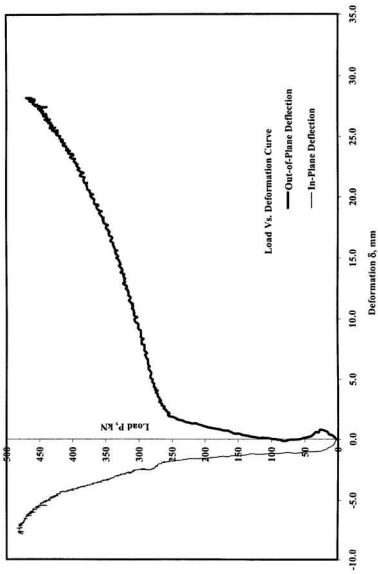
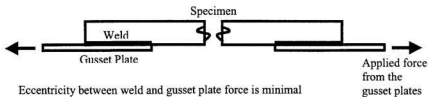
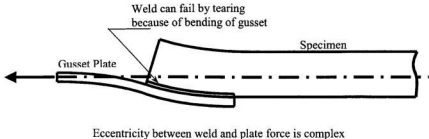


Figure 5-6 Load Deformation Curve for Specimen UEA2



**Figure 5-7 Specimen Loaded Through Gusset Plates**



**Figure 5-8 Specimen loaded through Gusset Plates**

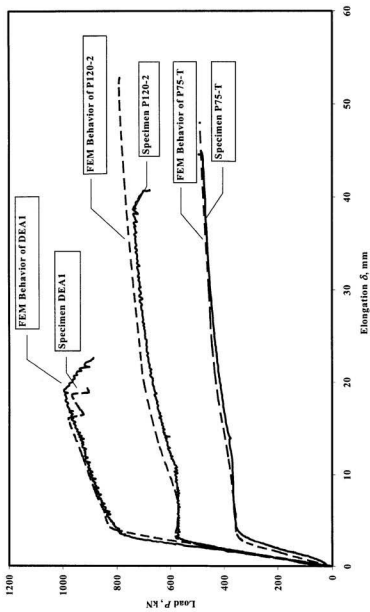
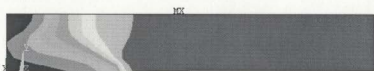


Figure 5-9 Comparison of Load-Elongation Curve from FEA and Experimental Results.



ANSYS 5.6.1	DMX =24.159
NOV 25 2001	SMN =-19.286
09:00:10	SMX =539.927
NODAL SOLUTION	
STEP=1	42.849
SUB =9	104.984
TIME=.25	167.118
SX (AVG)	229.253
MIDDLE	291.388
RSYS=0	353.523
PowerGraphics	415.658
EFACET=1	477.793
AVRES=Mat	539.927

Figure 5-10 Stress Variation at Ultimate Load for Specimen P120-1 (FEA)



ANSYS 5.6.1	DMX =25.58
NOV 25 2001	SMN =3.822
09:46:41	SMX =554.538
NODAL SOLUTION	
STEP=1	3.822
SUB =8	65.012
TIME=.275	126.203
SX (AVG)	187.394
MIDDLE	248.584
RSYS=0	309.775
PowerGraphics	370.966
EFACET=1	432.156
AVRES=Mat	493.347
	554.538

Figure 5-11 Stress Variation at Ultimate Load for Specimen P120-1.5 (FEA)

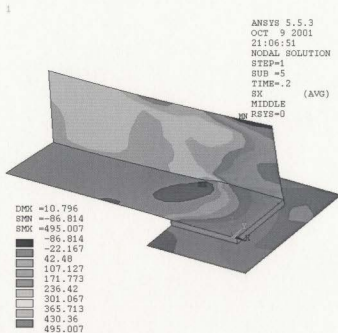


Figure 5-12 Stress Variation at Ultimate Load for Specimen DEAI

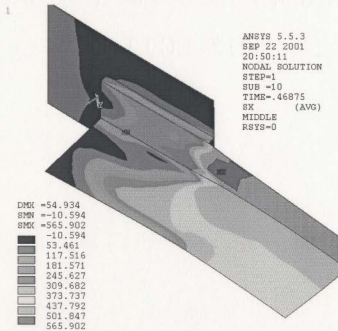


Figure 5-13 Stress Variation at Ultimate Load for Specimen UEA4

ANSYS 5.6.1  
DEC 7 2001  
20:38:44  
NODAL SOLUTION  
STEP=1  
SUB =10  
TIME=.45  
SX (AVG)  
MIDDLE  
RSYS=0  
PowerGraphics  
EFACET=1  
AVRES=All

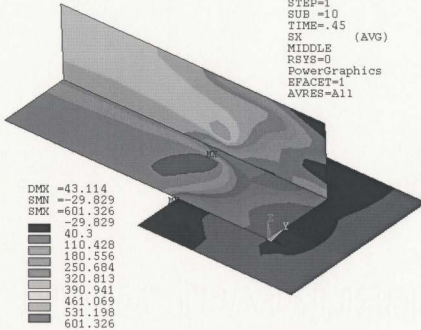


Figure 5-14 Stress Variation at Ultimate Load for Specimen EA1

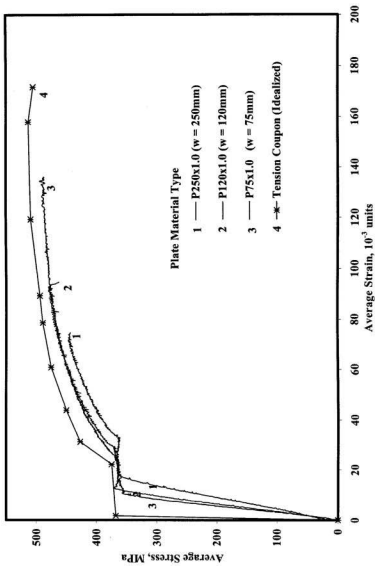


Figure 5-15 Effect of Size of Specimen on Shear Lag

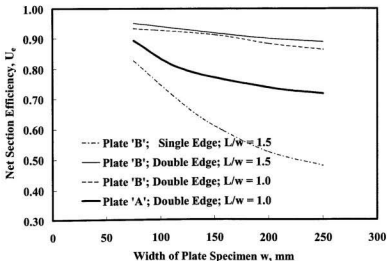


Figure 5-16 Effect of Width of Plate on Shear Lag (FEA)

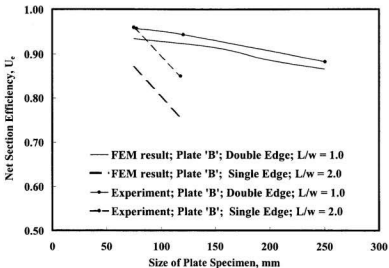


Figure 5-17 Comparison of Experimental and FEA Results on Size of Specimen

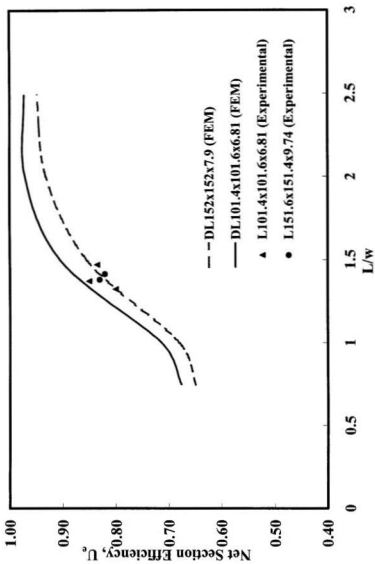


Figure 5-18 Effect of Size of Angles on Shear Lag

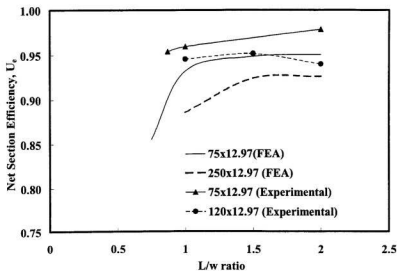


Figure 5-19 Effect of Length of Connection on Plate Welded on Both Edges

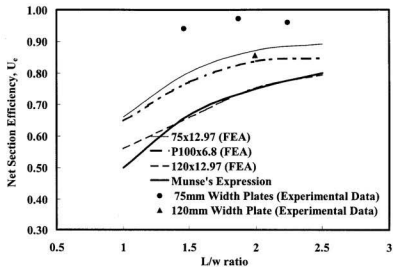


Figure 5-20 Effect of Length of Connection on Plates Welded Only on Single Edge

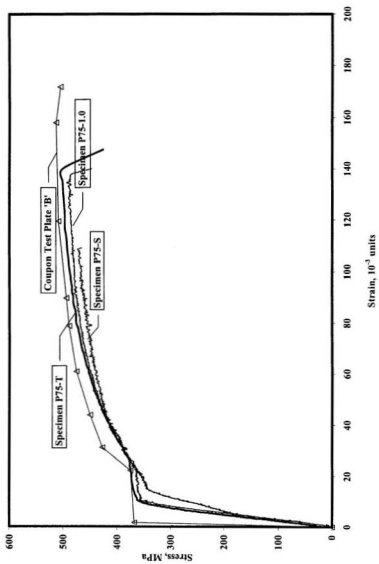


Figure 5-21 Behavior of 75mm Wide Plate Specimens

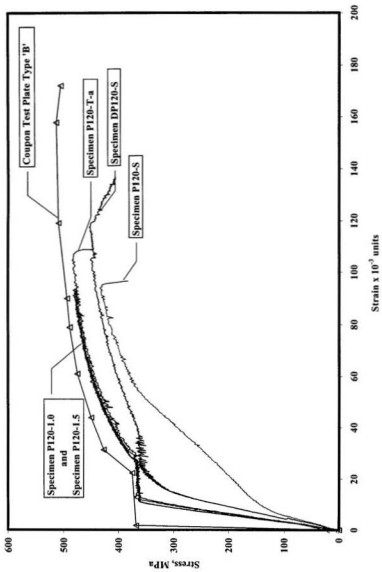
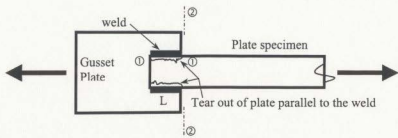
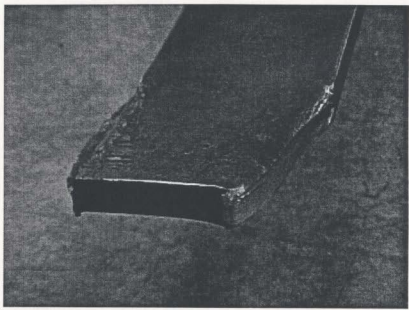


Figure 5-22 Behavior of 120mm wide Plate Specimen



**Figure 5-23 Plate Tear-Out in Shearing Mode**



**Figure 5-24 Failure of Specimen P75-0.87 in Shear-type Tearing**

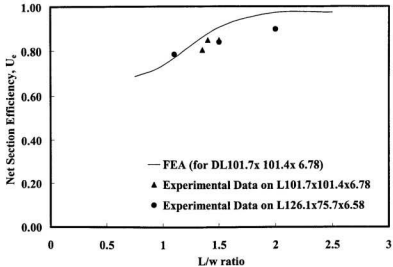


Figure 5-25 Effect of Length of Connection on Angles

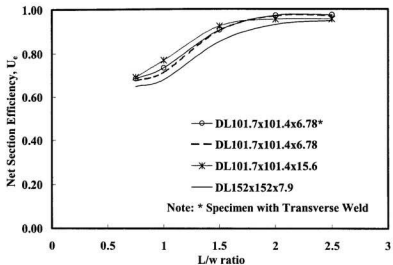


Figure 5-26 Effect of Length of Connection on Angles (FEA Study)

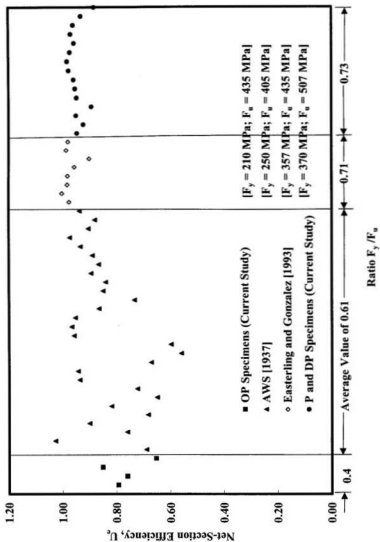


Figure 5-27 Effect of  $F_y/F_u$  (Steel Grade) on Efficiency of Plate Specimens

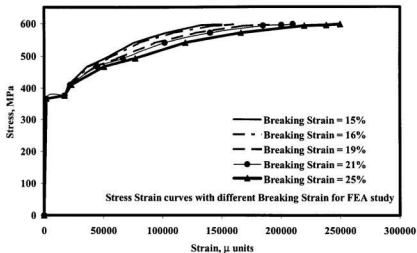
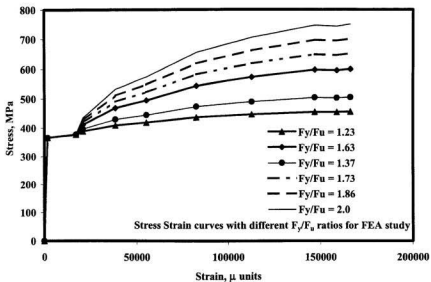


Figure 5-28 Stress Strain Pattern for FEA Parametric Study

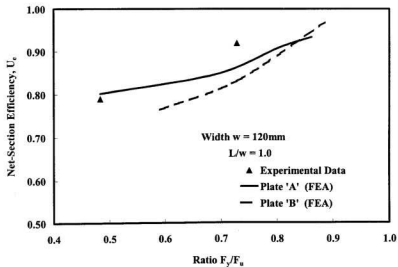


Figure 5-29 Effect of  $F_y/F_u$  on Plate Specimens ( $F_u$  kept Constant)

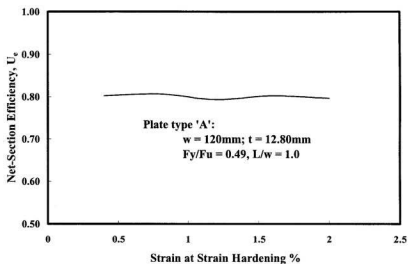


Figure 5-30 Effect of Initial Strain at Strain Hardening

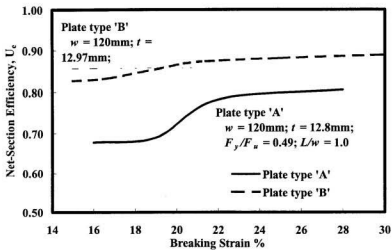


Figure 5-31 Effect of Breaking Strain on Shear Lag

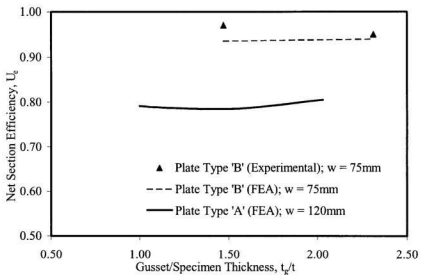


Figure 5-32 Effect of Eccentricity on Shear Lag

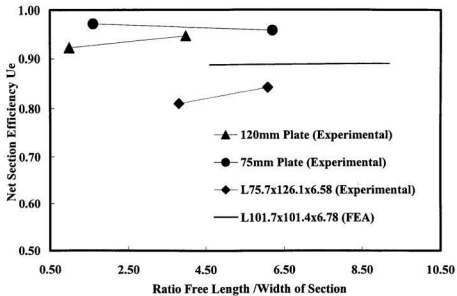


Figure 5-33 Effect of Free Length on Shear Lag

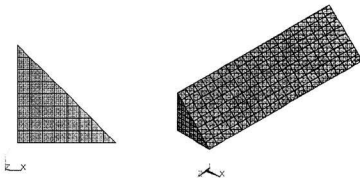
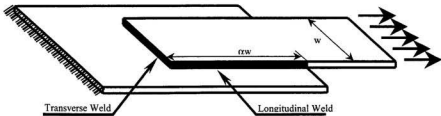
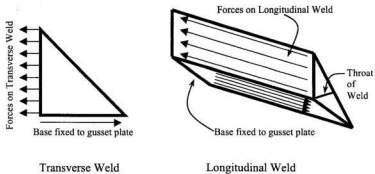


Figure 5-34 Finite element Model of a Typical Fillet Weld



**Figure 5-35 Plate Specimen with Both Longitudinal and Transverse Welds**



**Figure 5-36 Forces and Reactions on Transverse and Longitudinal Welds**

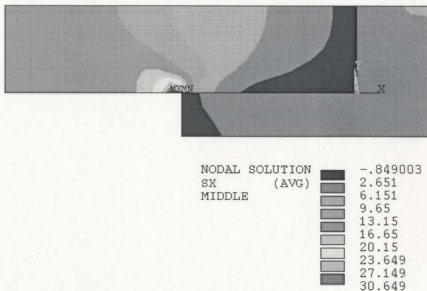


Figure 5-37 Elastic Stress Variation in a Plate connected by both Longitudinal and Transverse Welds ( $L_{longitudinal\ weld-length} / w = 1.0$ )

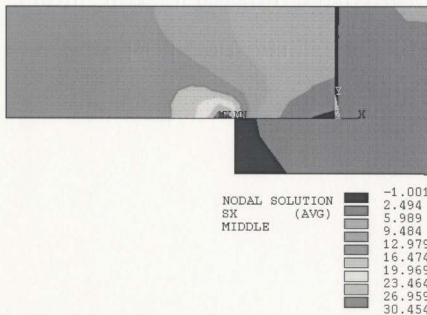


Figure 5-38 Elastic Stress Variation in Plate connected by both Longitudinal and Transverse Welds ( $L_{longitudinal\ weld-length} / w = 0.5$ )



Figure 5-39 Elastic Stress Variation in a Plate connected by both only Longitudinal Welds ( $L$ =longitudinal weld-length /  $w = 1.0$ )

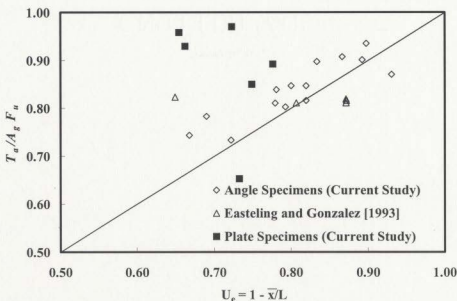


Figure 5-40 Comparison of  $1 - \bar{x}/L$  with Experimental Results

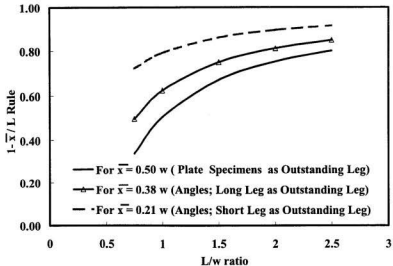


Figure 5-41 Variation of Munse's Expression for Plate and Angle Specimens

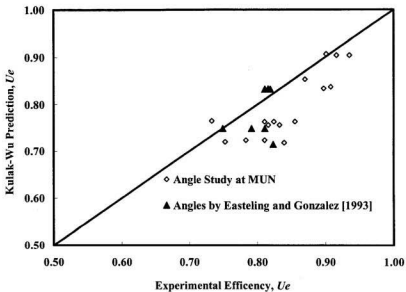


Figure 5-42 Comparison of Kulak Predictions with Test Results



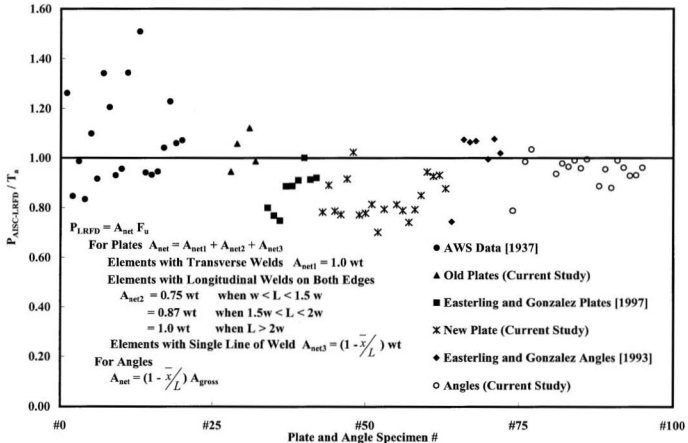


Figure 5-44 Comparison of AISC/LRFD Predictions with Test Results

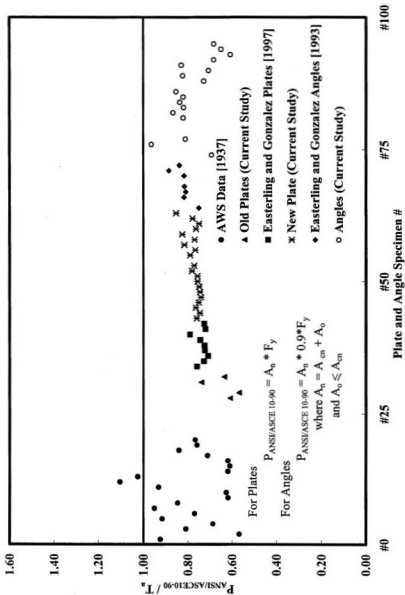


Figure 5-45 Comparison of ANSI/ASCE 10-90 Predictions with Test Results

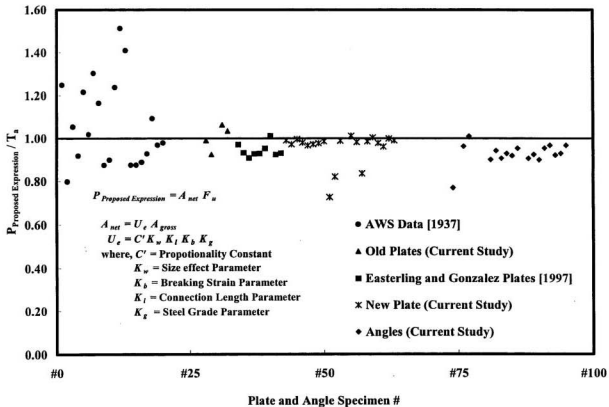


Figure 5-46 Comparison of Proposed Expression with Test Results

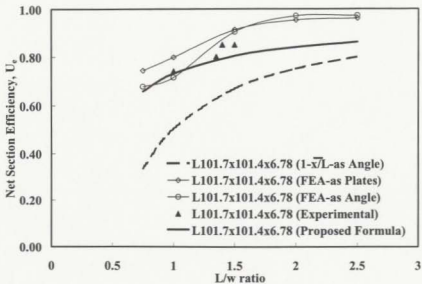


Figure 5-47 Comparison of Theoretical Predictions with Experimental Results

#### Comparison of Mean Values

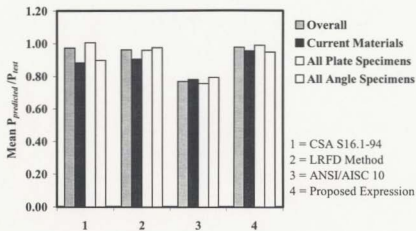


Figure 5-48 Comparison of Mean Values of Predictions of Current Design Standards and Proposed Expression

### Comparison of Standard Deviation (Scatter Band)

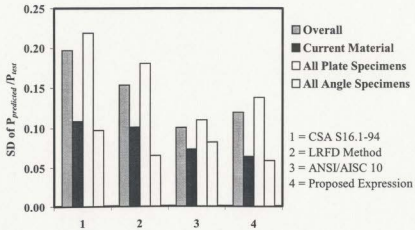


Figure 5-49 Comparison of Standard Deviation of Predictions of Current Design Standards and Proposed Expression

## Chapter 6

### Conclusions and Recommendations

#### 6.1 Summary

In the present thesis, the effect of Shear Lag on the net-section strength of plates and angle members connected by welds has been studied using experimental and theoretical investigations. Various influencing factors are investigated. The experimental study included twenty-seven plate specimens (75 mm, 120 mm and 250 mm wide) and twenty-two angle specimens (angle sizes involving L102x102x6.4, L152x152x9.5, L127x76x6.4 and L152x102x7.9). Both single and double member specimens were tested. All tests were under direct tension. Eccentricity is caused by the configuration of the connection. Nonlinear finite element models have been calibrated for validation and parametric study. Elastic theoretical analysis has also been carried out. The study included the effects of both physical and material parameters. Physical parameters such as length of connection ranging from  $0.87w$  to  $4.0w$ , free length of member varying from  $4w$  to  $7w$ , specimen sizes as described above, disposition of the angle section (Long Leg Connected and Short Leg Connected), weld configuration and the effect of thickness of gusset plate were investigated. The width of the specimen is taken as  $w$ . Material parameters such as grade of steel, location of strain hardening, effect of breaking strain (15-25% elongation) were studied numerically using non-linear finite element techniques. Only experimental study involving the material parameter was to study the effects of

grade of steel measured as a ratio of  $F_y/F_u$ . Comparisons have been made with the current design practices, and recommendations for design rules have been formulated.

## **6.2 Conclusions**

Based on the experimental results and the numerical analysis, the following conclusions are arrived at:

### **Failure Mechanisms**

1. All specimens yielded completely before the ultimate capacity of the specimen was attained. Yielding propagates from the critical net-section to the mid-length of the specimen.
2. Connected leg type plate specimens with weld lengths less than the width of the specimens tends to exhibit shearing type failure by tearing of the plate occurring along its length of weld. Such failure can be expected in out-standing leg type plate specimen with length of weld less than 1.5 times the width of the plate specimen. Such specimens have lower efficiencies and low ductility compared to similar specimens experiencing tensile failure.
3. When the welds on both heel and toe of the angle specimen are equal, the toe of the angle is the most common failure initiation point. The effective area available for load transfer at the toe is less than the area available at the heel. Since, the actual force transfer is same at the heel and the toe of the angle, stresses developed at the toe are higher resulting in yielding prior to the heel of the angle.

4. In all angle specimens failing at their net-section, complete rupture occurred through the connected leg prior to the outstanding leg. Such behavior was noticed even in large size angle specimens and unequal angle specimens with its long-leg as the connected leg. This behavior is exhibited even if the independent efficiency of the out-standing leg is less than the independent efficiency of the connected leg.
5. In some angles, failure occurred through pullout of the welds. This indicates that although the design equations used in practice neglect the effect of eccentricity that causes weld tear-out, it can be the governing failure mode in certain cases. The eccentricity in such cases, causes significant out of plane bending along with some twisting well before the onset of tear out. Such bending reduces the overall eccentricity of the applied load with respect to the centroid of the resisting force. As this is difficult to estimate, for weld design a minimum out of plane eccentricity caused by the distance between the member centroid and the weld line is recommended conservatively.

### **Physical Parameters**

6. *Plates with both longitudinal and transverse welds:*
  - The net-section provisions in Canadian Standard CSA-S16.1-94 neglect the shear lag in plates connected with both longitudinal and transverse welds and thereby overestimates the ultimate capacity. Tests show that such members are susceptible to Shear Lag effect.
  - The elastic stiffness of the longitudinal weld is at least twice as much as that of the transverse weld. Therefore, the longitudinal weld attracts considerably more force than the transverse weld. Hence, for specimens with small widths and

significant longitudinal welds, the addition of transverse welds (full or partial) does not result in significant increase in ultimate capacity.

- Experimental tests on 120 mm and 75 mm wide plate specimens with full transverse welds and longitudinal welds ranging between  $0.4w$  to  $0.8w$  showed efficiencies between 95% and 98%. In view of this, if a member is connected by transverse welds only, the efficiency can be taken as 100%. If longitudinal welds of length  $0.5w$ - $1.0w$  are also present, the efficiency can be taken as 95%. For longitudinal welds greater than  $1.0w$ , the effect of transverse weld can be neglected. This recommendation is applicable to all connected legs of angles as well as plates of small widths (upto 150mm).
7. Increasing weldlengths in plate specimens connected at both their longitudinal edges to values greater than the minimum length required for causing tensile failure showed no significant increase in the net-section capacity. Similarly, the efficiency of outstanding leg-type specimens increased significantly with increase in weldlength only up to weldlengths that was equal to twice the width of the specimen. The variation in net-section efficiency of angle specimens was significant only upto weldlengths equal to 1.5 times the width of the outstanding leg.
  8. The net-section capacity is affected by the size of the specimen. Increase in width of the section increases the effect of Shear Lag. This effect is prominent in the experimental results on plate specimens. It is also shown by the finite element study on various angle sizes having similar material properties.
  9. Double and single plate and angle specimen configurations have no significant effect on their ultimate capacities. However, double angle specimens experience lower out of plane deformations in comparison to single angle specimens.

10. Within the practical ranges of parameters, the effect on net-section capacity is negligible with variations in the thickness of specimens, length of specimens and thickness of the gusset plates. The stiffness of the gusset plate was studied by varying the length of the gusset member and the boundary conditions. This numerical study shows minor changes with the net-section efficiency.
11. Shear Lag effect is more prominent in specimens with lower yield stress to ultimate stress ratios. With the improvements in current steel quality and grades occurring with increasing  $F_y/F_u$  ratio, the effect of Shear Lag is expected to be less prominent, yielding higher net-section efficiencies. This is particularly true, when breaking strain (ductility) of the specimen is maintained.
12. Increase in the breaking strain beyond strain value of 22% has no significant effect on the ultimate capacity of the member. However, at lower values of breaking strain, the effect is dependent on the grade of steel. Based on numerical analysis, the decreased efficiency can be assumed to be 95% of the situation with 22% breaking strain.
13. For Long Leg Connected and Short Leg Connected unequal angle sections with equal connection lengths, the net section efficiency of the member with its long leg connected is higher than that of the short leg connected specimen. This is primarily because of the difference in the  $L/w_o$  ratio and also the size effect of the legs of the specimen.
14. Partial yielding of the angles during a few loading and unloading cycles does not seem having an appreciable effect on the ultimate capacity.

### **Comparison of Current Design Specifications**

15. Munse's equation [Munse and Chesson, 1963] for bolted members was used for welded angles. The net-section efficiencies predicted were similar to those of the experimental results. However for lower grades, i.e., lower ratios of  $F_y/F_u$ , this expression overestimates the net-section efficiencies. The effect of transverse welds on the net-section efficiency cannot be considered by this equation. The average ratio of the predicted capacity to the experimental capacity of only angle specimens is 0.95 with a standard deviation of 0.11.
  
16. The current provisions in CAN/CSA-S16.1-94 predict the efficiency of angle sections by superimposing the individual efficiencies of the connected leg and the outstanding leg. This approach is more appropriate than Munse's equation [Munse and Chesson, 1963] for predicting the net-section efficiency. The average ratio of the predicted capacity to the experimental capacity of only angle specimens is 0.90 with a standard deviation of 0.18.
  
17. ANSI/ASCE 10-90 design specification is highly conservative in predicting the net-section efficiencies. The average ratio of the predicted capacity to the experimental capacity of only angle specimens is 0.79 with a standard deviation of 0.08.

### **6.3 Suggested Changes to the Current Design Practice**

The recommended minimum weldlength for plates connected only along their longitudinal edges is  $1.0w$ . For outstanding leg-type plates with single line of welds, the minimum recommended weldlengths is  $1.5w$ . This minimum weldlength (or connection

length) would avoid shearing type failure in the specimens and also provide additional ductility before rupture of the specimen.

Net-section efficiency can be considered to be equal to unity for plates or elements connected by use of transverse welds only.

For elements or plates connected by combination of transverse and longitudinal welds, a factor of 0.90 is suggested for specimens with longitudinal weldlengths less than  $1.0w$ . However, for longitudinal weldlengths greater than width of the plate specimen, the effect of transverse welds may be neglected in determining the net-section efficiency.

Consideration of a minimum out-of-plane eccentricity caused by the distance between the member centroid and the weld line is recommended for the design of welds connections in angle specimens.

It is proposed that the efficiency of plates with only longitudinal welds and angles be calculated using the equation  $U_e = C' K_w K_l K_s K_g$  that accounts for effect of size, connection length, and material grade effects on shear lag.

where,  $C'$  the proportionality constant is 1.26 for connected-leg and 1.65 for outstanding leg,

Size effect parameter,  $K_w = 0.975 \left( 1 - \frac{w}{200t} \right)$  for Connected-leg type plates, and

$$K_w = \left( \frac{t}{w} \right)^{0.08} \quad \text{for Outstanding-leg type plates}$$

Connection length parameter,  $K_l = 0.95$  for Connected-leg type plates, and

$$K_l = 0.95 \left( 1 - \frac{w}{2L} \right) \quad \text{for Outstanding-leg type plates,}$$

Steel grade parameter,  $K_g = 0.35 + 0.7 \left( \frac{F_y}{F_u} \right)$

Breaking strain parameter,  $K_b = 1.0$  and  $0.95$ , when breaking strain  $\geq 22\%$ , and  $< 22\%$  respectively.

For yield stress,  $F_y = 300$  MPa and ultimate stress  $F_u = 450$  MPa, the above expression can be expressed in the following form.

For Connected-leg type plates,  $U_e = 0.9 \left( 1 - \frac{w}{200t} \right)$

For Outstanding-leg type plates,  $U_e = 1.28 \left( \frac{t}{w} \right)^{0.08} \left( 1 - \frac{w}{2L} \right)$

For angle sizes given in the CISC Handbook [CISC, 2000] the recommended expression

in simplified form is  $U_e = \frac{0.9 A_{cn} + \beta \left( 1 - \frac{w'}{2L} \right) A_o}{A_{net}}$

In the above equations,  $\phi$ , the resistance factor is equal to 0.90.

$w' = w - t$ , with  $w$  and  $t$  as width thickness of the plate under consideration.

$\beta = 0.95$  for angles,  $L$  is the length of connection and

$A_{cn}$ ,  $A_o$  and  $A_{net}$  as the net area of connected leg, out-standing leg and total area respectively, after accounting for reduction due to holes

## 6.4 Recommendations for Further Research

With the current knowledge on plate and angle section, it is possible to obtain the efficiency of channel sections connected along their web in tension. However, channels

connected by the flange and tee sections wherein the outstanding leg is not directly connected by welds, additional tests are necessary to obtain the factor  $\beta$  necessary to obtain its efficiency.

The behavior of members having a stiffer gusset plate may require additional tests to confirm the behaviour on shear lag effect. Additional tests are recommended on very large plates and extra large angle specimens to study their behaviour on shear lag effect.

Some additional experimental analysis is recommended to study the effect of length of connection and size of member on out-standing leg type plate specimens.

More analysis, both experimental and numerical, are required to study the combined effect of transverse welds and longitudinal welds on the behaviour of the specimen and its ultimate capacity.

## References

ABAQUS, 1999. *ABAQUS User's Manual, Vol. 1, 2 & 3, Theory Manual, Verification Manual, ABAQUS Post Manual*, Hibbit, Karlsson & Sorensen, Inc., Pawtucket, RI, USA.

Albert, C., 1996. "New Provisions for Shear Lag in Steel Tension Members," *Can. J. of Civil Eng.*, Vol. 23, pp. 305-309, Ottawa, Canada.

AISC-LRFD, 1993. *Load and Resistance Factor Design Specification for Structural Steel Buildings*, American Institute of Steel Construction (AISC), Chicago.

ASCE/ANSI 10-90, 1991. *Design of Latticed Steel Transmission Structures*, ASCE Standard, American Society of Civil Engineers, New York.

ANSYS Manuals, 1997. *User's Manual, Vol. 1 & 2, Theory Manual, User manuals for Theory, Commands, Elements and Procedures, Verification Manual, Structural analysis guide, Basic analysis procedures guide*, Swanson Analysis System, Inc., and ANSYS Inc., Houston, PA.

American Bureau of Welding, 1931. *Report of Structural Steel Welding Committee*, American Welding Society, New York.

ASTM-E-8M-96, *Standard Test Methods for Tension testing of Metallic Materials [Metric]*, Annual book of ASTM Standards

CISC, 2000. *Handbook of Steel Construction*, Seventh Edition, Canadian Institute of Steel Construction (CISC), Willowdale, Ontario, Canada.

CSA, 1994. *CAN/CSA-S16.1-94 Limit States Design of Steel Structures*, Canadian Standards Association, Rexdale, Ontario, Canada.

Davis, R.P., and Boomsliker, G.P., 1934. "Tensile tests of Welded and Riveted Structural Members," *J. of American Welding Society*, Vol. 13, April, pp. 21-27.

Easterling, W.S., and Gonzalez, L.S., 1993. "Shear Lag Effects in Steel Tension Members," *Eng. J. of American Institute of Steel Construction*, Third Quarter, pp. 77-89, Chicago.

Gonzalez, L., and Easterling, W.S., 1989. *Investigation of the Shear Lag Coefficient for Welded Tension Members*, M.S. Thesis, Virginia Polytechnic Institute and State University, Virginia, USA.

Gibson, G.J., and Wake, B.T., 1941. "An Investigation of Welded Connections for Angle Tension Members," *Welding Research Supplement*, October, pp. 44s-49s.

Hildebrand, F.B., 1943. *The Exact Solution of Shear-Lag Problems in Flat Panels and Box Beams assumed Rigid in the Transverse direction*, NACA Report No. 894, Technical Note, National Advisory Committee for Aeronautics, MIT, Cambridge, MA, USA.

Kulak, G.L., Adams, P.F., and Gilmor, M.L., 2000. *Limit States Design in Structural Steel*, Canadian Institute of Steel Construction, Universal Offset Ltd., Seventh Edition, Willodale, Ontario, Canada.

Kulak, G.L., and Wu, E.Y., 1997. "Shear Lag in Bolted Angle Tension Members," *J. Structural Eng.*, American Society of Civil Engineers, Vol.123, No.9, pp. 1144-1152, New York.

Marsh, C., 1969. "Single Angle Members in Tension and Compression," *J. Struct. Div.*, American Society of Civil Engineers, Vol. 95(ST5), May, pp. 1043-1049, New York.

Munse, W.H., and Chesson, E.Jr., 1963a. "Riveted and Bolted Joints: Net Section Design." *J. Struct. Div.*, American Society of Civil Engineers, Vol. 89(ST1), February, pp. 107-126.

Munse, W.H., and Chesson, E.Jr., 1963b. "Riveted and Bolted Joints: Truss-type Tensile Connections," *J. Struct. Div.*, American Society of Civil Engineers, Vol. 89(ST1), February, pp. 67-106.

Madugula, M.K.S., and Mohan, S., 1988. "Angles in Eccentric Tension." *J. Struct. Eng.*, American Society of Civil Engineers, Vol. 114, pp. 2387-2396, New York.

McCormac, J., 1992. *Structural Steel Design: ASD Method*, HarperCollins Publishers, Fourth Edition, USA.

SCI, 1992. *Steel Designers' Manual*, The Steel Construction Institute, Blackwell Scientific Publications, Fifth Edition, Cambridge, U.K.

Timoshenko, S., and Goodier, J.N., *Theory of Elasticity*, McGraw-Hill Book Co. Inc., Second Edition, Tokyo.

Young, W.C., 1989. *Roark's Formulas for Stress and Strain*, Sixth ed., McGraw-Hill Book Company, USA.

Wu, Y., and Kulak, G.L., 1993. *Shear Lag in Bolted Single and Double Angle Tension Members*, Struct. Eng. Rep. No. 187, Dept. of Civ. Engg., U. of Alberta, Edmonton, Canada.

## Appendices

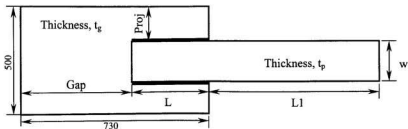
The generalized input file of “Plate Specimens” for numerical analysis involving both, material and geometric non-linearity is shown in APPENDIX A. Similarly APPENDIX B is the generalized input file for “Angle Specimens”. The effect of weld was studied using an elastic finite element model whose input file is shown in APPENDIX C. APPENDIX D summarizes the stress strain properties of all plates and angle specimens considered for this shear lag study.

APPENDIX E and APPENDIX F shows the failure of most plate and angle specimens, respectively.

## APPENDIX A

### FE Model of Plate connected by Longitudinal Welds

only



/TITLE CAPACITY OF SPECIMEN CONNECTED ON ONE EDGE ONLY

!\* MODEL DESCRIPTION

```
*set,w,250          !* Width of the Plate Specimen, mm
*set,l,250          !* Weld Length, mm
*set,l1,480/2       !* Free Length, mm
*set,tp,12.97      !* Plate Thickness, mm
*set,tg,19.1       !* Gusset Thickness, mm
*set,ecc,(tp+tg)/2
*set,gap,730-l     !* Free Length of Gusset, mm
*set,proj,250-w/2  !* Excess width of Gusset/2, mm
```

/prep7

```
nwd = NINT(w/(2*10))    !* Number of divisions along 1/2 width (w)
ngp = NINT(proj/25)    !* Number of divisions for projection (proj)
wn = NINT(l/20+1)      !* Number of node lines for the weld length
fl_nod = NINT(l1/20)   !* Number of node lines for the specimen free length
spn = wn + fl_nod      !* Total number of node lines along the length of the test
                        specimen
!*gelm = NINT(gap/10)  !* Number of divisions for the gusset free length for UTM
                        specimens
```

```
gelm = NINT(gap/35)      !* Number of divisions for the gusset free length for
                          Actuator specimens
gused = 2000+gelm+wn-1  !* Last node number for the first set of gusset plate nodes
```

!\* DEFINING THE MATERIAL PROPERTIES OF THE TEST SPECIMEN

```
ET,1,SHELL181
R,1,tp,tp,tp,,
mp,ex,1,210000
tb,miso,1
```

```
C*****
C*** Specimen properties shall be based on true stress and logarithmic strain      **
C*** True stress = engineering stress * (1+ engineering strain);                  **
C*** while logarithmic strain = ln(1+engineering strain)                        **
C*****
tbpt,defi,366/210000,366
tbpt,defi,0.017174667,375
tbpt,defi,0.020858932,409
tbpt,defi,0.038497375,467
tbpt,defi,0.055487686,492
tbpt,defi,0.082843704,540
tbpt,defi,0.112722251,570
tbpt,defi,0.146976723,594
tbpt,defi,0.158932657,595
tbpt,defi,0.16,6
```

!\* DEFINING THE MATERIAL PROPERTIES OF THE GUSSET PLATE

```
et,2,shell181
r,2,tg,tg,tg,,
mp,ex,2,2E+5
tb,biso,2
tbdata,1,400
```

!\* DEFINING THE MATERIAL PROPERTIES OF THE WELD MATERIAL

```
et,3,shell181
r,3,6,17,17,6
mp,ex,3,2e+5
```

!\* NODES FOR THE GENERATION OF THE TEST PLATE

```
n,1,0,0
n,wn,-1,0
fill,,,,,,,,1/2
n,spn,-1,1,0      !* spn = indicate specimen nodes
fill,wn,spn,,,,,2
ngen,nwd+1,spn,1,spn,1,,w/(2*nwd)
```

```

!* DEFINING THE PLATE SPECIMEN ELEMENTS
type,1
real,1
mat,1
e,1,2,spn+2,spn+1
egen,spn-1,1,1
egen,nwd,spn,1,spn-1
!* NODES FOR THE GENERATION OF THE GUSSET PLATE
!* Defining the first node number for the gusset plate as 2000
n,2000,gap,-proj,ecc
n,2000+gelm,0,-proj,ecc
fill,2000,2000+gelm,,,,,1/2
n,gusend,-1,-proj,ecc
fill,2000+gelm,gusend,,,,,1/2
ngen,ngp+1,gelm+wn,2000,gusend,1,,proj/ngp
gsend = gusend+ngp*(gelm+wn)
ngen,nwd/2+1,gelm+wn,2000+ngp*(gelm+wn),gsend,1,,w/(nwd)

```

```

!* DEFINING THE GUSSET ELEMENTS
gusset1=(spn-1)*nwd + 1      !* First gusset element
type,2
real,2
mat,2
e,2000,2001,gusend+2,gusend+1
egen,gelm+wn-1,1,gusset1
egen,ngp+nwd/2,gelm+wn,gusset1,gusset1+(gelm+wn-2)

```

```

!* DEFINING THE WELD ELEMENTS
weld1=(spn-1)*nwd+(nwd/2+ngp)*(gelm+wn-1)+1 !* Defining the first weld element
type,3
real,3
mat,3
e,1,2,2000+ngp*(gelm+wn)+gelm+1,2000+ngp*(gelm+wn)+gelm
egen,wn-1,1,weld1

```

finish

```

/solu !* Defining the solution procedure
antype,static
nset,all

```

```

!* DEFINING THE BC ALONG CENTER LINE OF THE PLATE SPECIMEN
nset,s,loc,x,-(l+1)
d,all,ux,0

```

```

d,all,roty,0
d,all,rotz,0

!* DEFINING THE BC ALONG THE MID SECTION OF THE PLATE
nset,all
nset,s,loc,y,w/2
d,all,uy,0
d,all,rotx,0
d,all,rotz,0

!* DEFINING THE BC ALONG THE GRIP ENDS OF THE SPECIMEN.
nset,all
nset,s,loc,x,gap
d,all,uy,0
d,all,uz,0
d,all,rotx,0
d,all,rotz,0

!* LOAD APPLICATION THROUGH DISPLACEMENT APPROACH
d,all,ux,30
nset,all
nlgeom,on
nropt,auto
nsubst,20,500
autots,on
neqit,100
lnsrch,on
outres,nsol,1
outres, strs,1
outres,epel,1
outres,eppl,1
outres,nload,1
eset,all
solve
nlist,all
finish

!* PROCESSING OF ANALYSIS RESULTS
/post26
round1 = 2*nwd + 4
k = 0
p = 0

timerange,0,1
prtime,0,1

```

```

numvar,100
!* Assigning the values to numerical variables
*do,i,1,nwd,1
esol,2*I,I*(spn-1),I*spn,f,x,
esol,2*I+1,I*(spn-1),(I+1)*spn,f,x,
*enddo

*do,j,2,2*nwd+1,3
k= k+1
add,round1 + k, j, j+1 j+2 ,,,2,2,2
*enddo

!* Next set first variable number is
*do,m, round1+1, round1 + k, 3
p = p + 1
add,round1+k+3+p, m, m+1, m+2,,,,1,1,1
prvar,round1+k+3+p
*enddo

*if,p,LE,3,then
add,round1+k+3+p+1,round1+k+1+p,round1+k+2+p,round1+k+3+p,,,,1,1,1
prvar,round1+k+3+p+1
*endif
finish

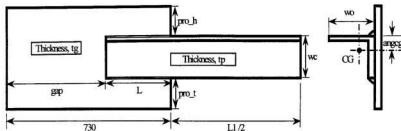
```

## APPENDIX B

### FE Model of Angle Specimens

```

C*****
C*** Input the following physical parameters, such as          **
C*** Angle Dimensions, Weld sizes and Weld Lengths, Material Properties, **
C*** Angle Configuration i.e., (double/single angle), with/without transverse welds **
C*****
  
```



title ULTIMATE CAPACITY OF ANGLE SECTION IN TENSION

!\* MODEL DESCRIPTION

```

C*****
C*** Input type: Angle A1 and its Material Properties          **
C*****
*set,wc,151.6          !* Width of Connected Leg of Angle Specimen, mm
*set,wo,151.4          !* Width of Outstanding Leg of Angle Specimen, mm
*set,l,153             !* Weld Length, mm
*set,angcg,45.1        !* CG of Angle from its Heel, mm
*set,l1,480/2          !* Free Length, mm
*set,tp,9.74           !* Angle Thickness, mm
*set,tg,19.1           !* Gusset Thickness, mm
*set,ecc,(tp+tg)/2     !* Free Length of Gusset, mm
*set,gap,730-l         !* Gusset Projection @ Heel, mm
*set,pro_h,250-angcg   !* Gusset Projection @ toe, mm
*set,pro_t,250+angcg-wc
  
```

/prep7

```

nwdc = NINT(wc/10) )      !* Number of divisions for width of connected leg, (wc)
nwdo = NINT(wo/10)       !* Number of divisions for width of outstanding leg, (wo)
wn = NINT(l/20+1)       !* Number of node lines for the weld length
fl_nod = NINT(l/20)     !* Number of node lines for the specimen free length
spn = wn + fl_nod      !* Total number of node lines along the length of the test specimen
!* Parameters defining modeling of Gusset Plate
ngph = NINT(pro_h/25)   !* Number of divisions for projection @ heel
ngpt = NINT(pro_t/25)   !* Number of divisions for projection @ toe
!*gelm = NINT(gap/10)   !* Number of divisions for gusset free length for UTM
Specimens.
gelm = NINT(gap/35)!* Number of divisions for gusset free length for Actuator
Specimens.
gusend = 2000+gelm+wn -1 !* Last node number for the first set gusset plate nodes

```

!\* DEFINING THE MATERIAL PROPERTIES OF THE TEST SPECIMEN

```

ET,1,SHELL181
R,1,tp,tp,tp,, ,
mp,ex,1,210000
tb,miso,1
C*****
C*** Specimen properties shall be based on true stress and logarithmic strain      **
C*** True stress = engineering stress * (1+ engineering strain);                  **
C*** while logarithmic strain = ln(1+engineering strain)                          **
C*****
!* For A1 type material only
tbpt,defi,358/210000,358
tbpt,defi,0.012916,364.680
tbpt,defi,0.019607,404.861
tbpt,defi,0.042197,478.783
tbpt,defi,0.079088,548.726
tbpt,defi,0.128393,601.473
tbpt,defi,0.211071,644.670
tbpt,defi,0.235862,644.394

```

!\* DEFINING THE MATERIAL PROPERTIES OF THE GUSSET PLATE

```

et,2,shell181
r,2,tg,tg,tg,, ,
mp,ex,2,2E+5
tb,biso,2
tbdata,1,400

```

!\* DEFINING THE MATERIAL PROPERTIES OF THE WELD MATERIAL

```

et,3,shell181
!* Weld Size depends on the Thickness of the Angle Specimen

```

```
r,3,6,17,17,6
mp,ex,3,2e+5
```

```
et,4,shell181
r,4,6,17,17,6
mp,ex,4,2e+5
```

```
!* NODES FOR THE GENERATION OF THE TEST PLATE
```

```
n,1,0,0
n,wn,-1,0
fill,,,,,,,,1/2
n,spn,-1-1,0          !* spn = indicate specimen nodes
fill,wn,spn,,,,,2
ngen,nwdc+1,spn,1,spn,1,,wc/nwdc
```

```
!* DEFINING THE NODES FOR OUTSTANDING LEG OF ANGLE SPECIMEN
```

```
ngen,nwdo+1,spn,nwdc*spn+1,(nwdc+1)*spn,1,,,wo/nwdo
```

```
!*   DEFINING THE ANGLE ELEMENTS
```

```
type,1
real,1
mat,1
e,1,2,spn+2,spn+1
egen,spn-1,1,1
egen,nwdc+nwdo,spn,1,spn-1
```

```
!*   NODES FOR THE GENERATION OF THE GUSSET PLATE
```

```
!*   Defining the first node number for the gusset plate as 2000
```

```
n,2000,gap,-pro_t,-ecc
n,2000+gelm,0,-pro_t,-ecc
fill,2000,2000+gelm,,,,,1/2
n,gusend,-1,-pro_t,-ecc
fill,2000+gelm,gusend,,,,,1/2
!* Creating nodes for gusset plate beyond toe
ngen,ngpt+1,gelm+wn,2000,gusend,1,,pro_t/ngpt
!* Creating nodes for gusset plate below connected angle leg
wnf = (gelm+wn)
ngen,nwdc+1,gelm+wn,2000+ngpt*wnf, gusend + ngpt*wnf,1,,wc/nwdc
!* Creating nodes for gusset plate beyond heel
ng = ngpt + nwdc
gsend1 = gusend + ng*wnf
ngen,ngph+1,gelm+wn,2000+ng*wnf,gsend1,1,,pro_h/ngph
```

```
!*   DEFINING THE GUSSET ELEMENTS
```

```
type,2
```

```

real,2
mat,2
gusset1= (spn-1)*(nwdc+nwdo) + 1  !* First Gusset Element
widthg= (ngpt+nwdc+ngph)
e,2000,2001,gusend+2,gusend+1
egen,gelm+wn-1,1,gusset1
egen,widthg,gelm+wn,gusset1,gusset1+(wnf-2)

!*   DEFINING THE WELD ELEMENTS AT TOE
weld1 =gusset1-1+widthg*(wnf-1)+1      !* First Weld Element # @ toe
type,3
real,3
mat,3
e,1,2,2000+ngpt*wnf+gelm+1,2000+ngpt*wnf+gelm
egen,wn-1,1,weld1

!*   DEFINING THE WELD ELEMENTS AT HEEL
weld2 = weld1 + wn-1                    !* First Weld Element # @ heel
type,4
real,4
mat,4
e,nwdc*spn+1,nwdc*spn+2,2000+ng*wnf+gelm+1,2000+ng*wnf+gelm
egen,wn-1,1,weld2

!*   THE FOLLOWING IS FOR TRANSVERSE WELD CONNECTION ONLY **
type,3
real,3
mat,3
*do,k,0,nwdc-1,1
Inode = k*spn + 1
IIInode = 2000 + (ngpt + k)*wnf + gelm
IIIInode = 2000 + (ngpt + k + 1)*wnf + gelm
IVnode = (k+ 1)*spn + 1
e,Inode,IIInode,IIIInode,IVnode
*enddo
finish

/solu                                !* Defining the solution procedure
antype,static
nset,all

!*   DEFINING THE BC ALONG CENTER LINE OF THE ANGLE SPECIMEN
nset,s,loc,x,-(l+l1)
d,all,ux,0
d,all,roty,0

```

```

d,all,rotz,0
nset,all

C*****
C*** The following condition should be applied for double angles      **
C*****
nset,s,loc,z,-ecc
d,all,uz,0
d,all,rotx,0
d,all,roty,0

!*   DEFINING THE BC ALONG THE GRIP ENDS OF THE SPECIMEN.
nset,all
nset,s,loc,x,gap
d,all,uy,0
d,all,uz,0
d,all,rotx,0
d,all,rotz,0

!*   LOAD APPLICATION THROUGH DISPLACEMENT APPROACH
d,all,ux,20

nset,all
nlgeom,on
nropt,auto
nsubst,10,500
autots,on
neqit,100
lnsrch,on
outres,nsol,1
outres, strs, 1
outres,epel,1
outres,eppl,1
outres,nload,1
esel,all
solve
finish

```

## APPENDIX C

### FE Model for Evaluating Weld Stiffness

```
/title, COMPARISON OF STIFFNESSES OF LONGITUDINAL & TRANSVERSE
      WELDS
*set,s,20
*set,ne,8           !* Max Number of Elements/row
*set,l,100          !* Weld Length
*set,nlength,l/5    !* Number of Elements along Length of Weld

/prep7
ct,1,solid45
ex,1,2,10000

!*   GENERATING NODES FOR THE WELD MODEL.
n,1,0,0
n,ne+1,s,0
fill
ngen,ne+1,ne+1,1,ne+1,1,,s/ne,
nsel,all
var1 = (ne+1)*(ne+1)
ngen,nlength,var1,1,var1,1,,l/nlength

!*   GENERATING WELD ELEMENTS
c,1,2,ne+3,ne+2,var1+1,var1+2,var1+ne+3,var1+ne+2
egen,ne-1,1,1
*do,1,1,ne-2,1
egen,2,1*(ne+1),1,ne-1-1,1
*enddo

!*   DEFINING THE FIRST WEDGE ELEMENT
*do,1,1,ne,1
var1a = var1+1*ne
var1b = var1a + ne
e,1*ne,1*ne+1,(1+1)*ne+1,(1+1)*ne+1,var1a,var1a+1,var1b+1,var1b+1
*enddo
nsel,all
esel,all
lastelem = ne*(ne+1)/2
```

```

!*   GENERATING ELEMENTS ALONG THE LENGTH
egen,nlength-1,var1,1,lastelem,1
csel,all
finish

/solu                               !* Defining the solution procedure

!*   DEFINING THE BC's
nset,s,loc,y,0
d,all,all,0

!*   LOAD APPLICATION THROUGH DISPLACEMENT APPROACH
nset,all
nset,s,loc,x,0
!* For longitudinal weld
!* f,all,fz,100
!* For transverse weld
f,all,fx,-100
nset,all
solve
save
finish

/post1
prnsol,u,comp
finish

```

## APPENDIX D

### True Stress vs. Logarithmic Strain of Plates and Angles

Plate Type 'A'		Plate Type 'B'	
Stress MPa	Strain $\mu$ units	Stress MPa	Strain $\mu$ units
0	0	0	0
210	1,000	366	1,830
212	4,000	375	17,174
334	29,000	409	20,859
424	60,000	467	38,498
472	106,000	492	55,488
535	215,000	540	82,844
545	278,000	570	112,722
5	289,000	596	166,361
		6	173,953

Table D-1 Stress Vs. Strain for Plate Specimens

Angle 'A1'		Angle 'B1'		Angle 'C1'	
Stress MPa	Strain $\mu$ units	Stress MPa	Strain $\mu$ units	Stress MPa	Strain $\mu$ units
0	0	0	0	0	0
358	1,704	358	1,704	350	1,667
364	9,160	370	22,153	357	20,293
404	19,607	402	28,587	388	27,421
478	42,197	464	54,393	455	54,204
548	79,088	519	94,583	506	90,298
601	128,393	551	133,044	539	125,751
644	211,071	589	199,670	585	211,071
10	215,000	10	200,000	589	241,376
				10	250,000

Table D-2 Stress Vs. Strain for Angle Sections

Angle 'F1'	
Stress MPa	Strain $\mu$ units
0	0
361	1,719
370	22,249
414	31,254
454	43,852
493	60,932
518	78,859
535	89,760
571	129,138
617	239,535
10	250,000

Angle 'E1'	
Stress MPa	Strain $\mu$ units
0	0
357	1,700
365	22,348
408	31,111
469	51,738
533	87,461
571	123,986
589	144,100
622	202,941
10	210,000

Angle 'D1'	
Stress MPa	Strain $\mu$ units
0	0
360	1,714
369	20,783
401	28,587
455	49,742
500	79,550
548	129,272
586	200,489
593	220,741
10	225,000

Table D-3 Stress Vs. Strain for Angle Section

## APPENDIX E

### Failure Pictures of Plate Specimens

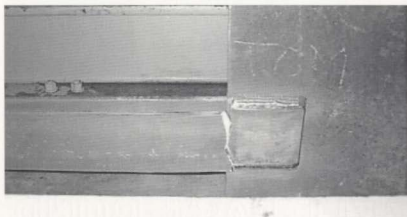
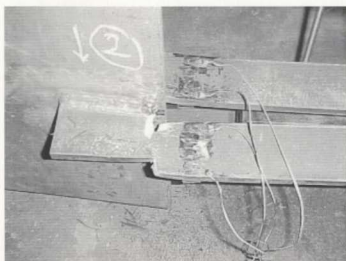


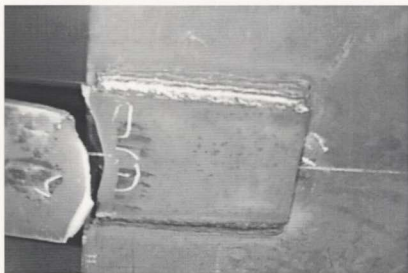
Figure E-1 Failure of Specimen DP120-1



Figure E-2 Failure of Specimen P120-S



**Figure E-3 Failure of Specimen DP75-S**



**Figure E-4 Failure of Specimen P120-1.5**

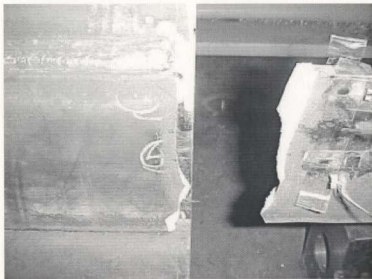


**Figure E-5 Failure of Specimen P120-1a**



**Figure E-6 Failure of Specimen P120-T-b**



**Figure E-7 Failure of Specimen P250-1**



**Figure E-8 Failure of Specimen P75-S-b**

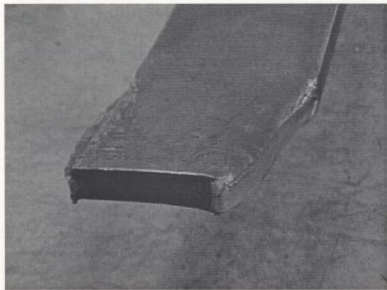


Figure E-9 Failure of Specimen P75-0.87

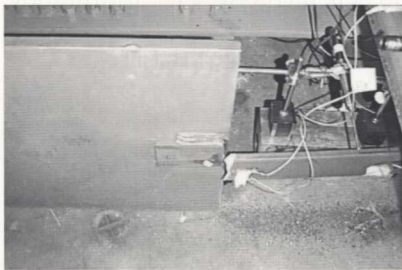


Figure E-10 Failure of Specimen P75-1

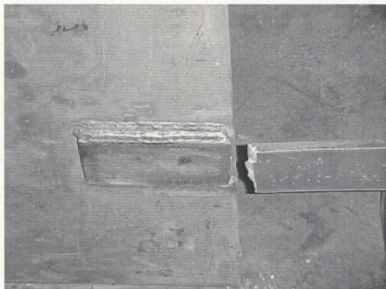


Figure E-11 Failure of Specimen P75-2

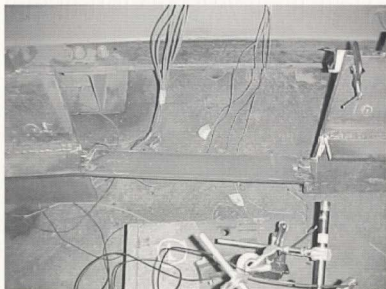


Figure E-12 Failure of Specimen P75-S



Figure E-13 Failure of Specimen P75-T



Figure E-14 Failure of Specimen OP120-1-a

## APPENDIX F

### Failure Pictures of Angle Specimens



Figure F-1 Failure of Specimen DEA2

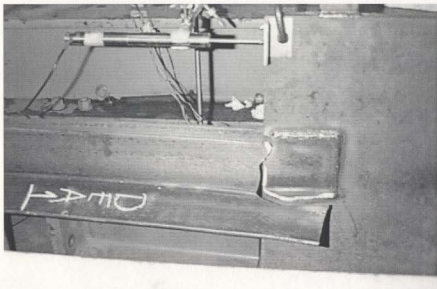
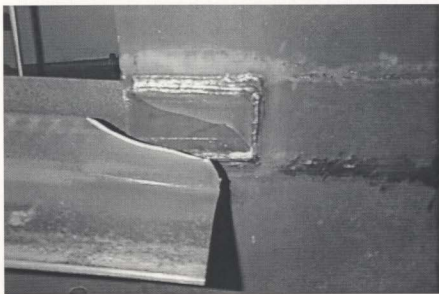


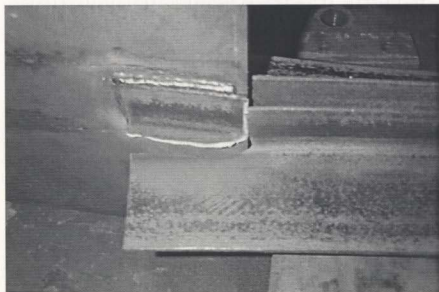
Figure F-2 Failure of Specimen DEA1



Figure F-3 Failure of Specimen DEA5



**Figure F-4 Failure of Specimen DUEA1**



**Figure F-5 Failure of Specimen DUEA2**



Figure F-6 Failure of Specimen EA1



Figure F-7 Failure of Specimen EA2



Figure F-8 Failure of Specimen EA3

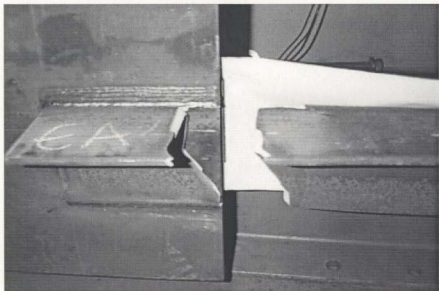


Figure F-9 Failure of Specimen EA4



Figure F-10 Failure of Specimen EAm

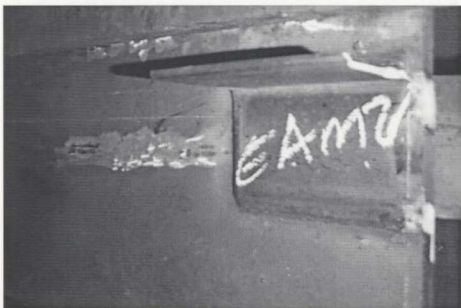
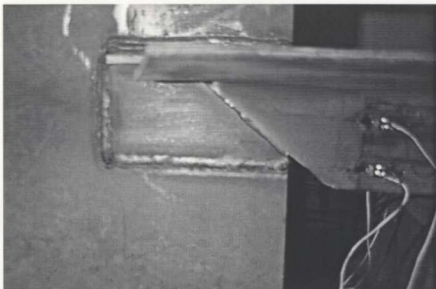


Figure F-11 Failure of Specimen EAm2



Figure F-12 Failure of Specimen UAE1



**Figure F-13 Failure of Specimen UEA2**



**Figure F-14 Failure of Specimen UEA3**



Figure F-15 Failure of Specimen UEA4

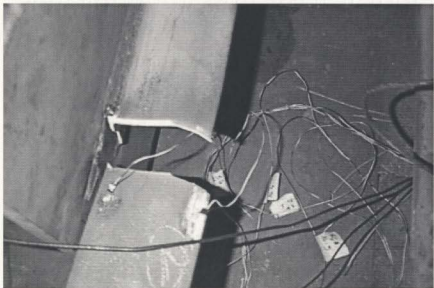
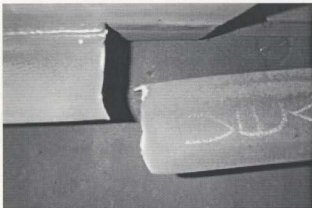


Figure F-16 Failure of Specimen UEA5



**Figure F-17 Failure of Specimen UEA6**



**Figure F-18 Failure of Specimen UEA8**



**Figure F-19 Failure of Specimen UEA9**







